

# When Does Preconditioning Help or Hurt Generalization?

\*Shun-ichi Amari<sup>†</sup>, Jimmy Ba<sup>‡</sup>, Roger Grosse<sup>‡</sup>, Xuechen Li<sup>§</sup>,  
Atsushi Nitanda<sup>¶</sup>, Taiji Suzuki<sup>¶</sup>, Denny Wu<sup>‡</sup>, Ji Xu<sup>||</sup>

June 12, 2022

## Abstract

While second order optimizers such as natural gradient descent (NGD) often speed up optimization, their effect on generalization remains controversial. For instance, it has been pointed out that gradient descent (GD), in contrast to second-order optimizers, converges to solutions with small Euclidean norm in many overparameterized models, leading to favorable generalization properties. In this work, we question the common belief that first-order optimizers generalize better. We provide a precise asymptotic bias-variance decomposition of the generalization error of overparameterized ridgeless regression under a general class of preconditioner  $\mathbf{P}$ , and consider the inverse population Fisher information matrix (used in NGD) as a particular example. We characterize the optimal  $\mathbf{P}$  for the bias and variance, and find that the relative generalization performance of different optimizers depends on the label noise and the “shape” of the signal (true parameters). Specifically, when the labels are noisy, the model is misspecified, or the signal is misaligned with the features, NGD can generalize better than GD. Conversely, in the setting with clean labels, a well-specified model, and well-aligned signal, GD achieves better generalization. Based on this analysis, we consider several approaches to manage the bias-variance tradeoff, and find that interpolating between GD and NGD may generalize better than either algorithm. We then extend our analysis to regression in the reproducing kernel Hilbert space and demonstrate that preconditioned GD can decrease the population risk faster than GD. In our empirical comparisons of first- and second-order optimization of neural networks, we observe robust trends matching our theoretical analysis.

## 1 Introduction

Due to the significant and growing cost of training large-scale machine learning systems (e.g. neural networks [RWC<sup>+</sup>]), there has been much interest in algorithms that speed up optimization. Many such algorithms make use of various types of second-order information, and can be interpreted as minimizing the empirical risk (or the training error)  $L(f_{\theta})$  via a preconditioned gradient descent update:

$$\theta_{t+1} = \theta_t - \eta \mathbf{P}(t) \nabla_{\theta_t} L(f_{\theta_t}), \quad t = 0, 1, \dots \quad (1.1)$$

Setting  $\mathbf{P} = \mathbf{I}$  gives ordinary gradient descent (GD). Choices of  $\mathbf{P}$  which exploit second-order information include the inverse Fisher information matrix, which gives the natural gradient descent (NGD) [Ama98]; the inverse Hessian, which gives Newton’s method [LBOM12]; and diagonal matrices estimated from past gradients, corresponding to various adaptive gradient methods [DHS11, KB14]. By using second-order information, these preconditioners often alleviate the effect of pathological curvature and speed up optimization.

\*Alphabetical ordering.

<sup>†</sup>RIKEN CBS. amari@brain.riken.jp

<sup>‡</sup>University of Toronto and Vector Institute. {jba, rgrosse, dennywu}@cs.toronto.edu

<sup>§</sup>Google Research, Brain Team. Member of the Google AI Residency Program. lxuechen@cs.toronto.edu

<sup>¶</sup>University of Tokyo and RIKEN AIP. {nitanda, taiji}@mist.i.u-tokyo.ac.jp

<sup>||</sup>Columbia University. jx2193@columbia.edu

However, the typical goal of learning is not to fit a finite training set, but to construct predictors that generalize beyond the training data. Although second-order methods lead to faster optimization, their effect on generalization has been largely under debate. NGD [Ama98], as well as Adagrad and its successors [DHS11, KB14], was originally justified in online learning, where efficiency in learning directly translates to generalization. Nonetheless, there remains the possibility that, in the finite data setting, these preconditioned updates are more (or less!) prone to overfitting than GD. For instance, several works reported that in neural network optimization, adaptive or second-order methods generalize worse than GD and its stochastic variants [WRS<sup>+</sup>17, WMW18, KS17], while other empirical studies suggested that second-order methods can achieve comparable, if not better generalization [XRM20, ZWXG18]. We aim to understand when preconditioning using second-order information can help or hurt generalization under fixed training data.

The comparison of the generalization performance of different optimizers relates to the discussion of *implicit regularization* [GLSS18a]. While many explanations have been proposed (see [ZBH<sup>+</sup>16] and Section 2), the starting point of this work is the well-known observation that GD often implicitly regularizes the Euclidean norm, leading to good generalization. For instance in overparameterized least squares regression [WRS<sup>+</sup>17], GD and many other first-order methods find the minimum Euclidean norm solution from zero initialization (without explicit regularization), but preconditioned updates often do not. However, while the minimum norm solution provides reasonable generalization in the overparameterized regime [HMRT19, BLT19], it is unclear whether preconditioned gradient descent always finds inferior solutions.

Motivated by the observations above, we focus on the analysis of overparameterized least squares regression, a setting that is convenient and also interesting for several reasons: (1) the Hessian and Fisher coincide and are not time varying (see Section 2), (2) the optimization trajectory and stationary solution admit an analytical form both with and without preconditioning. (3) due to overparameterization, different  $\mathbf{P}$  may give solutions with contrasting generalization properties. Despite its simplicity, linear regression often yields insights for neural network optimization; indeed we validate the main conclusions of our analysis with neural network experiments (although a rigorous connection is not established).

Our results are organized as follows. In Section 3, we compute the stationary ( $t \rightarrow \infty$ ) generalization error of update (1.1) for overparameterized linear regression under a fixed preconditioner. Extending the proportional asymptotic setup in [HMRT19, DW<sup>+</sup>18], we consider a more general random effects model and use random matrix theoretical tools to derive the exact population risk in its bias-variance decomposition. We characterize choices of  $\mathbf{P}$  that achieve the optimal bias or variance within a general class of preconditioners. Our analysis focuses on the comparison between GD, in which  $\mathbf{P}$  is identity, and NGD, in which  $\mathbf{P}$  is the inverse population Fisher information matrix<sup>1</sup>. Our characterization reveals that the comparison of generalization performance is affected by the following factors:

- **Label Noise:** Additive noise in the labels contributes to the variance term in the risk. We show that NGD achieves the optimal variance among a general class of preconditioned updates.
- **Model Misspecification:** Under misspecification, there does not exist  $f_{\theta}$  that achieves perfect generalization. While this influences the bias term in the risk, we argue that the impact is similar to label noise. Thus, NGD is also beneficial under model misspecification.
- **Data-Signal-Alignment:** Alignment describes how the target signal distributes among input features. We show that NGD achieves lower bias under misalignment — when large variance directions of the features match the small signal directions (learning is “difficult”) — whereas GD achieves lower bias under isotropic signals.

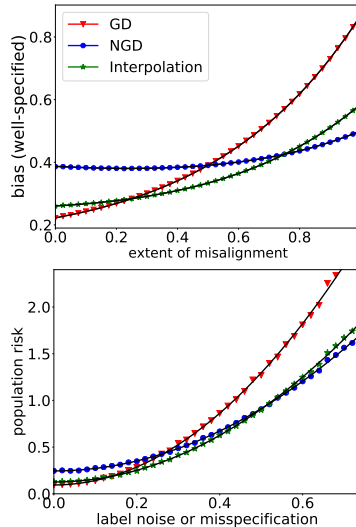


Figure 1: Population risk of the stationary solution of GD, NGD, and interpolation between the two in overparameterized ridgeless regression (detailed setup in Section 3). The relative generalization performance of optimizers depends on label noise, model misspecification and misalignment.

<sup>1</sup>From now on we use NGD to denote the preconditioned update with the inverse population Fisher, and we write “sample NGD” when  $\mathbf{P}$  is the inverse (or pseudo-inverse) of the sample Fisher.

Beyond decomposing the stationary risk, in Section 4 we characterize how the bias-variance tradeoff can be realized by different choices of  $\mathbf{P}$  (e.g. by interpolating between GD and NGD) or early stopping. We then extend the analysis to regression in the reproducing kernel Hilbert space (RKHS) and demonstrate that under early stopping, a particular preconditioner that interpolates between GD and NGD achieves the minimax convergence rate in much fewer steps, and thus reduces the population risk faster than GD. Lastly, in Section 5 we empirically test how well our predictions from the linear setting carry over to neural networks: under a student-teacher setup, we compare the generalization of GD with preconditioned updates and illustrate the influence of all aforementioned factors. The performance of neural networks under a variety of manipulations results in trends that closely match our analysis of linear model.

## 2 Background and Related Works

**Natural Gradient Descent.** NGD is a second-order optimization method proposed in [Ama97]. Consider a data distribution  $p(\mathbf{x})$  on the space  $\mathcal{X}$ , a function  $f_{\boldsymbol{\theta}} : \mathcal{X} \rightarrow \mathcal{Z}$  parameterized by  $\boldsymbol{\theta}$ , and a loss function  $L(\mathbf{X}, f_{\boldsymbol{\theta}}) = \frac{1}{n} \sum_{i=1}^n l(y_i, f_{\boldsymbol{\theta}}(\mathbf{x}_i))$ , where  $l : \mathcal{Y} \times \mathcal{Z} \rightarrow \mathbb{R}$ . Also suppose a probability distribution  $p(y|\mathbf{z}) = p(y|f_{\boldsymbol{\theta}}(\mathbf{x}))$  is defined on the space of labels as part of the model. Then, the natural gradient is the direction of steepest ascent in the Fisher information norm given by  $\tilde{\nabla}_{\boldsymbol{\theta}} L(\mathbf{X}, f_{\boldsymbol{\theta}}) = \mathbf{F}^{-1} \nabla_{\boldsymbol{\theta}} L(\mathbf{X}, f_{\boldsymbol{\theta}})$ , where

$$\mathbf{F} = \mathbb{E}[\nabla_{\boldsymbol{\theta}} \log p(\mathbf{x}, y|\boldsymbol{\theta}) \nabla_{\boldsymbol{\theta}} \log p(\mathbf{x}, y|\boldsymbol{\theta})^{\top}] = -\mathbb{E}[\nabla_{\boldsymbol{\theta}}^2 \log p(\mathbf{x}, y|\boldsymbol{\theta})] \quad (2.1)$$

is the *Fisher information matrix*, or simply the (population) Fisher. Note the expectations in (2.1) are under the joint distribution of the model  $p(\mathbf{x}, y|\boldsymbol{\theta}) = p(\mathbf{x})p(y|f_{\boldsymbol{\theta}}(\mathbf{x}))$ . In the literature, the Fisher is sometimes defined under the empirical data distribution, i.e. based on a finite set of examples  $\{\mathbf{x}_i\}_{i=1}^n$  [APF00]. We instead refer to this quantity as the *sample Fisher*, the properties of which influence optimization and has been studied in various works [KAA18, KAA19, KBH19]. It is known that in linear and kernel regression under the squared loss, preconditioning with the generalized inverse of the sample Fisher results in the same stationary solution as GD (see [ZMG19] and Section 3). Our analysis thus reveals a separation in the generalization performance between the population Fisher and its sample-based counterpart.

While the population Fisher is typically difficult to obtain, extra unlabeled data can be used in its estimation, which empirically leads to better generalization under appropriate damping [PB13]. Moreover, under structural assumptions, estimating the Fisher with parametric approaches can be more sample-efficient [MG15, GM16, Oll15, MCO16], and thus closing the gap between the sample and population Fisher.

When the per-instance loss  $l$  is the negative log-probability of an exponential family distribution, the sample Fisher coincides with the *generalized Gauss-Newton matrix* [Mar14, CGH<sup>+</sup>19]. In the case of least squares regression, which is the focus of this work, the quantity also coincides with the Hessian due to the linear prediction function. Therefore, in the following sections we take NGD as a representative example of preconditioned update, and we expect our findings to also translate to other second-order methods (not including adaptive gradient methods) applied to regression problems.

**Implicit Regularization in Optimization.** In overparameterized linear models, gradient descent converges to the minimum Euclidean norm solution under many loss functions. This characterization can be generalized to mirror descent, for which the implicit bias is determined by the Bregman divergence of the update [AH18, ALH19, GLSS18b, SPR18]. Under the exponential or logistic loss, recent works demonstrated that GD finds the max-margin direction in various setups [JT18, JT19, SHN<sup>+</sup>18, LL19, WLLM18, CB20]. The inductive bias of Adagrad [DHS11] has been analyzed under similar setting [QQ19]. The implicit regularization of the optimizer also relates to the model architecture; examples include matrix factorization [GWB<sup>+</sup>17, SMG13, GBLJ19, ACHL19] and various types of neural network [LMZ17, GLSS18b, WTS<sup>+</sup>19, WGL<sup>+</sup>20]. For networks in the kernel regime [JGH18], the implicit bias of GD relates to properties of the limiting neural tangent kernel (NTK) [ADH<sup>+</sup>19, BM19, XLS16]. We also note that the implicit bias of GD is not always explained by the minimum norm property [RC20].

**Asymptotics of Interpolating Estimators.** In Section 3 we analyze overparameterized estimators that interpolates the training data. Recent works have shown that interpolation may not lead to overfitting [LR18, BRT18, BHM18, BLLT19], and the optimal risk may be achieved by the unregularized estimator

under extreme overparameterization [BHMM18, XH19]. The asymptotic risk of overparameterized models has been characterized in various settings, such as linear regression [Kar13, DW<sup>+</sup>18, HMRT19], random features regression [MM19, dRBK20], and max-margin classifiers [MRSY19, DKT19]. Our analysis is based on tools from random matrix theory developed in [RM11, LP11]. Similar techniques can also be applied to study the gradient descent dynamics of linear regression models [LC18, AKT19].

**Analysis of Preconditioned Gradient Descent.** While [WRS<sup>+</sup>17] considered an example of fixed dataset where GD generalizes better than adaptive methods, in the online learning setting, for which optimization speed directly relates to generalization, several works have shown the advantage of preconditioned updates [DHS11, LD19, ZLN<sup>+</sup>19]. In addition, global convergence and generalization guarantees have been derived for the sample Fisher-based update in overparameterized neural networks [ZMG19, CGH<sup>+</sup>19], in which case the preconditioned update achieves comparable generalization as GD. Lastly, the generalization of different optimizers is often connected to the “sharpness” of the solution [KMN<sup>+</sup>16], and it has been argued that second-order updates tend to find sharper minima [WMW18].

### 3 Asymptotic Risk of Ridgeless Interpolants

We consider a student-teacher setup, in which labels are generated by a teacher model (target function)  $f^* : \mathbb{R}^d \rightarrow \mathbb{R}$  with additive noise  $y_i = f^*(\mathbf{x}_i) + \varepsilon_i$ , and we learn a linear student  $f_{\boldsymbol{\theta}}$  that minimizes the squared loss:  $L(\mathbf{X}, f) = \frac{1}{2n} \sum_{i=1}^n (y_i - \mathbf{x}_i^\top \boldsymbol{\theta})^2$ , where  $\mathbf{x}_i = \Sigma_{\mathbf{X}}^{1/2} \mathbf{z}_i$ ,  $\mathbf{z}_i$  is an i.i.d. random vector with zero-mean, unit-variance, and finite 12th moment, and  $\varepsilon$  is i.i.d. noise independent to  $\mathbf{z}$  with mean 0 and variance  $\sigma^2$ . To compute the population risk  $R(f) = \mathbb{E}_{P_{\mathbf{X}}} [(f^*(\mathbf{x}) - f(\mathbf{x}))^2]$ , we work under the following assumptions:

- **(A1) Proportional Asymptotics:**  $n, d \rightarrow \infty$ ,  $d/n \rightarrow \gamma \in (1, \infty)$ .
- **(A2) Converging Eigenvalues:**  $c_l \mathbf{I}_d \preceq \Sigma_{\mathbf{X}} \preceq c_u \mathbf{I}_d$  for some  $c_l, c_u > 0$  independent of  $d$ ; denote  $\kappa_X = c_u/c_l \in (0, \infty)$ . The spectral measure of  $\Sigma_{\mathbf{X}}$  converges weakly to the limiting  $F_{\Sigma_{\mathbf{X}}}$ .

(A1) entails that the number of features is larger than the number of samples. In this overparameterized setting, the population risk is equivalent to the generalization error, and there exist multiple empirical risk minimizers with potentially different generalization properties.

Denote  $\mathbf{X} = [\mathbf{x}_1^\top, \dots, \mathbf{x}_n^\top]^\top \in \mathbb{R}^{n \times d}$  the data matrix and  $\mathbf{y} \in \mathbb{R}^n$  the corresponding label vector. We optimize the parameters  $\boldsymbol{\theta}$  via gradient flow with the preconditioner  $\mathbf{P}(t) \in \mathbb{R}^{d \times d}$ ,

$$\frac{\partial \boldsymbol{\theta}(t)}{\partial t} = -\mathbf{P}(t) \frac{\partial L(\boldsymbol{\theta}(t))}{\partial \boldsymbol{\theta}(t)} = \frac{1}{n} \mathbf{P}(t) \mathbf{X}^\top (\mathbf{y} - \mathbf{X} \boldsymbol{\theta}(t)), \quad \boldsymbol{\theta}(0) = 0.$$

As previously mentioned, in this linear setup, many common choices of preconditioner do not change through time: under Gaussian likelihood, the sample Fisher (and also Hessian) corresponds to the sample covariance  $\mathbf{X}^\top \mathbf{X}/n$  up to variance scaling, whereas the population Fisher corresponds to the population covariance  $\mathbf{F} = \Sigma_{\mathbf{X}}$ . We thus limit our analysis to fixed preconditioner of the form  $\mathbf{P}(t) := \mathbf{P}$ .

Denote parameters at time  $t$  under preconditioned gradient update with fixed  $\mathbf{P}$  as  $\boldsymbol{\theta}_{\mathbf{P}}(t)$ . For positive definite  $\mathbf{P}$ , the gradient flow trajectory from zero initialization is given as

$$\boldsymbol{\theta}_{\mathbf{P}}(t) = \mathbf{P} \mathbf{X}^\top \left[ \mathbf{I}_n - \exp\left(-\frac{t}{n} \mathbf{X} \mathbf{P} \mathbf{X}^\top\right) \right] (\mathbf{X} \mathbf{P} \mathbf{X}^\top)^{-1} \mathbf{y},$$

The stationary solution is obtained by taking the large  $t$  limit, which we denote as:  $\hat{\boldsymbol{\theta}}_{\mathbf{P}} := \lim_{t \rightarrow \infty} \boldsymbol{\theta}_{\mathbf{P}}(t) = \mathbf{P} \mathbf{X}^\top (\mathbf{X} \mathbf{P} \mathbf{X}^\top)^{-1} \mathbf{y}$ . It is straightforward to check that preconditioned update with appropriately chosen step size converges to this solution as well.

**Remark.** For positive definite  $\mathbf{P}$ , the estimator  $\hat{\boldsymbol{\theta}}_{\mathbf{P}}$  is the minimum  $\|\boldsymbol{\theta}\|_{\mathbf{P}^{-1}}$  norm interpolant:  $\hat{\boldsymbol{\theta}}_{\mathbf{P}} = \arg \min_{\boldsymbol{\theta}} \|\boldsymbol{\theta}\|_{\mathbf{P}^{-1}}$ , s.t.  $\mathbf{X} \boldsymbol{\theta} = \mathbf{y}$ . For GD this translates to the Euclidean norm of the parameters, whereas for NGD ( $\mathbf{P} = \mathbf{F}^{-1} = \Sigma_{\mathbf{X}}^{-1}$ ), the implicit bias is the  $\|\boldsymbol{\theta}\|_{\mathbf{F}}$  norm. Since  $\mathbb{E}_{P_{\mathbf{X}}} [f(\mathbf{x})^2] = \|\boldsymbol{\theta}\|_{\Sigma_{\mathbf{X}}}^2$ , NGD finds an interpolating function with smallest norm under the data distribution (from zero initialization). This division between small parameter norm and function norm is also present in neural networks (see Appendix A).

We highlight the following choices of preconditioners and the corresponding stationary estimator  $\hat{\theta}_{\mathbf{P}}$  as  $t \rightarrow \infty$ .

- **Identity:**  $\mathbf{P} = \mathbf{I}_d$  recovers gradient descent that converges to the minimum-norm interpolant, which we write as  $\hat{\theta}_{\mathbf{I}} := \mathbf{X}^\top (\mathbf{X} \mathbf{X}^\top)^{-1} \mathbf{y}$  and refer to as the *GD solution*.
- **Population Fisher:**  $\mathbf{P} = \mathbf{F}^{-1} = \Sigma_{\mathbf{X}}^{-1}$ , i.e. preconditioning with the inverse *population Fisher*, leads to the estimator  $\hat{\theta}_{\mathbf{F}^{-1}}$ , which is referred to as the *NGD solution*.
- **Variants of Sample Fisher:** since the sample Fisher is rank-deficient, we may add a damping term to ensure invertibility  $\mathbf{P} = (\mathbf{X}^\top \mathbf{X} + \lambda \mathbf{I}_d)^{-1}$  or take the pseudo-inverse  $\mathbf{P} = (\mathbf{X}^\top \mathbf{X})^\dagger$ . In both cases, the gradient is still spanned by the rows of  $\mathbf{X}$ , and thus the preconditioned update also ends up at the unique minimum-norm solution  $\hat{\theta}_{\mathbf{I}}$ , although the trajectory differs, as shown in Figure 2.

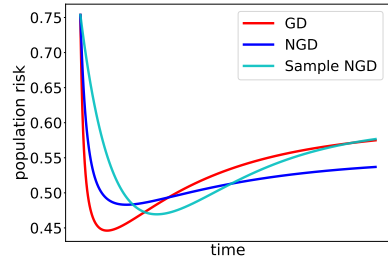


Figure 2: Population risk of preconditioned linear regression vs. time with the following  $\mathbf{P}$ :  $\mathbf{I}$  (red),  $\Sigma_{\mathbf{X}}^{-1}$  (blue) and  $(\mathbf{X}^\top \mathbf{X})^\dagger$  (cyan). Time is rescaled differently for each curve (convergence speed is not comparable). Note that GD and sample NGD give the same stationary risk.

**Remark.** *The above choices illustrate the gap between sample-based and population-based preconditioners: while the sample Fisher accelerates optimization [ZMG19], the following sections demonstrate the advantages of the population Fisher in generalization performance that the sample Fisher does not possess.*

We compare the population risk of the GD solution  $\hat{\theta}_{\mathbf{I}}$  and the NGD solution  $\hat{\theta}_{\mathbf{F}^{-1}}$  in its bias-variance decomposition w.r.t. the label noise, and discuss the two components separately:

$$R(\theta) = \underbrace{\mathbb{E}_{P_{\mathbf{X}}} [(f^*(\mathbf{x}) - \mathbf{x}^\top \mathbb{E}_{P_{\varepsilon}}[\theta])^2]}_{B(\theta), \text{ bias}} + \underbrace{\text{tr}(\text{Cov}(\theta) \Sigma_{\mathbf{X}})}_{V(\theta), \text{ variance}}.$$

### 3.1 The Variance Term: NGD is Optimal

We characterize the variance term which depends on the label noise but not the teacher model  $f^*$ . We restrict ourselves to preconditioners also satisfying (A2) and the additional assumption:

- **(A3) Codiagonalizability:**  $\Sigma_{\mathbf{X}}$  and  $\mathbf{P}$  can be decomposed as  $\Sigma_{\mathbf{X}} = \mathbf{U} \mathbf{D}_{\mathbf{X}} \mathbf{U}^\top$ ,  $\mathbf{P} = \mathbf{U} \mathbf{D}_{\mathbf{P}} \mathbf{U}^\top$  for orthogonal matrix  $\mathbf{U}$  and diagonal matrices  $\mathbf{D}_{\mathbf{X}}$ ,  $\mathbf{D}_{\mathbf{P}}$ .

Although (A3) does not cover all possible preconditioners<sup>2</sup>, it still allows us to characterize the solution of many common choices of  $\mathbf{P}$  previously mentioned, such as the inverse population Fisher, and the pseudo-inverse or ridge-regularized inverse of the sample Fisher<sup>3</sup>. The following theorem gives the asymptotic expression of the variance term and the optimal  $\mathbf{P}$  that minimizes the variances.

**Theorem 1.** *Given  $\mathbf{P}$  satisfying (A3) and  $\mathbf{X} \mathbf{P}$  satisfying the same condition as  $\Sigma_{\mathbf{X}}$  in (A2), then*

$$V(\hat{\theta}_{\mathbf{P}}) \rightarrow \sigma^2 \left( \lim_{\lambda \rightarrow 0^+} \frac{m'(-\lambda)}{m^2(-\lambda)} - 1 \right), \quad (3.1)$$

as  $n, d \rightarrow \infty$ , where  $m(z) > 0$  is the Stieltjes transform of the limiting distribution of eigenvalues of  $\frac{1}{n} \mathbf{X} \mathbf{P} \mathbf{X}^\top$  (for  $z$  beyond its support) defined as the solution to  $m^{-1}(z) = -z + \gamma \int \tau (1 + \tau m(z))^{-1} dF_{\mathbf{X} \mathbf{P}}(\tau)$ , where  $F_{\mathbf{X} \mathbf{P}}$  denotes the limiting spectral measure of  $\mathbf{D}_{\mathbf{X}} \mathbf{D}_{\mathbf{P}}$ .

Furthermore,  $V(\hat{\theta}_{\mathbf{P}}) \geq \sigma^2 (\gamma - 1)^{-1}$ , and the equality is obtained by  $\hat{\theta}_{\mathbf{F}^{-1}}$ , i.e. when  $\mathbf{P} = \Sigma_{\mathbf{X}}^{-1}$ .

Formula (3.1) is a direct extension of [HMRT19, Theorem 4], which can be obtained from [DW<sup>+</sup>18, Theorem 2.1] or the general result of [LP11, Theorem 1.2]. Theorem 1 implies that preconditioning with the inverse population Fisher leads to the optimal stationary variance, which is supported by Figure 3(a). In

<sup>2</sup>This assumption is not required by [RM11] but we included it for simple and interpretable result.

<sup>3</sup>Variants of the sample Fisher do not satisfy (A3), yet from the previous discussion we know that preconditioned update with  $\mathbf{P} = (\mathbf{X}^\top \mathbf{X})^\dagger$  or  $(\mathbf{X}^\top \mathbf{X} + \lambda \mathbf{I}_d)^{-1}$  also converges to the min-norm solution  $\hat{\theta}_{\mathbf{I}}$ .

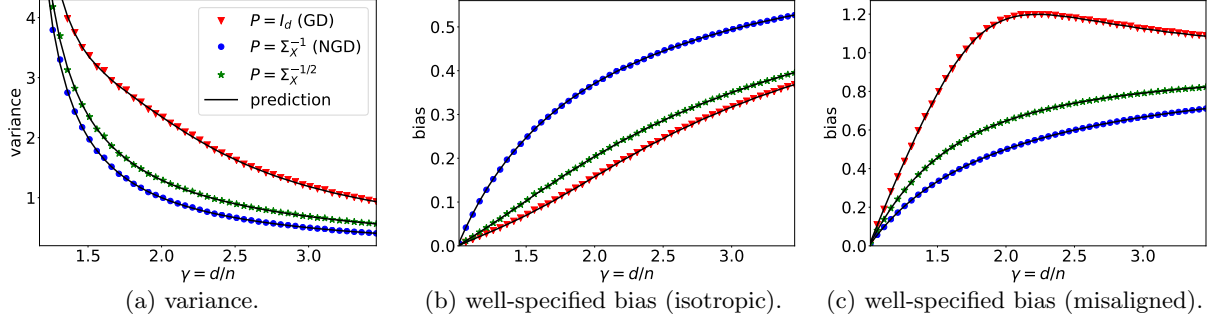


Figure 3: Experiments with  $\mathbf{D}_X$  as two equally-weighted point masses with  $\kappa_X = 20$ ; for the empirical values (dots) we set  $n = 300$ . (a) NGD achieves minimum variance. (b) GD achieves lower bias under isotropic signal:  $\Sigma_\theta = \mathbf{I}_d$ . (c) NGD achieves lower bias under “misalignment”:  $\Sigma_X = \Sigma_\theta^{-1}$ .

other words, when the labels contain large amount of noise, i.e. the generalization error is dominated by the variance term, we expect NGD to generalize better upon convergence. We emphasize that this advantage is only present when the population Fisher is used, but not the sample-based counterpart.

### 3.2 The Bias Term: Well-specified Case

We first consider the case where the teacher is also linear and well-specified, i.e.  $y_i = \mathbf{x}_i^\top \boldsymbol{\theta}^*$ . We assume a random effects model that is more general than that in [DW<sup>+</sup>18] and place the following prior on  $\boldsymbol{\theta}^*$ :

- **(A4) Anisotropic Prior:**  $\mathbb{E}[\boldsymbol{\theta}^*] = 0$ ,  $\text{Cov}(\boldsymbol{\theta}^*) = d^{-1} \Sigma_\theta$ .  $\Sigma_\theta$  satisfies (A2-3). The empirical distributions of diagonal elements of  $\mathbf{D}_X$ ,  $\mathbf{D}_\theta$ , and  $\mathbf{D}_{X\mathbf{P}}$  jointly converge to non-negative random variables  $(v_x, v_\theta, v_{xp})$ .

When  $\mathbf{P} = \mathbf{I}_d$ , previous works have considered the special case of the isotropic prior  $\Sigma_\theta = d^{-1} \mathbf{I}_d$  [DW<sup>+</sup>18, XH19]. We note that our more general prior leads to many interesting phenomena that are not captured by simplified settings, such as the non-monotonicity of the bias and variance for  $\gamma > 1$  (see Figure 12), and the epoch-wise double descent (see Appendix A for discussion). Under our general setup, the asymptotic bias and the optimal  $\mathbf{P}$  can be characterize as follow:

**Theorem 2.** Under (A1-4), the expected bias  $B(\hat{\boldsymbol{\theta}}_{\mathbf{P}}) := \mathbb{E}_{\boldsymbol{\theta}^*}[B(\hat{\boldsymbol{\theta}}_{\mathbf{P}})]$  is given as

$$B(\hat{\boldsymbol{\theta}}_{\mathbf{P}}) \rightarrow \lim_{\lambda \rightarrow 0^+} \frac{m'(-\lambda)}{m^2(-\lambda)} \mathbb{E} \left[ \frac{v_x v_\theta}{(1 + v_{xp} m(-\lambda))^2} \right],$$

where expectation is taken over  $v$  and  $m(z)$  is the Stieltjes transform defined in Theorem 1.

Furthermore, we have  $B(\hat{\boldsymbol{\theta}}_{\mathbf{P}}) \geq \lim_{\lambda \rightarrow 0^+} [\gamma^{-1} m^{-1}(-\lambda)]$ ; the equality is obtained when  $\mathbf{P} = \Sigma_\theta$ .

This result implies that the optimal preconditioner does not depend on the data covariance  $\Sigma_X$ , but only on the distribution of the teacher  $\Sigma_\theta$ , which is usually not known *a priori*. Consequently, when parameters of the teacher model have roughly equal magnitude (isotropic), then GD achieves lower bias (see Figure 3(a), in which  $\Sigma_\theta = \mathbf{I}_d$ ). In contrast, when  $\Sigma_X$  is “misaligned” with  $\Sigma_\theta$ , i.e. when the most varying directions of the features  $\mathbf{X}$  contain little information about the signal  $\boldsymbol{\theta}^*$  (see Figure 3(b), in which  $\Sigma_\theta = \Sigma_X^{-1}$ ), in which case the teacher is difficult to learn, the NGD solution has lower bias. This is in contrast to the variance term, for which the NGD solution  $\hat{\boldsymbol{\theta}}_{\mathbf{F}^{-1}}$  always dominates.

### 3.3 Misspecification $\approx$ Label Noise

Under model misspecification, there does not exist a predictor  $\boldsymbol{\theta} \in \mathbb{R}^d$  s.t.  $B(\boldsymbol{\theta}) = 0$ . In this case, we may decompose the teacher into a well-specified component and its residual:  $f^*(\mathbf{x}) = \mathbf{x}^\top \boldsymbol{\theta}^* + f_c^*(\mathbf{x})$ .

For simplicity, we first consider the residual to be a linear function of unobserved features (from [HMRT19, Section 5]). Formally, the label is generated as  $y_i = \mathbf{x}_i^\top \boldsymbol{\theta}^* + \mathbf{x}_{c,i}^\top \boldsymbol{\theta}^c + \varepsilon_i$ , where  $\mathbf{x}_{c,i} \in \mathbb{R}^{d_c}$  are unobserved

features independent on  $\mathbf{x}_i$ . Similar to the previous calculation, we assume  $\mathbf{x}_c$  has zero-mean and covariance  $\Sigma_{\mathbf{X}}^c$  and place the prior  $\mathbb{E}[\boldsymbol{\theta}^c] = 0$ ,  $\text{Cov}(\boldsymbol{\theta}^c) = d_c^{-1}\Sigma_{\boldsymbol{\theta}}^c$ , where  $\Sigma_{\mathbf{X}}^c, \Sigma_{\boldsymbol{\theta}}^c$  satisfy (A2-3).

**Proposition 3.** *Under model misspecification with unobserved features described above, the bias can be decomposed as  $B(\hat{\boldsymbol{\theta}}) = B_{\boldsymbol{\theta}}(\hat{\boldsymbol{\theta}}_{\mathbf{P}}) + B_c(\hat{\boldsymbol{\theta}}_{\mathbf{P}})$ , where  $B_{\boldsymbol{\theta}}$  is the well-specified bias defined in Theorem 2, and  $B_c = d_c^{-1}\text{tr}(\Sigma_{\mathbf{X}}^c\Sigma_{\boldsymbol{\theta}}^c)(V(\hat{\boldsymbol{\theta}}_{\mathbf{P}}) + 1)$ , where  $V(\hat{\boldsymbol{\theta}}_{\mathbf{P}})$  is the variance in Theorem 1.*

In other words, the misspecification bias is the same as a scaled variance (also noted in [HMRT19, Theorem 4]). Thus, Theorem 1 implies that NGD likely achieves lower bias when the model is very misspecified. While Proposition 3 only describes one example of misspecification, we expect such characterization to hold under broader settings. In particular, [MM19, Remark 5] indicates that for many nonlinear  $f_c^*$ , the misspecified bias is the same as variance caused by label noise. This result is only rigorously shown under isotropic data, but we empirically verify that the same observation holds under general covariances in Figure 1: we take  $\Sigma_{\boldsymbol{\theta}} = \mathbf{I}_d$  (favors GD) and  $f_c^*(\mathbf{x}) = \alpha(\langle \mathbf{x}, \mathbf{x} \rangle - \text{tr}(\Sigma_{\mathbf{X}}))$ , where  $\alpha$  controls the extent of nonlinearity. Predictions are generated by adding the same level of noise as the second moment of  $f_c$ . Note that as we further misspecify the model by increasing the nonlinearity of the teacher, NGD results in lower bias than GD.

## 4 Bias-variance Tradeoff

Our characterization of stationary risk suggests that the preconditioners that achieve the optimal bias and variance can be different. This section discusses how the bias and the variance can be balanced by interpolating between preconditioners or by early stopping. In addition, we show that a preconditioner that interpolates between GD and NGD also leads to faster decrease in the test error compared to GD.

### 4.1 Interpolating between Preconditioners

Depending on the orientation of the teacher model, we may expect a bias-variance tradeoff in choosing  $\mathbf{P}$ . Intuitively, given  $\mathbf{P}_1$  that minimizes the bias and  $\mathbf{P}_2$  that minimizes the variance, we may expect a preconditioner that interpolates between  $\mathbf{P}_1$  and  $\mathbf{P}_2$  to balance the bias and variance and thus generalize better. In the following proposition, we confirm this intuition in a setup of general data covariance and isotropic prior on the teacher<sup>4</sup>, for which GD ( $\mathbf{P} = \mathbf{I}_d$ ) achieves optimal bias and NGD ( $\mathbf{P} = \mathbf{F}^{-1}$ ) achieves optimal variance.

**Proposition 4 (Informal).** *Let  $\Sigma_{\mathbf{X}} \neq \mathbf{I}_d$  and  $\Sigma_{\boldsymbol{\theta}} = \mathbf{I}_d$ . Consider the following three interpolating preconditioners (under appropriate scaling of  $\Sigma_{\mathbf{X}}$ ): (i)  $\mathbf{P}_{\alpha} = \alpha\Sigma_{\mathbf{X}}^{-1} + (1-\alpha)\mathbf{I}_d$ , (ii)  $\mathbf{P}_{\alpha} = (\alpha\Sigma_{\mathbf{X}} + (1-\alpha)\mathbf{I}_d)^{-1}$ , (iii)  $\mathbf{P}_{\alpha} = \Sigma_{\mathbf{X}}^{-\alpha}$ . The stationary variance monotonically decreases with  $\alpha \in [0, 1]$  for all three choices. For (i), the stationary bias monotonically increases with  $\alpha \in [0, 1]$ , whereas for (ii) and (iii), the bias monotonically increases with  $\alpha$  in a range that depends on  $\Sigma_{\mathbf{X}}$ .*

This proposition implies that as the signal-to-noise ratio (SNR) decreases (i.e., more label noise), one can increase  $\alpha$ , which makes the update closer to NGD to improve generalization, and vice versa<sup>5</sup> (small  $\alpha$  entails GD-like update). Figure 4 and 15 validates Proposition 4 and suggests that in general, for a given SNR, a preconditioner that interpolates between  $\Sigma_{\mathbf{X}}^{-1}$  and  $\Sigma_{\boldsymbol{\theta}}$  may achieve lower stationary risk.

**Remark.** *Two of the interpolation schemes above align with common choices in practice: additive interpolation (ii) corresponds to damping added to the Fisher to stabilize its inverse, while geometric interpolation (iii) includes the “conservative” square-root scaling in many adaptive gradient methods [DHS11, KB14].*

<sup>4</sup>Note that this setup reduces to the random effects model studied in [DW+18, XH19].

<sup>5</sup>While Proposition 4 does not show the monotonicity of the bias of (ii)(iii) for all  $\Sigma_{\mathbf{X}}$  and  $\alpha \in [0, 1]$ , in Appendix C.5 we empirically verify that the bias is monotone over  $\alpha \in [0, 1]$  for a wide range of distributions beyond the proposition.

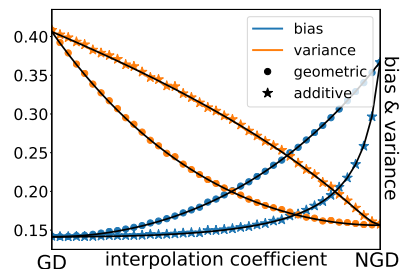


Figure 4: illustration of the bias-variance tradeoff with  $\kappa_X = 25$ ,  $\Sigma_{\boldsymbol{\theta}} = \mathbf{I}_d$  and  $\text{SNR}=32/5$ . As we additively or geometrically interpolate from GD to NGD (left to right), the stationary bias (blue) increases and the stationary variance (orange) decreases.

## 4.2 The Role of Early Stopping

Previously, we considered the stationary solution with no regularization applied. It is known that the bias-variance tradeoff can also be controlled by either explicit or algorithmic regularization. Here we briefly comment on the effect of early stopping, starting from the variance term.

**Proposition 5.** *For all  $\mathbf{P}$  satisfying (A2-3), the variance  $V(\boldsymbol{\theta}_{\mathbf{P}}(t))$  monotonically increases with  $t$ .*

This confirms the common knowledge that early stopping reduces overfitting to label noise (i.e., lower variance). Variance reduction can be beneficial to GD in its comparison with NGD, which always achieves the lowest stationary variance possible, and the same would also hold for the misspecification bias which is analogous to the variance term. Indeed, Figure 2 and 14 demonstrate that GD may have better early stopping risk even when its stationary risk is larger than NGD.

On the other hand, early stopping may not always improve the bias in the well-specified case. While we do not give a full characterization due to the difficulty in handling the potentially non-monotonic bias term (see Appendix A), we speculate that previous observations on the stationary bias also translate to early stopping. To give a concrete example, we consider well-specified settings under in GD or NGD achieves the optimal stationary bias, and demonstrate that such optimality is preserved under early stopping.

**Proposition 6.** *Denote the optimal early stopping bias as  $B^{\text{opt}}(\boldsymbol{\theta}) = \inf_{t \geq 0} B(\boldsymbol{\theta}(t))$ . Then for all  $\mathbf{P}$  satisfying (A2-3), when  $\boldsymbol{\Sigma}_{\boldsymbol{\theta}} = \boldsymbol{\Sigma}_{\mathbf{X}}^{-1}$ ,  $B^{\text{opt}}(\boldsymbol{\theta}_{\mathbf{P}}) \geq B^{\text{opt}}(\boldsymbol{\theta}_{\mathbf{F}-1})$ . Whereas when  $\boldsymbol{\Sigma}_{\boldsymbol{\theta}} = \mathbf{I}_d$ ,  $B^{\text{opt}}(\boldsymbol{\theta}_{\mathbf{I}}) \leq B^{\text{opt}}(\boldsymbol{\theta}_{\mathbf{F}-1})$ .*

Figure 14 shows that the observed trend in the stationary bias (well-specified) is indeed preserved in early stopping: GD or NGD achieves lower early stopping bias under isotropic or misaligned teacher model, respectively. We leave the precise characterization of this observation as future work.

## 4.3 Fast Decay of Population Risk

Our previous analysis suggests that certain preconditioners can achieve lower population risk, but does not compare which method decreases the risk more efficiently. Knowing that preconditioned updates often lead to faster optimization, one natural question to ask is, is this speedup also present for the population risk (generalization error) under fixed dataset? We answer this question in the affirmative for a slightly different model: we study least squares regression in the RKHS, and show that a preconditioned gradient update that interpolates between GD and NGD can achieve the minimax optimal rate in much fewer iterations than GD.

We defer the details to Appendix C and briefly outline the setup here. Let  $\mathcal{H}$  be an RKHS included in  $L_2(P_X)$  equipped with a bounded kernel function  $k$ , and  $K_{\mathbf{x}} \in \mathcal{H}$  be the Riesz representation of the kernel function. Define an operator  $S$  as the canonical embedding from  $\mathcal{H}$  to  $L_2(P_X)$ , and write  $\Sigma = S^*S$  and  $L = SS^*$ . We consider a student-teacher setup with teacher model  $f^*$  and make the following assumptions:

- **(A5):** There exist  $r \in (0, \infty)$  and  $M > 0$  such that  $f^* = L^r h^*$  for some  $h^* \in L_2(P_X)$  and  $\|f^*\|_{\infty} \leq M$ .
- **(A6):** There exists  $s > 1$  such that  $\text{tr}(\Sigma^{1/s}) < \infty$  and  $2r + s^{-1} > 1$ .
- **(A7):** There exist  $\mu \in [s^{-1}, 1]$  and  $C_{\mu} > 0$  such that  $\sup_{\mathbf{x} \in \text{supp}(P_X)} \|\Sigma^{1/2-1/\mu} K_{\mathbf{x}}\|_{\mathcal{H}} \leq C_{\mu}$ .

The coefficient  $r$  in (A5) controls the complexity of the teacher model and relates to the notions of model misalignment and misspecification discussed in Section 3. In particular, large  $r$  implies a smoother teacher model which is “easier” to learn, and vice versa. We remark that previous works mostly consider  $r \geq 1/2$  which implies  $f^* \in \mathcal{H}$ . On the other hand, (A6)(A7) are common assumptions that control the capacity and the regularity of the RKHS [CDV07, PVRB18]. Given  $n$  training points  $\{(\mathbf{x}_i, y_i)\}_{i=1}^n$ , we consider the following preconditioned update on the student model  $f_t \in \mathcal{H}$ :

$$f_t = f_{t-1} - \eta(\Sigma + \alpha I)^{-1}(\hat{\Sigma} f_{t-1} - \hat{S}^* Y), \quad f_0 = 0, \quad (4.1)$$

where  $\hat{\Sigma} = \frac{1}{n} \sum_{i=1}^n K_{\mathbf{x}_i} \otimes K_{\mathbf{x}_i}$  and  $\hat{S}^* Y = \frac{1}{n} \sum_{i=1}^n y_i K_{\mathbf{x}_i}$ . In this setup, the population Fisher corresponds to the covariance operator  $\Sigma$ , and thus (4.1) can be interpreted an interpolation between GD and NGD (discussed in Section 4.1): we expect update with large  $\alpha$  to behave like GD, and small  $\alpha$  like NGD. The following theorem illustrates the benefit of preconditioning in terms of the fast decrease of population risk.

**Theorem 7 (Informal).** Under (A5-7) and sufficiently large  $n$ , the population risk of  $f_t$  can be written as  $R(f_t) = \|Sf_t - f^*\|_{L_2(P_X)}^2 \leq C(B(t) + V(t))$ , where  $B(t)$  and  $V(t)$  are defined in Appendix C. Given  $r > 1/2$  or  $\mu \leq 2r$ , the preconditioned update (4.1) with  $\alpha = n^{-\frac{2s}{2rs+1}}$  achieves the minimax optimal convergence rate  $R(f_t) = \tilde{O}\left(n^{-\frac{2rs}{2rs+1}}\right)$  in  $t = \Theta(\log n)$  steps, whereas naive gradient descent requires  $t = \Theta\left(n^{\frac{2rs}{2rs+1}}\right)$  steps.

We remark that the faster convergence of the preconditioned update is due to the more rapid decay of the bias term. Note that the interpolation coefficient  $\alpha$  depends on the teacher model in the following way: for  $n > 1$ ,  $\alpha$  decreases as  $r$  becomes smaller, which corresponds to non-smooth and “difficult” teacher, and vice versa. This agrees with our previous observation that NGD is advantageous when the teacher is difficult to learn (either misaligned or misspecified). We defer empirical verification of this result to Appendix B.

## 5 Neural Network Experiments

### 5.1 Protocol

We empirically demonstrate similar trends as our theoretical results in neural network settings that NGD finds solutions that generalize better compared to GD when (i) labels of the training data are noisy, and (ii) the model is misspecified, (iii) the teacher is “misaligned”, and vice versa.

We consider the MNIST and CIFAR10 [KH<sup>+</sup>09] datasets. To create a student-teacher setup, we split the original training set into two equal halves, one of which along with the original labels is used to pretrain the teacher, and the other along with the teacher’s labels is used to distill [HVD15, BCNM06] the student. We refer to the splits as the *pretrain* and *distill* split, respectively. In all scenarios, the teacher is either a two-layer fully-connected ReLU network [NH10] or a ResNet [HZRS16]; whereas the student model is a two-layer ReLU net. We normalize the teacher’s labels (logits) following [BC14] before potentially adding label noise and fit the student model by minimizing the L2 loss. Student models are trained on a subset of the distill split with full-batch updates. We implement NGD using Hessian-free optimization [Mar10]. To estimate the population Fisher, we use 100k training data obtained by possibly applying data augmentation. We report the test error when the training error is below 0.2% of the training error at initialization as a proxy for the stationary risk. We defer detailed setup to Appendix D and additional results to Appendix B.

### 5.2 Empirical Findings

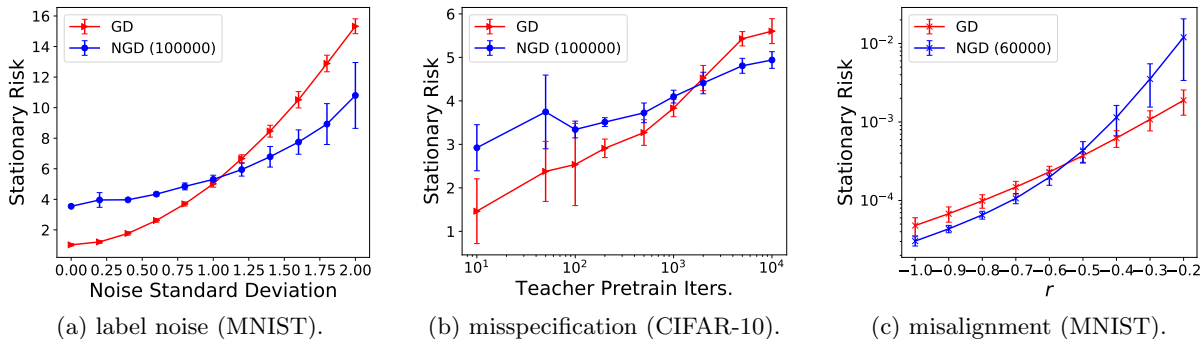


Figure 5: Comparison between NGD and GD. Error bar is one standard deviation away from mean over five independent runs. Numbers in parentheses denote amount of unlabeled examples for estimating the Fisher.

**Label Noise.** We pretrain the teacher with the full pretrain split and use 1024 examples from the distill split to fit the student. For both the student and teacher, we use a two-layer ReLU net with 80 hidden units. We corrupt the labels with isotropic Gaussian noise whose standard deviation we vary. Figure 5(a) shows that as the noise increases (variance begins to dominate), the stationary risk of both NGD and GD worsen, with GD worsening faster, which aligns with our observation in Figure 3.

**Misspecification.** We use ResNet-20 [HZRS16] for the teacher and the same two-layer student from the label noise experiment. To vary the misspecification, we take teacher models with the same initialization but varying amount of pretraining. Intuitively, large teacher models that are trained more should be more complex and thus more likely to be outside of functions that a small two-layer student can represent (therefore the problem is more misspecified). Indeed, Figure 5(b) shows that NGD eventually achieves better generalization as the number of training steps for the teacher increases. As a heuristic measure of misspecification, in Figure 6 we report  $\sqrt{2\mathbf{y}^\top \mathbf{K}^{-1} \mathbf{y}/n}$  studied in [ADH<sup>+</sup>19], in which  $\mathbf{y}$  is the label vector and  $\mathbf{K}$  is the student’s NTK matrix [JGH18]. We observe that the quantity is increasing as more label noise is added and as the teacher is trained longer. In Appendix A we provide a non-rigorous interpretation of how this quantity relates to label noise and misspecification.

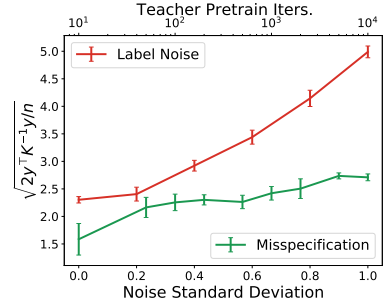
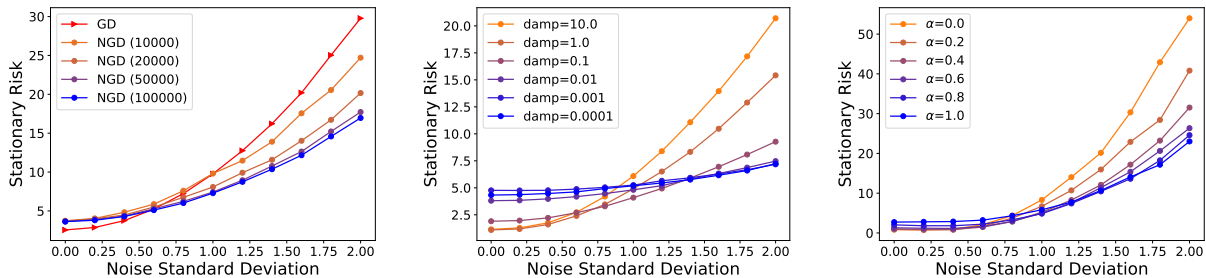


Figure 6: A heuristic measure of misspecification and label noise.

**Misalignment.** We use the same two-layer ReLU net (60 neurons) for the student and teacher (thus the setting is intuitively well-specified). We construct the teacher model by perturbing the student’s initialization. The direction of the random perturbation is given by  $\mathbf{F}^r$ , where  $\mathbf{F}$  is the student’s population Fisher and  $r \in [-1, 0]$ . Intuitively, as  $r$  approaches -1, the “important” parameters of the teacher (i.e. larger update directions) lie in the small eigendirections of the student’s Hessian, and we therefore interpret the problem to be more misaligned, and vice versa. While this analogy is rather superficial due to the non-convex nature of neural network optimization, Figure 5(c) shows that as  $r$  becomes smaller (setup is more misaligned), NGD begins to generalize better than GD in terms of stationary risk.

**Interpolating between Preconditioners.** We also validate our observations in Section 3 and 4 on the difference between the sample Fisher and population Fisher, and the potential benefit of interpolating between GD and NGD. Figure 7(a) shows that as we decrease the number of unlabeled data in estimating the Fisher, which renders the preconditioner closer to the sample Fisher, the stationary risk becomes more akin to that of GD, especially in the large noise setting. This agrees with our remark on sample vs. population Fisher in Section 3 and Appendix A.

Figure 7(b)(c) confirms the finding in Section 4.1 that interpolating preconditioners provides bias-variance tradeoff also holds in neural network settings. In particular, we interpret the left end to correspond to a bias-dominant regime (due to the same architecture of two-layer MLP for the student and teacher), and the right end to correspond to the variance-dominant regime (due to the added label noise). Observe that at a certain SNR, a preconditioner that interpolates between GD and NGD achieves lower stationary risk.



(a) interpolation between sample and population Fisher (CIFAR-10). (b) additive interpolation between GD and NGD (MNIST). (c) geometric interpolation between GD and NGD (MNIST).

Figure 7: (a) numbers in parentheses indicate the amount of unlabeled data used in estimating the Fisher; we expect the estimated Fisher to be closer to the sample Fisher when the number of unlabeled data is small. (a) additive interpolation  $\mathbf{P} = (\hat{\mathbf{F}} + \alpha \mathbf{I}_d)^{-1}$ ; larger damping parameter yields update closer to GD. (b) geometric interpolation  $\mathbf{P} = \hat{\mathbf{F}}^{-\alpha}$ ; larger  $\alpha$  parameter yields update closer to that of NGD (blue). We use the singular value decomposition to compute the minus  $\alpha$  power of the Fisher, as CG is not applicable in this scenario.

## 6 Discussion and Conclusion

We analyzed the generalization properties of a general class of preconditioned gradient descent under the squared loss, with particular emphasis on natural gradient descent. Our analysis identifies three factors that affects the relative generalization performance, the influence of which we also empirically observed in neural network experiments. We additionally determined the corresponding optimal preconditioner for each of the factors. While the optimal preconditioner is usually not known in practice, we provided justification for common algorithmic choices by discussing the bias-variance tradeoff. We remark that our least squares regression setup dealt with a fixed preconditioner and thus does not cover many adaptive gradient methods; an interesting problem is to characterize the generalization of these optimizers in similar setting. In addition, beyond the analysis of this work, there are many other ingredients that influence the generalization of different optimizers, such as different loss functions [TPT20, MNS<sup>+</sup>20], and explicit (e.g. weight decay<sup>6</sup>) or implicit regularization (e.g. learning rate and gradient noise); understanding their impact in the overparameterized regime would be a fruitful future direction.

It is worth noting that our optimal preconditioner requires knowledge on the population second-order statistics, which we empirically approximate using extra unlabeled data. Consequently, our characterization suggests that different “types” (sample vs. population) of second-order information may affect generalization differently. Broadly speaking, there are two types of practical approximate second-order optimizers for neural networks. Some algorithms, such as Hessian-free optimization [Mar10, MS12, DPCB13], approximate second-order matrices (typically the Hessian or Fisher) using the exact matrix on finite training examples. In high-dimensional problems, this sample-based approximation may be very different from the population quantity (e.g. it is necessarily degenerate in the overparameterized regime). Other algorithms fit a parametric approximation to the Fisher, such as diagonal [DHS11, KB14], quasi-diagonal [Oll15], or Kronecker-factored [MG15]. If the parametric assumption is accurate, these parametric approximations are more statistically efficient and thus may lead to better approximation of the population Fisher. Our analysis reveals a separation between sample- and population-based preconditioned updates, which is present in simple neural network problems as well (see Appendix A). As future work, we intend to investigate whether similar separation is also present for different approximate second-order optimizers in real-world problems.

## Acknowledgement

The authors would like to thank Murat A. Erdogdu, Fartash Faghri, Ryo Karakida, Yiping Lu, Jiaxin Shi, Shengyang Sun, Guodong Zhang and Michael Zhang for helpful comments and discussions. The authors are also grateful to Tomoya Murata for his contribution to the preliminary studies on regression in the RKHS.

JB and RG were supported by the CIFAR AI Chairs program. JB and DW were partially supported by LG Electronics and NSERC. AN was partially supported by JSPS Kakenhi (19K20337) and JST-PRESTO. TS was partially supported by JSPS Kakenhi (26280009, 15H05707 and 18H03201), Japan Digital Design and JST-CREST. JX was supported by a Cheung-Kong Graduate School of Business Fellowship. Resources used in preparing this research were provided, in part, by the Province of Ontario, the Government of Canada through CIFAR, and companies sponsoring the Vector Institute.

---

<sup>6</sup>in a companion work [WX20] we characterize the impact of  $\ell_2$  regularization in overparameterized models.

## References

- [ACHL19] Sanjeev Arora, Nadav Cohen, Wei Hu, and Yuping Luo, *Implicit regularization in deep matrix factorization*, Advances in Neural Information Processing Systems, 2019, pp. 7411–7422.
- [ADH<sup>+</sup>19] Sanjeev Arora, Simon S Du, Wei Hu, Zhiyuan Li, and Ruosong Wang, *Fine-grained analysis of optimization and generalization for overparameterized two-layer neural networks*, arXiv preprint arXiv:1901.08584 (2019).
- [AH18] Navid Azizan and Babak Hassibi, *Stochastic gradient/mirror descent: Minimax optimality and implicit regularization*, arXiv preprint arXiv:1806.00952 (2018).
- [AKT19] Alnur Ali, J Zico Kolter, and Ryan J Tibshirani, *A continuous-time view of early stopping for least squares*, International Conference on Artificial Intelligence and Statistics, vol. 22, 2019.
- [ALH19] Navid Azizan, Sahin Lale, and Babak Hassibi, *Stochastic mirror descent on overparameterized nonlinear models: Convergence, implicit regularization, and generalization*, arXiv preprint arXiv:1906.03830 (2019).
- [Ama97] Shun-ichi Amari, *Neural learning in structured parameter spaces-natural riemannian gradient*, Advances in neural information processing systems, 1997, pp. 127–133.
- [Ama98] Shun-Ichi Amari, *Natural gradient works efficiently in learning*, Neural computation **10** (1998), no. 2, 251–276.
- [APF00] Shun-Ichi Amari, Hyeyoung Park, and Kenji Fukumizu, *Adaptive method of realizing natural gradient learning for multilayer perceptrons*, Neural computation **12** (2000), no. 6, 1399–1409.
- [BBV04] Stephen Boyd, Stephen P Boyd, and Lieven Vandenberghe, *Convex optimization*, Cambridge university press, 2004.
- [BC14] Jimmy Ba and Rich Caruana, *Do deep nets really need to be deep?*, Advances in neural information processing systems, 2014, pp. 2654–2662.
- [BCNM06] Cristian Bucilu, Rich Caruana, and Alexandru Niculescu-Mizil, *Model compression*, Proceedings of the 12th ACM SIGKDD international conference on Knowledge discovery and data mining, 2006, pp. 535–541.
- [BHM18] Mikhail Belkin, Daniel J Hsu, and Partha Mitra, *Overfitting or perfect fitting? risk bounds for classification and regression rules that interpolate*, Advances in neural information processing systems, 2018, pp. 2300–2311.
- [BHMM18] Mikhail Belkin, Daniel Hsu, Siyuan Ma, and Soumik Mandal, *Reconciling modern machine learning and the bias-variance trade-off*, arXiv preprint arXiv:1812.11118 (2018).
- [BLLT19] Peter L Bartlett, Philip M Long, Gábor Lugosi, and Alexander Tsigler, *Benign overfitting in linear regression*, arXiv preprint arXiv:1906.11300 (2019).
- [BM19] Alberto Bietti and Julien Mairal, *On the inductive bias of neural tangent kernels*, Advances in Neural Information Processing Systems, 2019, pp. 12873–12884.
- [BRT18] Mikhail Belkin, Alexander Rakhlin, and Alexandre B Tsybakov, *Does data interpolation contradict statistical optimality?*, arXiv preprint arXiv:1806.09471 (2018).
- [CB20] Lenaic Chizat and Francis Bach, *Implicit bias of gradient descent for wide two-layer neural networks trained with the logistic loss*, arXiv preprint arXiv:2002.04486 (2020).
- [CDV07] Andrea Caponnetto and Ernesto De Vito, *Optimal rates for the regularized least-squares algorithm*, Foundations of Computational Mathematics **7** (2007), no. 3, 331–368.

- [CFW<sup>+</sup>19] Yuan Cao, Zhiying Fang, Yue Wu, Ding-Xuan Zhou, and Quanquan Gu, *Towards understanding the spectral bias of deep learning*, arXiv preprint arXiv:1912.01198 (2019).
- [CGH<sup>+</sup>19] Tianle Cai, Ruiqi Gao, Jikai Hou, Siyu Chen, Dong Wang, Di He, Zhihua Zhang, and Liwei Wang, *A gram-gauss-newton method learning overparameterized deep neural networks for regression problems*, arXiv preprint arXiv:1905.11675 (2019).
- [DHLZ19] Bin Dong, Jikai Hou, Yiping Lu, and Zhihua Zhang, *Distillation  $\approx$  early stopping? harvesting dark knowledge utilizing anisotropic information retrieval for overparameterized neural network*, arXiv preprint arXiv:1910.01255 (2019).
- [DHS11] John Duchi, Elad Hazan, and Yoram Singer, *Adaptive subgradient methods for online learning and stochastic optimization*, Journal of machine learning research **12** (2011), no. Jul, 2121–2159.
- [DKT19] Zeyu Deng, Abba Kammoun, and Christos Thrampoulidis, *A model of double descent for high-dimensional binary linear classification*, arXiv preprint arXiv:1911.05822 (2019).
- [DPCB13] Guillaume Desjardins, Razvan Pascanu, Aaron Courville, and Yoshua Bengio, *Metric-free natural gradient for joint-training of boltzmann machines*, arXiv preprint arXiv:1301.3545 (2013).
- [dRBK20] Stéphane d’Ascoli, Maria Refinetti, Giulio Biroli, and Florent Krzakala, *Double trouble in double descent: Bias and variance (s) in the lazy regime*, arXiv preprint arXiv:2003.01054 (2020).
- [DW<sup>+</sup>18] Edgar Dobriban, Stefan Wager, et al., *High-dimensional asymptotics of prediction: Ridge regression and classification*, The Annals of Statistics **46** (2018), no. 1, 247–279.
- [GBLJ19] Gauthier Gidel, Francis Bach, and Simon Lacoste-Julien, *Implicit regularization of discrete gradient dynamics in deep linear neural networks*, arXiv preprint arXiv:1904.13262 (2019).
- [GLSS18a] Suriya Gunasekar, Jason Lee, Daniel Soudry, and Nathan Srebro, *Characterizing implicit bias in terms of optimization geometry*, arXiv preprint arXiv:1802.08246 (2018).
- [GLSS18b] Suriya Gunasekar, Jason D Lee, Daniel Soudry, and Nati Srebro, *Implicit bias of gradient descent on linear convolutional networks*, Advances in Neural Information Processing Systems, 2018, pp. 9461–9471.
- [GM16] Roger Grosse and James Martens, *A kronecker-factored approximate fisher matrix for convolution layers*, International Conference on Machine Learning, 2016, pp. 573–582.
- [GWB<sup>+</sup>17] Suriya Gunasekar, Blake E Woodworth, Srinadh Bhojanapalli, Behnam Neyshabur, and Nati Srebro, *Implicit regularization in matrix factorization*, Advances in Neural Information Processing Systems, 2017, pp. 6151–6159.
- [HMRT19] Trevor Hastie, Andrea Montanari, Saharon Rosset, and Ryan J Tibshirani, *Surprises in high-dimensional ridgeless least squares interpolation*, arXiv preprint arXiv:1903.08560 (2019).
- [HVD15] Geoffrey Hinton, Oriol Vinyals, and Jeff Dean, *Distilling the knowledge in a neural network*, arXiv preprint arXiv:1503.02531 (2015).
- [HZRS16] Kaiming He, Xiangyu Zhang, Shaoqing Ren, and Jian Sun, *Deep residual learning for image recognition*, Proceedings of the IEEE conference on computer vision and pattern recognition, 2016, pp. 770–778.
- [JGH18] Arthur Jacot, Franck Gabriel, and Clément Hongler, *Neural tangent kernel: Convergence and generalization in neural networks*, Advances in neural information processing systems, 2018, pp. 8571–8580.
- [JT18] Ziwei Ji and Matus Telgarsky, *Gradient descent aligns the layers of deep linear networks*, arXiv preprint arXiv:1810.02032 (2018).

- [JT19] ———, *The implicit bias of gradient descent on nonseparable data*, Conference on Learning Theory, 2019, pp. 1772–1798.
- [KAA18] Ryo Karakida, Shotaro Akaho, and Shun-ichi Amari, *Universal statistics of fisher information in deep neural networks: Mean field approach*, arXiv preprint arXiv:1806.01316 (2018).
- [KAA19] ———, *The normalization method for alleviating pathological sharpness in wide neural networks*, Advances in Neural Information Processing Systems, 2019, pp. 6403–6413.
- [Kar13] Noureddine El Karoui, *Asymptotic behavior of unregularized and ridge-regularized high-dimensional robust regression estimators: rigorous results*, arXiv preprint arXiv:1311.2445 (2013).
- [KB14] Diederik P Kingma and Jimmy Ba, *Adam: A method for stochastic optimization*, arXiv preprint arXiv:1412.6980 (2014).
- [KBH19] Frederik Kunstner, Lukas Balles, and Philipp Hennig, *Limitations of the empirical fisher approximation*, arXiv preprint arXiv:1905.12558 (2019).
- [KH<sup>+</sup>09] Alex Krizhevsky, Geoffrey Hinton, et al., *Learning multiple layers of features from tiny images*.
- [KMN<sup>+</sup>16] Nitish Shirish Keskar, Dheevatsa Mudigere, Jorge Nocedal, Mikhail Smelyanskiy, and Ping Tak Peter Tang, *On large-batch training for deep learning: Generalization gap and sharp minima*, arXiv preprint arXiv:1609.04836 (2016).
- [KS17] Nitish Shirish Keskar and Richard Socher, *Improving generalization performance by switching from adam to sgd*, arXiv preprint arXiv:1712.07628 (2017).
- [LBOM12] Yann A LeCun, Léon Bottou, Genevieve B Orr, and Klaus-Robert Müller, *Efficient backprop*, Neural networks: Tricks of the trade, Springer, 2012, pp. 9–48.
- [LC18] Zhenyu Liao and Romain Couillet, *The dynamics of learning: a random matrix approach*, arXiv preprint arXiv:1805.11917 (2018).
- [LD19] Daniel Levy and John C Duchi, *Necessary and sufficient geometries for gradient methods*, Advances in Neural Information Processing Systems, 2019, pp. 11491–11501.
- [LL19] Kaifeng Lyu and Jian Li, *Gradient descent maximizes the margin of homogeneous neural networks*, arXiv preprint arXiv:1906.05890 (2019).
- [LMZ17] Yuanzhi Li, Tengyu Ma, and Hongyang Zhang, *Algorithmic regularization in over-parameterized matrix sensing and neural networks with quadratic activations*, arXiv preprint arXiv:1712.09203 (2017).
- [LP11] Olivier Ledoit and Sandrine Piché, *Eigenvectors of some large sample covariance matrix ensembles*, Probability Theory and Related Fields **151** (2011), no. 1-2, 233–264.
- [LR17] Junhong Lin and Lorenzo Rosasco, *Optimal rates for multi-pass stochastic gradient methods*, The Journal of Machine Learning Research **18** (2017), no. 1, 3375–3421.
- [LR18] Tengyuan Liang and Alexander Rakhlin, *Just interpolate: Kernel” ridgeless” regression can generalize*, arXiv preprint arXiv:1808.00387 (2018).
- [LSO19] Mingchen Li, Mahdi Soltanolkotabi, and Samet Oymak, *Gradient descent with early stopping is provably robust to label noise for overparameterized neural networks*, arXiv preprint arXiv:1903.11680 (2019).
- [Mar10] James Martens, *Deep learning via hessian-free optimization.*, ICML, vol. 27, 2010, pp. 735–742.
- [Mar14] ———, *New insights and perspectives on the natural gradient method*, arXiv preprint arXiv:1412.1193 (2014).

- [MCO16] Gaétan Marceau-Caron and Yann Ollivier, *Practical riemannian neural networks*, arXiv preprint arXiv:1602.08007 (2016).
- [MG15] James Martens and Roger Grosse, *Optimizing neural networks with kronecker-factored approximate curvature*, International conference on machine learning, 2015, pp. 2408–2417.
- [Min17] Stanislav Minsker, *On some extensions of Bernstein’s inequality for self-adjoint operators*, Statistics & Probability Letters **127** (2017), 111–119.
- [MM19] Song Mei and Andrea Montanari, *The generalization error of random features regression: Precise asymptotics and double descent curve*, arXiv preprint arXiv:1908.05355 (2019).
- [MNS<sup>+</sup>20] Vidya Muthukumar, Adhyayan Narang, Vignesh Subramanian, Mikhail Belkin, Daniel Hsu, and Anant Sahai, *Classification vs regression in overparameterized regimes: Does the loss function matter?*, arXiv preprint arXiv:2005.08054 (2020).
- [MRSY19] Andrea Montanari, Feng Ruan, Youngtak Sohn, and Jun Yan, *The generalization error of max-margin linear classifiers: High-dimensional asymptotics in the overparametrized regime*, arXiv preprint arXiv:1911.01544 (2019).
- [MS12] James Martens and Ilya Sutskever, *Training deep and recurrent networks with hessian-free optimization*, Neural networks: Tricks of the trade, Springer, 2012, pp. 479–535.
- [NH10] Vinod Nair and Geoffrey E Hinton, *Rectified linear units improve restricted boltzmann machines*, Proceedings of the 27th international conference on machine learning (ICML-10), 2010, pp. 807–814.
- [NKB<sup>+</sup>19] Preetum Nakkiran, Gal Kaplun, Yamini Bansal, Tristan Yang, Boaz Barak, and Ilya Sutskever, *Deep double descent: Where bigger models and more data hurt*, arXiv preprint arXiv:1912.02292 (2019).
- [NW06] Jorge Nocedal and Stephen Wright, *Numerical optimization*, Springer Science & Business Media, 2006.
- [Oll15] Yann Ollivier, *Riemannian metrics for neural networks i: feedforward networks*, Information and Inference: A Journal of the IMA **4** (2015), no. 2, 108–153.
- [PB13] Razvan Pascanu and Yoshua Bengio, *Revisiting natural gradient for deep networks*, arXiv preprint arXiv:1301.3584 (2013).
- [PVRB18] Loucas Pillaud-Vivien, Alessandro Rudi, and Francis Bach, *Statistical optimality of stochastic gradient descent on hard learning problems through multiple passes*, Advances in Neural Information Processing Systems, 2018, pp. 8114–8124.
- [QQ19] Qian Qian and Xiaoyuan Qian, *The implicit bias of adagrad on separable data*, Advances in Neural Information Processing Systems, 2019, pp. 7759–7767.
- [RC20] Noam Razin and Nadav Cohen, *Implicit regularization in deep learning may not be explainable by norms*, arXiv preprint arXiv:2005.06398 (2020).
- [RM11] Francisco Rubio and Xavier Mestre, *Spectral convergence for a general class of random matrices*, Statistics & probability letters **81** (2011), no. 5, 592–602.
- [RR17] Alessandro Rudi and Lorenzo Rosasco, *Generalization properties of learning with random features*, Advances in Neural Information Processing Systems, 2017, pp. 3215–3225.
- [RWC<sup>+</sup>] Alec Radford, Jeffrey Wu, Rewon Child, David Luan, Dario Amodei, and Ilya Sutskever, *Language models are unsupervised multitask learners*.

- [SHN<sup>+</sup>18] Daniel Soudry, Elad Hoffer, Mor Shpigel Nacson, Suriya Gunasekar, and Nathan Srebro, *The implicit bias of gradient descent on separable data*, The Journal of Machine Learning Research **19** (2018), no. 1, 2822–2878.
- [SMG13] Andrew M Saxe, James L McClelland, and Surya Ganguli, *Exact solutions to the nonlinear dynamics of learning in deep linear neural networks*, arXiv preprint arXiv:1312.6120 (2013).
- [SPR18] Arun Suggala, Adarsh Prasad, and Pradeep K Ravikumar, *Connecting optimization and regularization paths*, Advances in Neural Information Processing Systems, 2018, pp. 10608–10619.
- [SY19] Lili Su and Pengkun Yang, *On learning over-parameterized neural networks: A functional approximation perspective*, Advances in Neural Information Processing Systems, 2019, pp. 2637–2646.
- [TPT20] Hossein Taheri, Ramtin Pedarsani, and Christos Thrampoulidis, *Sharp asymptotics and optimal performance for inference in binary models*, arXiv preprint arXiv:2002.07284 (2020).
- [WGL<sup>+</sup>20] Blake Woodworth, Suriya Gunasekar, Jason D Lee, Edward Moroshko, Pedro Savarese, Itay Golan, Daniel Soudry, and Nathan Srebro, *Kernel and rich regimes in overparametrized models*, arXiv preprint arXiv:2002.09277 (2020).
- [WLLM18] Colin Wei, Jason D Lee, Qiang Liu, and Tengyu Ma, *On the margin theory of feedforward neural networks*, arXiv preprint arXiv:1810.05369 (2018).
- [WMW18] Lei Wu, Chao Ma, and E Weinan, *How sgd selects the global minima in over-parameterized learning: A dynamical stability perspective*, Advances in Neural Information Processing Systems, 2018, pp. 8279–8288.
- [WRS<sup>+</sup>17] Ashia C Wilson, Rebecca Roelofs, Mitchell Stern, Nati Srebro, and Benjamin Recht, *The marginal value of adaptive gradient methods in machine learning*, Advances in Neural Information Processing Systems, 2017, pp. 4148–4158.
- [WTS<sup>+</sup>19] Francis Williams, Matthew Trager, Claudio Silva, Daniele Panozzo, Denis Zorin, and Joan Bruna, *Gradient dynamics of shallow univariate relu networks*, arXiv preprint arXiv:1906.07842 (2019).
- [WX20] Denny Wu and Ji Xu, *On the optimal weighted  $\ell_2$  regularization in overparameterized linear regression*, arXiv preprint arXiv:2006.05800 (2020).
- [XH19] Ji Xu and Daniel Hsu, *How many variables should be entered in a principal component regression equation?*, arXiv preprint arXiv:1906.01139 (2019).
- [XLS16] Bo Xie, Yingyu Liang, and Le Song, *Diverse neural network learns true target functions*, arXiv preprint arXiv:1611.03131 (2016).
- [XRM20] Peng Xu, Fred Roosta, and Michael W Mahoney, *Second-order optimization for non-convex machine learning: An empirical study*, Proceedings of the 2020 SIAM International Conference on Data Mining, SIAM, 2020, pp. 199–207.
- [ZBH<sup>+</sup>16] Chiyuan Zhang, Samy Bengio, Moritz Hardt, Benjamin Recht, and Oriol Vinyals, *Understanding deep learning requires rethinking generalization*, arXiv preprint arXiv:1611.03530 (2016).
- [ZLN<sup>+</sup>19] Guodong Zhang, Lala Li, Zachary Nado, James Martens, Sushant Sachdeva, George Dahl, Chris Shallue, and Roger B Grosse, *Which algorithmic choices matter at which batch sizes? insights from a noisy quadratic model*, Advances in Neural Information Processing Systems, 2019, pp. 8194–8205.
- [ZMG19] Guodong Zhang, James Martens, and Roger B Grosse, *Fast convergence of natural gradient descent for over-parameterized neural networks*, Advances in Neural Information Processing Systems, 2019, pp. 8080–8091.
- [ZWXG18] Guodong Zhang, Chaoqi Wang, Bowen Xu, and Roger Grosse, *Three mechanisms of weight decay regularization*, arXiv preprint arXiv:1810.12281 (2018).

# A Discussions of Additional Results

## A.1 Implicit Bias of GD vs. NGD

It is known that gradient descent is the steepest descent with respect to the  $\ell_2$  norm, i.e., the update direction is constructed to decrease the loss under small changes in the parameters measured by the  $\ell_2$  norm [GLSS18a]. Following this analogy, NGD is the steepest descent in which changes are measured by the KL divergence on the predictive distributions [Mar14]; this can be interpreted as a proximal update which penalizes how much the predictions change on the data distribution.

Intuitively, the above discussion suggests GD tend to find solution that is close to the initialization in the Euclidean distance between parameters, whereas NGD prefers solution close to the initialization in terms of the function values. This observation turns out to be exact in the case of ridgeless interpolant under the squared loss, as remarked in Section 3. Moreover, Figure 8 confirms the same trend in neural network optimization. In particular, we observe that

- GD results in small changes in the parameters, whereas NGD results in small changes in the function.
- preconditioning with the pseudo-inverse of the sample Fisher, i.e.,  $\mathbf{P} = (\mathbf{J}^\top \mathbf{J})^\dagger$ , leads to implicit bias similar to that of GD (also pointed out in [ZMG19]), but not NGD with the population Fisher.
- interpolating between GD and NGD, e.g.,  $\mathbf{P} = \mathbf{F}^{-1/2}$  (green), results in solution with properties in between GD and NGD.

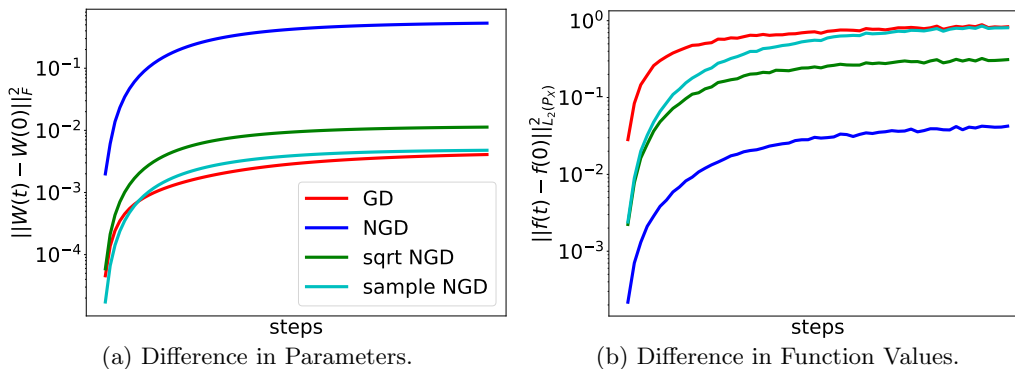


Figure 8: Illustration of the different implicit bias of GD and NGD. We set  $n = 100$ ,  $d = 50$ , and regress a two-layer ReLU network with 50 hidden units towards a teacher model of the same architecture on Gaussian input. The x-axis is rescaled for each optimizer such that the final training error is below  $10^{-3}$ . GD finds solution with small changes in the parameters, whereas NGD finds solution with small changes in the function. Note that the sample Fisher (cyan) has implicit bias similar to GD and does not resemble NGD (population Fisher).

In addition, we also speculate that as we interpolate from GD to NGD, the distance traveled by the parameter space would gradually increase, and distance traveled in the function space would decrease. Figure 9 and 20 demonstrate that this is indeed the case for linear model as well as neural network.

We remark that this observation also implies that wide neural networks trained with NGD (population Fisher) is less likely to stay in the kernel regime, since the distance traveled from initialization can be large (see Figure 8(a)) and thus the Taylor expansion around the initialization is no longer an accurate description of the training dynamics. In other words, the analogy between wide neural net and its linearized kernel model (which we partially employed in Section 5) may not be valid in models trained with NGD<sup>7</sup>.

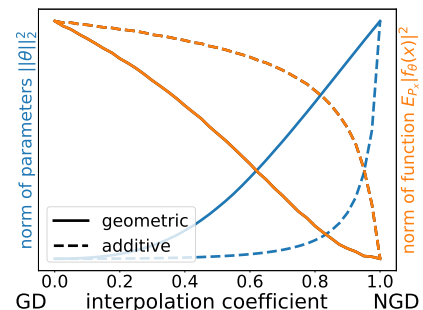


Figure 9: Euclidean and  $\|\cdot\|_\Sigma$  norm (log scale) under additive and geometric interpolation in ridgeless regression.

<sup>7</sup>Note that this gap is only present when the population Fisher is used; previous works have shown the NTK-type global convergence for sample Fisher-related preconditioned update [ZMG19, CGH<sup>+</sup>19].

## A.2 Non-monotonicity of the Bias Term

As mentioned earlier, many previous works on the high-dimensional characterization of linear regression assumed a random effects model with an isotropic prior on the true parameters [DW<sup>+</sup>18, HMRT19, XH19], which may not be realistic. As an example of the limitation of this assumption, we note that when  $\Sigma_{\theta} = \mathbf{I}_d$ , it can be shown that the expected bias  $B(\hat{\theta}(t))$  monotonically decreases through time (see proof of Proposition 6 for details). In contrast, when the target parameters do not follow an isotropic prior, the bias term can exhibit non-monotonicity, which gives rise to the “epoch-wise double descent” phenomenon also observed in deep learning [NKB<sup>+</sup>19].

We empirically demonstrate this non-monotonicity when the model is close to the interpolation threshold in Figure 10. We set  $\mathbf{D}_{\mathbf{X}}$  to be two equally-weighted point masses with  $\kappa_{\mathbf{X}} = 32$ ,  $\Sigma_{\theta} = \Sigma_{\mathbf{X}}^{-1}$  and  $\gamma = 16/15$ . Note that the GD trajectory (red) exhibits non-monotonicity in the bias term, whereas for NGD the bias is monotonically decreasing through time (which we show in the proof of Proposition 6). We remark that this mechanism of epoch-wise double descent may not be related to the empirical findings in deep neural networks (the robustness of which is also largely unknown), in which it is usually speculated that the variance term exhibits non-monotonicity.

## A.3 Interpretation of $\sqrt{\mathbf{y}^{\top} \mathbf{K}^{-1} \mathbf{y} / n}$

The quantity which we empirically evaluated in Section 5 was first proposed as a measure of generalization for wide neural networks in the kernel regime. This quantity can be interpreted as a proxy for measuring how much signal and noise are distributed along the eigendirections of the NTK (see [LSO19, DHLZ19, SY19, CFW<sup>+</sup>19] for detailed discussion). Intuitively speaking, large  $\sqrt{\mathbf{y}^{\top} \mathbf{K}^{-1} \mathbf{y} / n}$  implies that the problem is difficult to learn by GD, and vice versa.

Here we give a heuristic argument on how this quantity relates to label noise and misspecification in our setup. For the ridgeless regression model considered in Section 3, if we write the label as  $y_i = f^*(\mathbf{x}_i) + f^c(\mathbf{x}_i) + \varepsilon_i$ , where  $f^*(\mathbf{x}) = \mathbf{x}^{\top} \theta^*$ ,  $f^c$  is the misspecified component that is independent to  $f^*$ , and  $\varepsilon_i$  is the label noise, we have the following heuristic calculation:

$$\begin{aligned} & \mathbb{E}[\mathbf{y}^{\top} \mathbf{K}^{-1} \mathbf{y}] \\ &= \mathbb{E}\left[(f^*(\mathbf{X}) + f^c(\mathbf{X}) + \varepsilon)^{\top} (\mathbf{X} \mathbf{X}^{\top})^{-1} (f^*(\mathbf{X}) + f^c(\mathbf{X}) + \varepsilon)\right] \\ &\stackrel{(i)}{\approx} \text{tr}\left(\theta^* \theta^{*\top} \mathbf{X}^{\top} (\mathbf{X} \mathbf{X}^{\top})^{-1} \mathbf{X}\right) + (\sigma^2 + \sigma_c^2) \text{tr}\left((\mathbf{X} \mathbf{X}^{\top})^{-1}\right), \quad (\text{A.1}) \end{aligned}$$

where we heuristically replaced the misspecified component with i.i.d. noise of the same variance  $\sigma_c^2$  (as argued in Section 3). The first term of (A.1) resembles an RKHS norm of the true coefficients  $\theta^*$ , whereas the second term is small when the data is well-conditioned (i.e. the inverse of  $\mathbf{X} \mathbf{X}^{\top}$  is stable) or when the amount of label noise  $\sigma$  and misspecification  $\sigma_c^2$  is small, as illustrated in Figure 11 (note that these are conditions under which GD generalizes well, as shown in Theorem 1). We also expect this characterization to hold for neural networks close to the kernel regime. This provides a non-rigorous explanation of the increasing trend we observed in Figure 6 as we add more label noise or further misspecify the model.

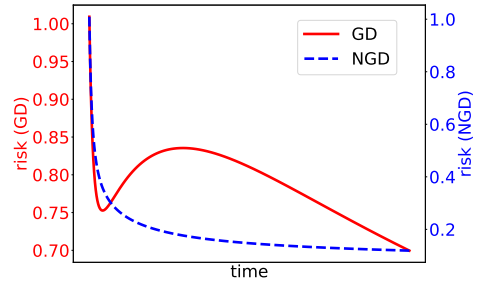


Figure 10: Epoch-wise double descent. Note that non-monotonicity of the bias term is present in GD but not NGD.

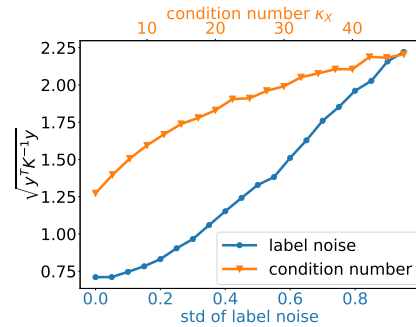


Figure 11: Demonstration of the growth of  $\sqrt{\mathbf{y}^{\top} \mathbf{K}^{-1} \mathbf{y}}$  in linear model as the amount of label noise (orange) or the condition number of  $\Sigma_{\mathbf{X}}$  (blue) increases.

## B Additional Figures

### B.1 Additional Figures for Ridgeless Regression

**Non-monotonicity of the Risk.** Under our generalized (anisotropic) assumption on the covariance of the features and the target coefficients, both the bias and the variance term can exhibit non-monotonicity w.r.t. the overparameterization level  $\gamma > 1$ . For instance, in Figure 12 we observe two peaks in the bias term and three peaks in the variance term.

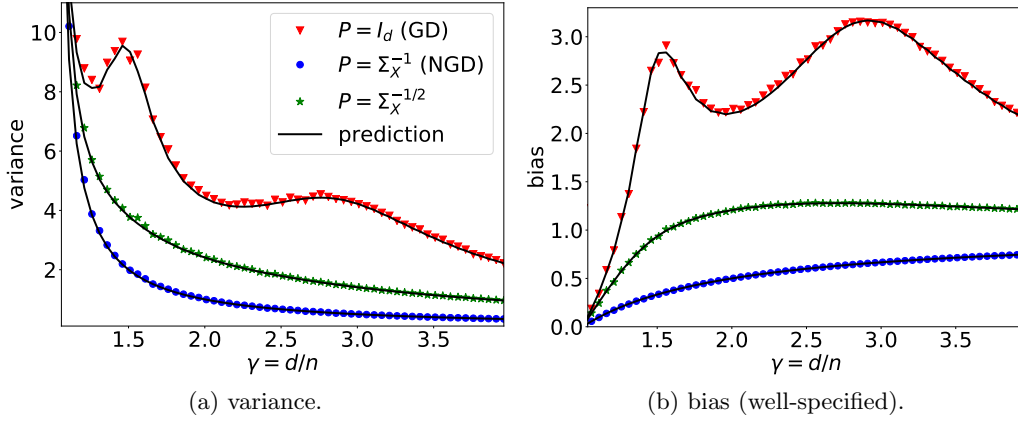


Figure 12: Illustration of the “multiple-descent” curve of the risk for  $\gamma > 1$ . We take  $n = 300$ ,  $\mathbf{D}_X$  as three equally-spaced point masses with  $\kappa_X = 5000$  and  $\|\Sigma_X\|_F^2 = d$ , and  $\mathbf{D}_\theta = \mathbf{D}_X^{-1}$  (misaligned). Note that for GD, both the bias and the variance are highly non-monotonic for  $\gamma > 1$ .

**Early Stopping Risk.** Figure 13 compares the stationary risk with the optimal early stopping risk under varying misalignment level. To increase the extent of misalignment, we set  $\Sigma_\theta = \Sigma_X^{-\alpha}$  and vary  $\alpha$  from 0 to 1: larger  $\alpha$  entails more “misaligned” teacher, and vice versa. Note that as the problem becomes more misaligned, NGD achieves lower stationary and early stopping risk.

Figure 14 reports the optimal early stopping risk under misspecification (exact same trend can be obtained when the x-axis is label noise). In contrast to the stationary risk (Figure 1), GD can be advantageous under early stopping even with large extent of misspecification (if the well-specified bias favors GD). This indicates that early stopping reduces the variance and the misspecified bias.

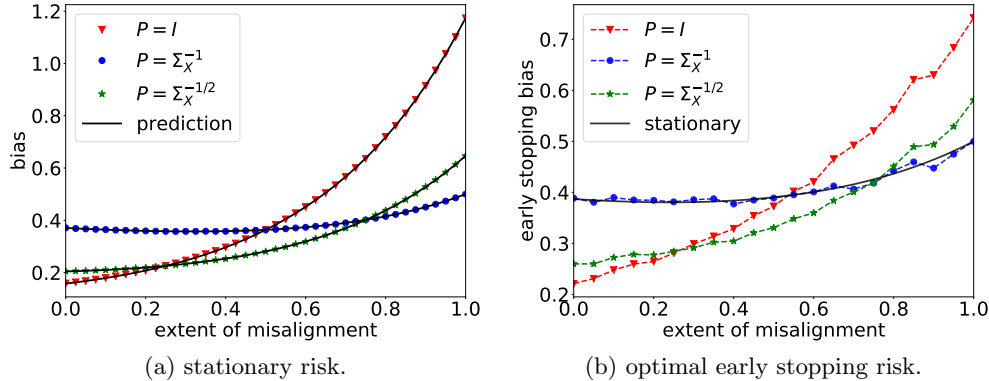


Figure 13: Well-specified bias against different extent of “alignment”. We set  $n = 300$ ,  $\mathbf{D}_X$  as two point masses with  $\kappa_X = 20$  and  $\|\Sigma_X\|_F^2 = d$ , and take  $\Sigma_\theta = \Sigma_X^{-\alpha}$  and vary  $\alpha$  from 0 to 1. (a) GD achieves lower bias when  $\Sigma_\theta$  is isotropic, whereas NGD dominates when  $\Sigma_X = \Sigma_\theta^{-1}$ ;  $P = \Sigma_X^{-1/2}$  (interpolates between GD and NGD) is advantageous in between. (b) optimal early stopping bias follows similar trend as stationary risk (the optimal early stopping bias for NGD is the same as its stationary risk due to the monotonic bias term).

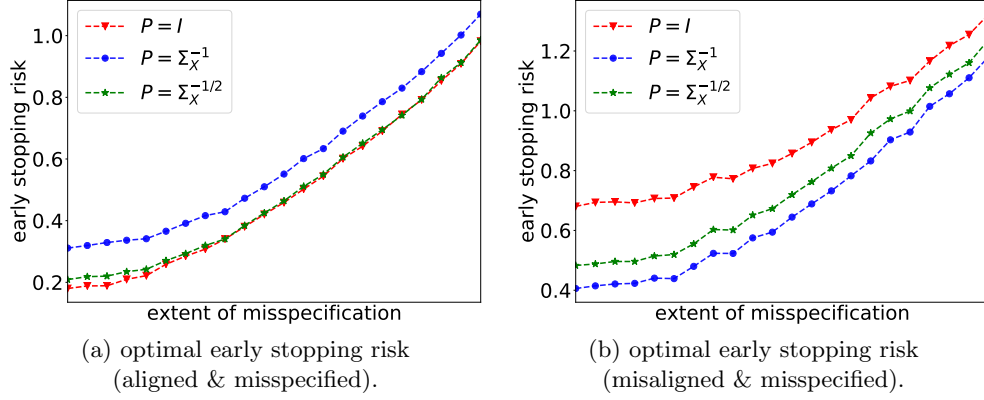


Figure 14: Optimal early stopping risk vs. increasing model misspecification. We follow the same setup as Figure 3(c). (a)  $\Sigma_\theta = I_d$  (favors GD); unlike Figure 3(c), GD has lower early stopping risk even under large extent of misspecification. (b)  $\Sigma_\theta = \Sigma_X^{-1}$  (favors NGD); NGD is also advantageous under early stopping.

**Complementary Figures for Section 3 and 4.** We include additional figures on (a) well-specified bias when  $\Sigma_\theta = I_d$  (GD is optimal); (b) misspecified bias under unobserved features (predicted by Proposition 3); (c) bias-variance tradeoff by interpolating between preconditioners (SNR=5). Note that in all cases the experimental values match the theoretical predictions.

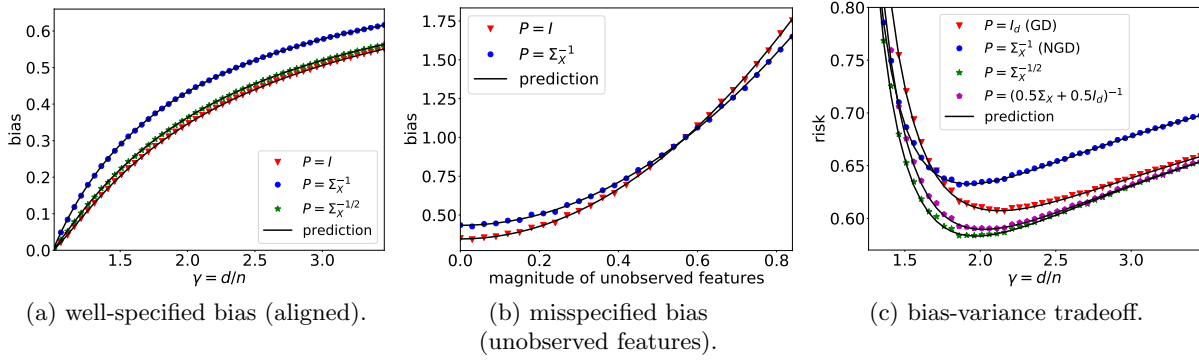


Figure 15: We set  $D_X$  as a uniform distribution with  $\kappa_X = 20$  and  $\|\Sigma_X\|_F^2 = d$ .

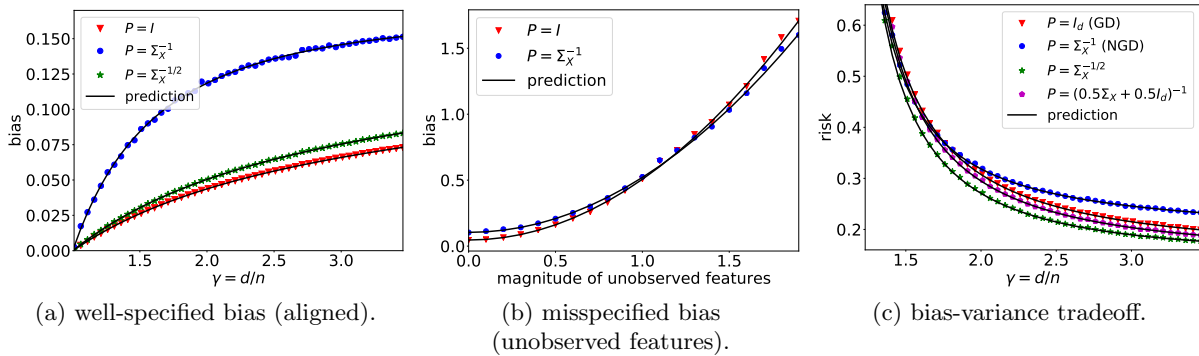


Figure 16: We construct  $D_X$  with a polynomial decay:  $\lambda_i(D_X) = i^{-1}$  and then rescale the eigenvalues such that  $\kappa_X = 500$  and  $\|\Sigma_X\|_F^2 = d$ .

## B.2 Additional Figures for RKHS Regression

We simulate the optimization in the coordinates of RKHS via a finite-dimensional approximation (using extra unlabeled data). In particular, we consider the teacher model in the form of  $f^*(\mathbf{x}) = \sum_{i=1}^N h_i \mu_i^T \phi_i(\mathbf{x})$  for some square summable  $\{h_i\}_{i=1}^N$ , in which  $r$  controls the “difficulty” of the learning problem. We find  $\{\mu_i\}_{i=1}^N$  and  $\{\phi_i\}_{i=1}^N$  by solving the eigenfunction problem for some kernel  $k$ . The student model takes the form of  $f(\mathbf{x}) = \sum_{i=1}^N \frac{a_i}{\sqrt{\mu_i}} \phi_i(\mathbf{x})$  and we optimize the coefficients  $\{a_i\}_{i=1}^N$  via the preconditioned update (4.1). We set  $n = 1000$ ,  $d = 5$ ,  $N = 2500$  and consider the inverse multiquadratic (IMQ) kernel:  $k(\mathbf{x}, \mathbf{y}) = \frac{1}{\sqrt{1 + \|\mathbf{x} - \mathbf{y}\|_2^2}}$ .

Recall that Theorem 7 suggests that for small  $r$ , i.e., “difficult” problem, the damping coefficient  $\lambda$  would need to be small (which makes the update NGD-like), and vice versa. This result is (qualitatively) supported by Figure 17, from which we can see that small  $\lambda$  is beneficial when  $r$  is small, and vice versa. We remark that this observed trend is rather fragile and sensitive to various hyperparameters. We leave a more comprehensive characterization of this observation as future work.

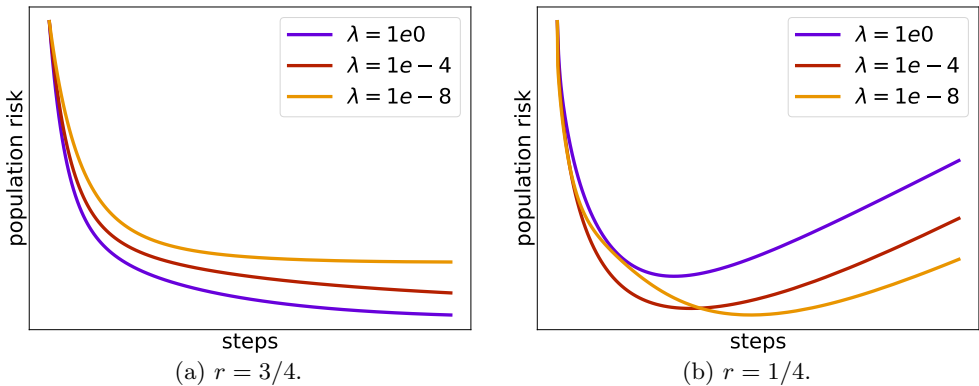


Figure 17: Population risk of the preconditioned update in RKHS that interpolates between GD and NGD. We use the IMQ kernel and set  $n = 1000$ ,  $d = 5$ ,  $N = 2500$ ,  $\sigma^2 = 5 \times 10^{-4}$ . The x-axis has been rescaled for each curve and thus convergence speed is not directly comparable. Note that (a) large  $\lambda$  (i.e., GD-like update) is beneficial when  $r$  is large, and (b) small  $\lambda$  (i.e., NGD-like update) is beneficial when  $r$  is small.

## B.3 Additional Figures for Neural Network Experiments

**Label Noise.** In Figure 18, (a) we observe the same phenomenon that NGD generalizes better as more label noise is added to the training data on CIFAR-10. Figure 18 (b) shows that in all cases with varying amounts of label noise, the early stopping risk is however worse than that of GD, regardless of whether the preconditioner is the (pseudo-)inverse of the Fisher or its sample-based counterpart. This is consistent with the observation in Section 4 and Figure 14(a) that early stopping can potentially favor GD due to the reduced variance.

**Misalignment.** We illustrate the finding in Proposition 6 and Figure 13(b) in neural networks under synthetic data: we consider 50-dimensional Gaussian input, and both the teacher model and the student model are two-layer ReLU networks with 50 hidden units. We construct the teacher by perturbing the initialization of the student, as described in Section 5. Figure 19 shows that as we decrease  $r$ , which we interpret as the problem becoming more “misaligned”<sup>8</sup>, NGD eventually achieves lower early stopping risk (b), whereas GD dominates the early stopping risk is less misaligned setting (a). We remark that this phenomenon is difficult to observe in practical neural networks training on real-world data, which we partially attribute to the fragility of the analogy between neural nets and linear models, especially under NGD (discussed in Appendix A).

<sup>8</sup>We remark that this  $r$  is slightly different than that defined in the RKHS regression experiment.

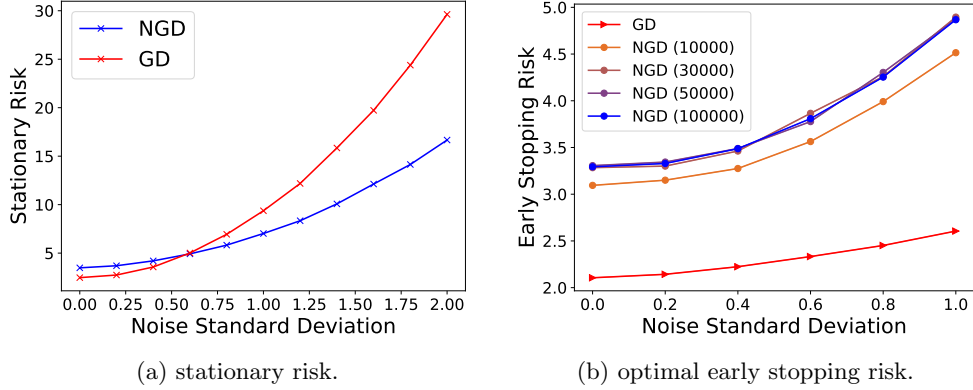


Figure 18: Additional label noise experiment on CIFAR-10.

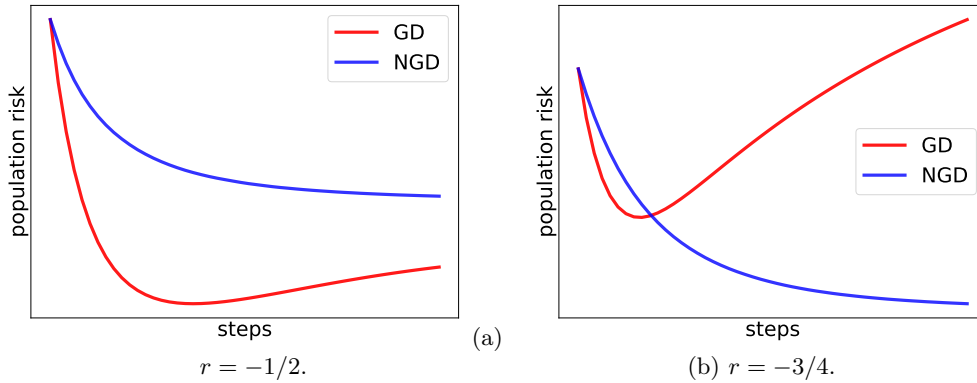


Figure 19: Population risk of two-layer neural networks in the misalignment setup (noiseless) with synthetic Gaussian data. We set  $n = 200$ ,  $d = 50$ , the damping coefficient  $\lambda = 10^{-6}$ , and both the student and the teacher are two-layer ReLU networks with 50 hidden units. The x-axis and the learning rate have been rescaled for each curve. When  $r$  is sufficiently small, NGD achieves lower early stopping risk, and vice versa.

**Implicit Bias of Interpolating Preconditioners.** Figure 20 demonstrates that the implicit bias of preconditioned update that interpolates between GD and NGD. We use the same two-layer MLP setup on MNIST as in Figure 7. Note that updates that are closer to GD result in smaller change in the parameters, whereas ones close to NGD lead to smaller change in the function.

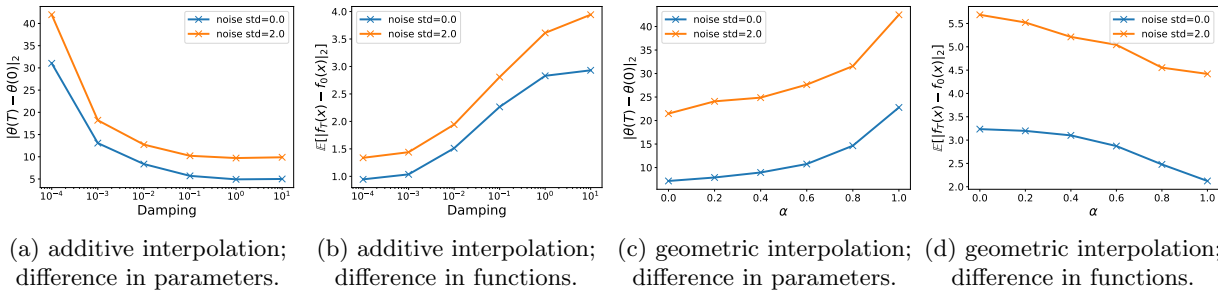


Figure 20: Illustration of the implicit bias of preconditioned gradient descent that interpolates between GD and NGD on MNIST. Note that as the update becomes more similar to NGD (smaller damping or larger  $\alpha$ ), the distance traveled in the parameter space increases, whereas the distance traveled on the output space decreases.

## C Proofs and Derivations

### C.1 Missing Derivations in Section 3

**Gradient Flow of Preconditioned Updates.** Given positive definite  $\mathbf{P}$  and  $\gamma > 1$ , it is clear that the gradient flow solution at time  $t$  can be written as

$$\boldsymbol{\theta}_{\mathbf{P}}(t) = \mathbf{P}\mathbf{X}^\top \left[ \mathbf{I}_n - \exp\left(-\frac{t}{n}\mathbf{X}\mathbf{P}\mathbf{X}^\top\right) \right] (\mathbf{X}\mathbf{P}\mathbf{X}^\top)^{-1}\mathbf{y}.$$

Taking  $t \rightarrow \infty$  yields the stationary solution  $\hat{\boldsymbol{\theta}}_{\mathbf{P}} = \mathbf{P}\mathbf{X}^\top(\mathbf{X}\mathbf{P}\mathbf{X}^\top)^{-1}\mathbf{y}$ . We remark that the damped inverse of the sample Fisher  $\mathbf{P} = (\mathbf{X}\mathbf{X}^\top + \lambda\mathbf{I}_d)^{-1}$  leads to the same minimum-norm solution as GD  $\hat{\boldsymbol{\theta}}_{\mathbf{I}} = \mathbf{X}^\top(\mathbf{X}\mathbf{X}^\top)^{-1}\mathbf{y}$  since  $\mathbf{P}\mathbf{X}^\top$  and  $\mathbf{X}$  share the same eigenvectors. On the other hand, when  $\mathbf{P}$  is the pseudo-inverse of the sample Fisher  $(\mathbf{X}\mathbf{X}^\top)^\dagger$  which is not full-rank, the trajectory can be obtained via the variation of constants formula:

$$\boldsymbol{\theta}(t) = \left[ \frac{t}{n} \sum_{k=0}^{\infty} \frac{1}{(k+1)!} \left( -\frac{t}{n} \mathbf{X}^\top (\mathbf{X}\mathbf{X}^\top)^{-1} \mathbf{X} \right)^k \right] \mathbf{X}^\top (\mathbf{X}\mathbf{X}^\top)^{-1} \mathbf{y},$$

for which taking the large  $t$  limit also yields the minimum-norm solution  $\mathbf{X}^\top(\mathbf{X}\mathbf{X}^\top)^{-1}\mathbf{y}$ .

**Minimum  $\|\boldsymbol{\theta}\|_{\mathbf{P}^{-1}}$  Norm Interpolant.** For positive definite  $\mathbf{P}$  and the corresponding stationary solution  $\hat{\boldsymbol{\theta}}_{\mathbf{P}} = \mathbf{P}\mathbf{X}^\top(\mathbf{X}\mathbf{P}\mathbf{X}^\top)^{-1}\mathbf{y}$ , note that given any other interpolant  $\hat{\boldsymbol{\theta}}'$ , we have  $(\hat{\boldsymbol{\theta}}_{\mathbf{P}} - \hat{\boldsymbol{\theta}}')\mathbf{P}^{-1}\hat{\boldsymbol{\theta}}_{\mathbf{P}} = 0$  because both  $\hat{\boldsymbol{\theta}}_{\mathbf{P}}$  and  $\hat{\boldsymbol{\theta}}'$  achieves zero empirical risk. Therefore,  $\|\hat{\boldsymbol{\theta}}'\|_{\mathbf{P}^{-1}}^2 - \|\hat{\boldsymbol{\theta}}_{\mathbf{P}}\|_{\mathbf{P}^{-1}}^2 = \|\hat{\boldsymbol{\theta}}' - \hat{\boldsymbol{\theta}}_{\mathbf{P}}\|_{\mathbf{P}^{-1}}^2 \geq 0$ . This confirms that  $\hat{\boldsymbol{\theta}}_{\mathbf{P}}$  is the minimum  $\|\boldsymbol{\theta}\|_{\mathbf{P}^{-1}}$  norm solution.

### C.2 Proof of Theorem 1

**Proof.** By the definition of the variance term and the stationary  $\hat{\boldsymbol{\theta}}$ ,

$$V(\hat{\boldsymbol{\theta}}) = \text{tr}\left(\text{Cov}(\hat{\boldsymbol{\theta}})\boldsymbol{\Sigma}_{\mathbf{X}}\right) = \sigma^2 \text{tr}\left(\mathbf{P}\mathbf{X}^\top(\mathbf{X}\mathbf{P}\mathbf{X}^\top)^{-2}\mathbf{X}^\top\mathbf{P}\boldsymbol{\Sigma}_{\mathbf{X}}\right).$$

Write  $\bar{\mathbf{X}} = \mathbf{X}\mathbf{P}^{1/2}$  with covariance  $\mathbf{D}_{\mathbf{X}\mathbf{P}} = \mathbf{D}_{\mathbf{X}}\mathbf{D}_{\mathbf{P}}$ . Similarly, we define  $\boldsymbol{\Sigma}_{\mathbf{X}\mathbf{P}} = \boldsymbol{\Sigma}_{\mathbf{X}}\boldsymbol{\Sigma}_{\mathbf{P}}$ . The equation above thus simplifies to

$$V(\hat{\boldsymbol{\theta}}_{\mathbf{P}}) = \sigma^2 \text{tr}\left(\bar{\mathbf{X}}^\top(\bar{\mathbf{X}}\bar{\mathbf{X}}^\top)^{-2}\bar{\mathbf{X}}^\top\boldsymbol{\Sigma}_{\mathbf{X}\mathbf{P}}\right).$$

The analytic expression of the variance term follows from a direct application of [HMRT19, Theorem 4], in which the conditions on the population covariance are satisfied by (A2).

Taking the derivative of  $m(-\lambda)$  yields

$$m'(-\lambda) = \left( \frac{1}{m^2(-\lambda)} - \gamma \int \frac{\tau^2}{(1 + \tau m(-\lambda))^2} dF_{\mathbf{X}\mathbf{P}}(\tau) \right)^{-1}.$$

Plugging the quantity into the expression of the variance (omitting the scaling  $\sigma^2$  and constant shift),

$$\frac{m'(-\lambda)}{m^2(-\lambda)} = \left( 1 - \gamma m^2(-\lambda) \int \frac{\tau^2}{(1 + \tau m(-\lambda))^2} dF_{\mathbf{X}\mathbf{P}}(\tau) \right)^{-1}.$$

From the monotonicity of  $\frac{x}{1+x}$  on  $x > 0$  or the Jensen's inequality we know that

$$1 - \gamma \int \left( \frac{\tau m(-\lambda)}{1 + \tau m(-\lambda)} \right)^2 dF_{\mathbf{X}\mathbf{P}}(\tau) \leq 1 - \gamma \left( \int \frac{\tau m(-\lambda)}{1 + \tau m(-\lambda)} dF_{\mathbf{X}\mathbf{P}}(\tau) \right)^2.$$

Taking  $\lambda \rightarrow 0$ , the RHS evaluates to  $1 - 1/\gamma$ , and thus omitting the scalar  $\sigma^2$ , we arrive at the lower bound  $V \geq (\gamma - 1)^{-1}$ . Note that the equality is only achieved when  $F_{\mathbf{X}\mathbf{P}}$  is a point mass, i.e.  $\mathbf{P} = \Sigma_{\mathbf{X}}^{-1}$ . In other words, the minimum variance is achieved by NGD. As a verification, the variance of the NGD solution  $\hat{\boldsymbol{\theta}}_{\mathbf{P}^{-1}}$  agrees with the calculation in [HMRT19, A.3].  $\square$

### C.3 Proof of Theorem 2

**Proof.** By the definition of the bias term,

$$\begin{aligned}
B(\hat{\boldsymbol{\theta}}_{\mathbf{P}}) &= \mathbb{E}_{\boldsymbol{\theta}^*} \left[ \left\| \mathbf{P}\mathbf{X}^\top (\mathbf{X}\mathbf{P}\mathbf{X}^\top)^{-1} \mathbf{X}\boldsymbol{\theta}_* - \boldsymbol{\theta}^* \right\|_{\Sigma_{\mathbf{X}}}^2 \right] \\
&= \frac{1}{d} \text{tr} \left( \Sigma_{\boldsymbol{\theta}} \left( \mathbf{I}_d - \mathbf{P}\mathbf{X}^\top (\mathbf{X}\mathbf{P}\mathbf{X}^\top)^{-1} \mathbf{X} \right)^\top \Sigma_{\mathbf{X}} \left( \mathbf{I}_d - \mathbf{P}\mathbf{X}^\top (\mathbf{X}\mathbf{P}\mathbf{X}^\top)^{-1} \mathbf{X} \right) \right) \\
&\stackrel{(i)}{=} \frac{1}{d} \text{tr} \left( \Sigma_{\boldsymbol{\theta}/\mathbf{P}} \left( \mathbf{I}_d - \bar{\mathbf{X}}^\top (\bar{\mathbf{X}}\bar{\mathbf{X}}^\top)^{-1} \bar{\mathbf{X}} \right)^\top \Sigma_{\mathbf{X}\mathbf{P}} \left( \mathbf{I}_d - \bar{\mathbf{X}}^\top (\bar{\mathbf{X}}\bar{\mathbf{X}}^\top)^{-1} \bar{\mathbf{X}} \right) \right) \\
&\stackrel{(ii)}{=} \lim_{\lambda \rightarrow 0_+} \frac{\lambda^2}{d} \text{tr} \left( \Sigma_{\boldsymbol{\theta}/\mathbf{P}} \left( \frac{1}{n} \bar{\mathbf{X}}^\top \bar{\mathbf{X}} + \lambda \mathbf{I}_d \right)^{-1} \Sigma_{\mathbf{X}\mathbf{P}} \left( \frac{1}{n} \bar{\mathbf{X}}^\top \bar{\mathbf{X}} + \lambda \mathbf{I}_d \right)^{-1} \right) \\
&\stackrel{(iii)}{=} \lim_{\lambda \rightarrow 0_+} \frac{\lambda^2}{d} \text{tr} \left( \left( \frac{1}{n} \hat{\mathbf{X}}^\top \hat{\mathbf{X}} + \lambda \mathbf{D}_{\boldsymbol{\theta}/\mathbf{P}}^{-1} \right)^{-2} \Sigma_{\mathbf{X}\mathbf{P}} \Sigma_{\boldsymbol{\theta}/\mathbf{P}}^{-1} \right),
\end{aligned}$$

where we utilized (A3) and defined  $\bar{\mathbf{X}} = \mathbf{X}\mathbf{P}^{1/2}$ ,  $\Sigma_{\mathbf{X}\mathbf{P}} = \Sigma_{\mathbf{X}}\mathbf{P}$ ,  $\Sigma_{\boldsymbol{\theta}/\mathbf{P}} = \Sigma_{\boldsymbol{\theta}}\mathbf{P}^{-1}$  in (i), applied the equality  $(\mathbf{A}\mathbf{A}^\top)^\dagger \mathbf{A} = \lim_{\lambda \rightarrow 0} (\mathbf{A}^\top \mathbf{A} + \lambda \mathbf{I})^{-1} \mathbf{A}$  in (ii), and defined  $\hat{\mathbf{X}} = \mathbf{X}\Sigma^{-1/2}\mathbf{P}$  with covariance  $\mathbf{D}_{\mathbf{X}\mathbf{P}}\mathbf{D}_{\boldsymbol{\theta}/\mathbf{P}}^{-1}$  in (iii) (note that  $\mathbf{D}_{\boldsymbol{\theta}/\mathbf{P}}$  is invertible by (A2-4)). To proceed, we first observe the following relation via a leave-one-out argument similar to that in [XH19],

$$\begin{aligned}
&\frac{1}{d} \text{tr} \left( \frac{1}{n} \hat{\mathbf{X}}^\top \hat{\mathbf{X}} \left( \frac{1}{n} \hat{\mathbf{X}}^\top \hat{\mathbf{X}} + \lambda \mathbf{D}_{\boldsymbol{\theta}/\mathbf{P}}^{-1} \right)^{-2} \right) \tag{C.1} \\
&\stackrel{(i)}{=} \frac{1}{d} \sum_{i=1}^n \frac{\frac{1}{n} \hat{\mathbf{x}}_i^\top \left( \frac{1}{n} \hat{\mathbf{X}}^\top \hat{\mathbf{X}} + \lambda \mathbf{D}_{\boldsymbol{\theta}/\mathbf{P}}^{-1} \right)^{-2}_{-i} \hat{\mathbf{x}}_i}{\left( 1 + \frac{1}{n} \hat{\mathbf{x}}_i^\top \left( \frac{1}{n} \hat{\mathbf{X}}^\top \hat{\mathbf{X}} + \lambda \mathbf{D}_{\boldsymbol{\theta}/\mathbf{P}}^{-1} \right)^{-1}_{-i} \hat{\mathbf{x}}_i \right)^2} \\
&\stackrel{(ii)}{\xrightarrow{p}} \frac{\frac{1}{d} \text{tr} \left( \left( \frac{1}{n} \hat{\mathbf{X}}^\top \hat{\mathbf{X}} + \lambda \mathbf{D}_{\boldsymbol{\theta}/\mathbf{P}}^{-1} \right)^{-2} \Sigma_{\mathbf{X}\mathbf{P}} \Sigma_{\boldsymbol{\theta}/\mathbf{P}}^{-1} \right)}{\left( 1 + \frac{1}{n} \text{tr} \left( \left( \frac{1}{n} \bar{\mathbf{X}}^\top \bar{\mathbf{X}} + \lambda \mathbf{I}_d \right)^{-1} \Sigma_{\mathbf{X}\mathbf{P}} \right) \right)^2}, \tag{C.2}
\end{aligned}$$

where (i) is due to the Woodbury identity and we defined  $\left( \frac{1}{n} \hat{\mathbf{X}}^\top \hat{\mathbf{X}} + \lambda \mathbf{D}_{\boldsymbol{\theta}/\mathbf{P}}^{-1} \right)^{-2}_{-i} = \frac{1}{n} \hat{\mathbf{X}}^\top \hat{\mathbf{X}} - \frac{1}{n} \hat{\mathbf{x}}_i \hat{\mathbf{x}}_i^\top + \lambda \mathbf{D}_{\boldsymbol{\theta}/\mathbf{P}}^{-1}$  which is independent to  $\hat{\mathbf{x}}_i$  (see [XH19, Eq. 58] for details), and in (ii) we used (A2), the convergence to trace [LP11, Lemma 2.1] and its stability under low-rank perturbation (e.g., see [LP11, Eq. 18]) which we elaborate below. In particular, denote  $\hat{\Sigma} = \frac{1}{n} \hat{\mathbf{X}}^\top \hat{\mathbf{X}} + \lambda \mathbf{D}_{\boldsymbol{\theta}/\mathbf{P}}^{-1}$ , for the denominator we have

$$\begin{aligned}
&\sup_i \left| \frac{\lambda}{n} \text{tr} \left( \hat{\Sigma}^{-1} \Sigma_{\mathbf{X}\mathbf{P}} \Sigma_{\boldsymbol{\theta}/\mathbf{P}}^{-1} \right) - \frac{\lambda}{n} \text{tr} \left( \hat{\Sigma}_{-i}^{-1} \Sigma_{\mathbf{X}\mathbf{P}} \Sigma_{\boldsymbol{\theta}/\mathbf{P}}^{-1} \right) \right| \\
&\leq \frac{\lambda}{n} \left\| \Sigma_{\mathbf{X}\mathbf{P}} \Sigma_{\boldsymbol{\theta}/\mathbf{P}}^{-1} \right\|_2 \sup_i \left| \text{tr} \left( \hat{\Sigma}^{-1} \left( \hat{\Sigma} - \hat{\Sigma}_{-i} \right) \hat{\Sigma}_{-i}^{-1} \right) \right| \\
&\leq \frac{\lambda}{n} \left\| \Sigma_{\mathbf{X}\mathbf{P}} \Sigma_{\boldsymbol{\theta}/\mathbf{P}}^{-1} \right\|_2 \left\| \hat{\Sigma}^{-1} \right\|_2 \sup_i \left\| \hat{\Sigma}_{-i}^{-1} \right\|_2 \text{tr} \left( \hat{\Sigma} - \hat{\Sigma}_{-i} \right) \stackrel{(i)}{\rightarrow} O_p \left( \frac{1}{n} \right),
\end{aligned}$$

where (i) is due to the definition of  $\hat{\Sigma}_{-i}$  and (A1)(A2)(A4), which implies that the non-zero eigenvalues of  $\Sigma_{\mathbf{X}\mathbf{P}}$ ,  $\Sigma_{\boldsymbol{\theta}/\mathbf{P}}$ ,  $\hat{\Sigma}$  and  $\hat{\Sigma}_{-i}$  are finite and lower-bounded away from zero as  $n, d \rightarrow \infty$  (we take the pseudo-inverse of  $\hat{\Sigma}$  when  $\lambda \rightarrow 0$ ). The result on the numerator can be obtained by a similar calculation, the details of which we omit.

Note that the denominator can be evaluated by previous results (e.g. [DW<sup>+</sup>18, Theorem 2.1]) as follows,

$$\frac{1}{n} \text{tr} \left( \left( \frac{1}{n} \bar{\mathbf{X}}^\top \bar{\mathbf{X}} + \lambda \mathbf{I}_d \right)^{-1} \Sigma_{\mathbf{X}\mathbf{P}} \right) \xrightarrow{a.s.} \frac{1}{\lambda m(-\lambda)} - 1. \quad (\text{C.3})$$

On the other hand, following the same derivation as [DW<sup>+</sup>18, HMRT19], (C.1) can be decomposed as

$$\begin{aligned} & \frac{1}{d} \text{tr} \left( \frac{1}{n} \hat{\mathbf{X}}^\top \hat{\mathbf{X}} \left( \frac{1}{n} \hat{\mathbf{X}}^\top \hat{\mathbf{X}} + \lambda \mathbf{D}_{\boldsymbol{\theta}/\mathbf{P}}^{-1} \right)^{-2} \right) \\ &= \frac{1}{d} \text{tr} \left( \left( \frac{1}{n} \bar{\mathbf{X}}^\top \bar{\mathbf{X}} + \lambda \mathbf{I}_d \right)^{-1} \Sigma_{\boldsymbol{\theta}/\mathbf{P}} \right) - \frac{\lambda}{d} \text{tr} \left( \left( \frac{1}{n} \bar{\mathbf{X}}^\top \bar{\mathbf{X}} + \lambda \mathbf{I}_d \right)^{-2} \Sigma_{\boldsymbol{\theta}/\mathbf{P}} \right) \\ &= \frac{1}{d} \text{tr} \left( \left( \frac{1}{n} \bar{\mathbf{X}}^\top \bar{\mathbf{X}} + \lambda \mathbf{I}_d \right)^{-1} \Sigma_{\boldsymbol{\theta}/\mathbf{P}} \right) + \frac{\lambda}{d} \frac{d}{d\lambda} \text{tr} \left( \left( \frac{1}{n} \bar{\mathbf{X}}^\top \bar{\mathbf{X}} + \lambda \mathbf{I}_d \right)^{-1} \Sigma_{\boldsymbol{\theta}/\mathbf{P}} \right). \end{aligned} \quad (\text{C.4})$$

We employ [RM11, Theorem 1] to characterize (C.4). In particular, For any deterministic sequence of matrices  $\Theta_n \in \mathbb{R}^{d \times d}$  with finite trace norm, as  $n, d \rightarrow \infty$  we have

$$\text{tr} \left( \Theta_n \left( \frac{1}{n} \bar{\mathbf{X}}^\top \bar{\mathbf{X}} - z \mathbf{I}_d \right)^{-1} - \Theta_n (c_n(z) \Sigma_{\mathbf{X}\mathbf{P}} - z \mathbf{I}_d)^{-1} \right) \xrightarrow{a.s.} 0,$$

in which  $c_n(z) \rightarrow -zm(z)$  for  $z \in \mathbb{C} \setminus \mathbb{R}^+$  and  $m(z)$  is defined in Theorem 1 due to the dominated convergence theorem. By (A2)(A4) we are allowed to take  $\Theta_n = \frac{1}{d} \Sigma_{\boldsymbol{\theta}/\mathbf{P}}$ . Thus we have

$$\begin{aligned} \frac{\lambda}{d} \text{tr} \left( \Sigma_{\boldsymbol{\theta}/\mathbf{P}} \left( \frac{1}{n} \bar{\mathbf{X}}^\top \bar{\mathbf{X}} + \lambda \mathbf{I}_d \right)^{-1} \right) &\rightarrow \frac{\lambda}{d} \text{tr} \left( \Sigma_{\boldsymbol{\theta}/\mathbf{P}} (\lambda m(-\lambda) \Sigma_{\mathbf{X}\mathbf{P}} + \lambda \mathbf{I}_d)^{-1} \right) \\ &\stackrel{(i)}{=} \mathbb{E} \left[ \frac{v_x v_\theta v_{xp}^{-1}}{1 + m(-\lambda) v_{xp}} \right], \quad \forall \lambda > -c_l, \end{aligned} \quad (\text{C.5})$$

in which (i) is due to (A2)(A4), the fact that the LHS is almost surely bounded for  $\lambda > -c_l$ , where  $c_l$  is the lowest non-zero eigenvalue of  $\frac{1}{n} \bar{\mathbf{X}}^\top \bar{\mathbf{X}}$ , and the application of the dominated convergence theorem. Differentiating (C.5) (note that the derivative is also bounded on  $\lambda > -c_l$ ) yields

$$\frac{\lambda}{d} \frac{d}{d\lambda} \text{tr} \left( \left( \frac{1}{n} \bar{\mathbf{X}}^\top \bar{\mathbf{X}} + \lambda \mathbf{I}_d \right)^{-1} \Sigma_{\boldsymbol{\theta}/\mathbf{P}} \right) \rightarrow \mathbb{E} \left[ \frac{v_x v_\theta v_{xp}^{-1}}{\lambda(1 + m(-\lambda) v_{xp})} - \frac{m'(-\lambda) v_x v_\theta}{(1 + m(-\lambda) v_{xp})^2} \right]. \quad (\text{C.6})$$

Finally, note that the numerator of (C.2) is the quantity of interest. Combining (C.1) (C.2) (C.3) (C.4) (C.5) (C.6) and taking  $\lambda \rightarrow 0$  yields the formula of the bias term. We remark that similar (but less general) characterization can also be obtained by [LP11, Theorem 1.2] when the eigenvalues of  $\mathbf{D}_{\mathbf{X}\mathbf{P}}$  and  $\mathbf{D}_{\boldsymbol{\theta}/\mathbf{P}}$  exhibit certain relations.

To show that  $\mathbf{P} = \Sigma_{\boldsymbol{\theta}}$  achieves the lowest bias, first note that under the definition of random variables in (A4), our claimed optimal preconditioner is equivalent to  $v_{xp} \stackrel{a.s.}{=} v_x v_\theta$ . We therefore define an interpolation  $v_\alpha = \alpha v_x v_\theta + (1 - \alpha) \bar{v}$  for some  $\bar{v}$  and write the corresponding Stieltjes transform as  $m_\alpha(-\lambda)$  and the bias term as  $B_\alpha$ . We aim to show that  $\text{argmin}_{\alpha \in [0,1]} B_\alpha = 1$ .

For notational convenience define  $g_\alpha \triangleq m_\alpha(0) v_x v_\theta$  and  $h_\alpha \triangleq m_\alpha(0) v_\alpha$ . One can check that

$$B_\alpha = \mathbb{E} \left[ \frac{v_x v_\theta}{(1 + h_\alpha)^2} \right] \mathbb{E} \left[ \frac{h_\alpha}{(1 + h_\alpha)^2} \right]^{-1}; \quad \left. \frac{dm_\alpha(-\lambda)}{d\alpha} \right|_{\lambda \rightarrow 0} = \frac{m_\alpha(0) \mathbb{E} \left[ \frac{h_\alpha - g_\alpha}{(1 + h_\alpha)^2} \right]}{(1 - \alpha) \mathbb{E} \left[ \frac{h_\alpha}{(1 + h_\alpha)^2} \right]}.$$

We now verify that the derivative of  $B_\alpha$  w.r.t.  $\alpha$  is non-positive for  $\alpha \in [0, 1]$ . A standard simplification of the derivative yields

$$\begin{aligned} \frac{dB_\alpha}{d\alpha} &\propto -2\mathbb{E}\left[\frac{(g_\alpha - h_\alpha)^2}{(1 + h_\alpha)^3}\right] \left(\mathbb{E}\left[\frac{h_\alpha}{(1 + h_\alpha)^2}\right]\right)^2 - 2\left(\mathbb{E}\left[\frac{g_\alpha - h_\alpha}{(1 + h_\alpha)^2}\right]\right)^2 \mathbb{E}\left[\frac{h_\alpha^2}{(1 + h_\alpha)^3}\right] \\ &\quad + 4\mathbb{E}\left[\frac{h_\alpha(g_\alpha - h_\alpha)}{(1 + h_\alpha)^3}\right] \mathbb{E}\left[\frac{g_\alpha - h_\alpha}{(1 + h_\alpha)^2}\right] \mathbb{E}\left[\frac{h_\alpha}{(1 + h_\alpha)^2}\right] \\ &\stackrel{(i)}{\leq} -4\sqrt{\mathbb{E}\left[\frac{(g_\alpha - h_\alpha)^2}{(1 + h_\alpha)^3}\right] \mathbb{E}\left[\frac{h_\alpha^2}{(1 + h_\alpha)^3}\right] \left(\mathbb{E}\left[\frac{g_\alpha - h_\alpha}{(1 + h_\alpha)^2}\right]\right)^2 \left(\mathbb{E}\left[\frac{h_\alpha}{(1 + h_\alpha)^2}\right]\right)^2} \\ &\quad + 4\mathbb{E}\left[\frac{h_\alpha(g_\alpha - h_\alpha)}{(1 + h_\alpha)^3}\right] \mathbb{E}\left[\frac{g_\alpha - h_\alpha}{(1 + h_\alpha)^2}\right] \mathbb{E}\left[\frac{h_\alpha}{(1 + h_\alpha)^2}\right] \stackrel{(ii)}{\leq} 0, \end{aligned}$$

where (i) is due to AM-GM and (ii) due to Cauchy-Schwarz on the first term. Note that the two equalities hold when  $g_\alpha = h_\alpha$ , from which one can easily deduce that the optimum is achieved when  $v_{xp} \stackrel{a.s.}{=} v_x v_\theta$ , and thus we know that  $\mathbf{P} = \boldsymbol{\Sigma}_\theta$  is the optimal preconditioner for the bias term.  $\square$

### C.4 Proof of Proposition 3

**Proof.** Via a similar calculation as in [HMRT19, Section 5], the bias term can be decomposed as

$$\begin{aligned} \mathbb{E}[B(\hat{\boldsymbol{\theta}}_{\mathbf{P}})] &= \mathbb{E}_{\mathbf{x}, \hat{\mathbf{x}}, \boldsymbol{\theta}^*, \boldsymbol{\theta}^c} \left[ \left( \mathbf{x}^\top \mathbf{P} \mathbf{X}^\top (\mathbf{X} \mathbf{P} \mathbf{X}^\top)^{-1} (\mathbf{X} \boldsymbol{\theta}^* + \mathbf{X}^c \boldsymbol{\theta}^c) - (\mathbf{x}^\top \boldsymbol{\theta}^* + \hat{\mathbf{x}}^\top \boldsymbol{\theta}^c) \right)^2 \right] \\ &\stackrel{(i)}{=} \mathbb{E}_{\mathbf{x}, \boldsymbol{\theta}^*} \left[ \left( \mathbf{x}^\top \mathbf{P} \mathbf{X}^\top (\mathbf{X} \mathbf{P} \mathbf{X}^\top)^{-1} \mathbf{X} \boldsymbol{\theta}^* - \mathbf{x}^\top \boldsymbol{\theta}^* \right)^2 \right] + \mathbb{E}_{\mathbf{x}^c, \boldsymbol{\theta}^c} \left[ (\hat{\mathbf{x}}^\top \boldsymbol{\theta}^c)^2 \right] \\ &\quad + \mathbb{E}_{\mathbf{x}, \boldsymbol{\theta}^c} \left[ \left( \mathbf{x}^\top \mathbf{P} \mathbf{X}^\top (\mathbf{X} \mathbf{P} \mathbf{X}^\top)^{-1} \mathbf{X}^c \boldsymbol{\theta}^c \boldsymbol{\theta}^{c\top} \mathbf{X}^{c\top} (\mathbf{X} \mathbf{P} \mathbf{X}^\top)^{-1} \mathbf{X} \mathbf{P} \mathbf{x} \right)^2 \right] \\ &\stackrel{(ii)}{\rightarrow} B_\theta(\hat{\boldsymbol{\theta}}_{\mathbf{P}}) + \frac{1}{d^c} \text{tr}(\boldsymbol{\Sigma}_{\mathbf{X}}^c \boldsymbol{\Sigma}_\theta^c) (1 + V(\hat{\boldsymbol{\theta}}_{\mathbf{P}})), \end{aligned}$$

where we used the independence of  $\mathbf{x}$ ,  $\hat{\mathbf{x}}$  and  $\boldsymbol{\theta}^*$ ,  $\boldsymbol{\theta}^c$  in (i), and (A2-4) as well as the definition of the well-specified bias  $B_\theta(\hat{\boldsymbol{\theta}}_{\mathbf{P}})$  and variance  $V(\hat{\boldsymbol{\theta}}_{\mathbf{P}})$  in (ii).  $\square$

### C.5 Proof of Proposition 4

**Proof.** We first outline a more general setup where  $\mathbf{P}_\alpha = f(\boldsymbol{\Sigma}_{\mathbf{X}}; \alpha)$  for continuous and differentiable function of  $\alpha$  and  $f$  applied to the eigenvalues of  $\boldsymbol{\Sigma}_{\mathbf{x}}$ . For any interval  $\mathcal{I} \subseteq [0, 1]$ , we claim that

- Suppose all four functions  $\frac{1}{xf(x;\alpha)}$ ,  $f(x;\alpha)$ ,  $\frac{\partial f(x;\alpha)}{\partial \alpha}/f(x;\alpha)$  and  $x \frac{\partial f(x;\alpha)}{\partial \alpha}$  are decreasing functions of  $x$  on the support of  $v_x$  for all  $\alpha \in \mathcal{I}$ . In addition,  $\frac{\partial f(x;\alpha)}{\partial \alpha} \geq 0$  on the support of  $v_x$  for all  $\alpha \in \mathcal{I}$ . Then the stationary bias is an increasing function of  $\alpha$  on  $\mathcal{I}$ .
- For all  $\alpha \in \mathcal{I}$ , suppose  $xf(x;\alpha)$  is a monotonic function of  $x$  on the support of  $v_x$  and  $\frac{\partial f(x;\alpha)}{\partial \alpha}/f(x;\alpha)$  is a decreasing function of  $x$  on the support of  $v_x$ . Then the stationary variance is a decreasing function of  $\alpha$  on  $\mathcal{I}$ .

Let us verify the three choices of  $\mathbf{P}_\alpha$  in Proposition 4 one by one.

- When  $\mathbf{P}_\alpha = (1 - \alpha)\mathbf{I}_d + \alpha(\boldsymbol{\Sigma}_{\mathbf{X}})^{-1}$ , the corresponding  $f(x;\alpha)$  is  $(1 - \alpha) + \alpha x$ . It is clear that it satisfies all conditions in (a) and (b) for all  $\alpha \in [0, 1]$ . Hence, the stationary variance is a decreasing function and the stationary bias is an increasing function of  $\alpha \in [0, 1]$ .

- When  $\mathbf{P}_\alpha = (\boldsymbol{\Sigma}_X)^{-\alpha}$ , the corresponding  $f(x; \alpha)$  is  $x^{-\alpha}$ . It is clear that it satisfies all conditions in (a) and (b) for all  $\alpha \in [0, 1]$  except for the condition that  $x \frac{\partial f(x; \alpha)}{\partial \alpha} = -x^{1-\alpha} \ln x$  is a decreasing function of  $x$ . Note that  $x \frac{\partial f(x; \alpha)}{\partial \alpha} = -x^{1-\alpha} \ln x$  is a decreasing function of  $x$  on the support of  $v_x$  only for  $\alpha \geq \frac{\ln(\kappa)-1}{\ln(\kappa)}$  where  $\kappa = \sup v_x / \inf v_x$ . Hence, the stationary variance is a decreasing function of  $\alpha \in [0, 1]$  and the stationary bias is an increasing function of  $\alpha \in [\max(0, \frac{\ln(\kappa)-1}{\ln(\kappa)}), 1]$ .
- When  $\mathbf{P}_\alpha = (\alpha \boldsymbol{\Sigma}_X + (1-\alpha) \mathbf{I}_d)^{-1}$ , the corresponding  $f(x; \alpha)$  is  $1/(\alpha x + (1-\alpha))$ . It is clear that it satisfies all conditions in (a) and (b) for all  $\alpha \in [0, 1]$  except for the condition that  $x \frac{\partial f(x; \alpha)}{\partial \alpha} = \frac{x(1-x)}{(\alpha x + (1-\alpha))^2}$  is a decreasing function of  $x$ . Note that  $x \frac{\partial f(x; \alpha)}{\partial \alpha} = \frac{x(1-x)}{(\alpha x + (1-\alpha))^2}$  is a decreasing function of  $x$  on the support of  $v_x$  only for  $\alpha \geq \frac{\kappa-2}{\kappa-1}$ . Hence, the stationary variance is a decreasing function of  $\alpha \in [0, 1]$  and the stationary bias is an increasing function of  $\alpha \in [\max(0, \frac{\kappa-2}{\kappa-1}), 1]$ .

To show (a) and (b), note that under the conditions on  $\boldsymbol{\Sigma}_x$  and  $\boldsymbol{\Sigma}_\theta$  assumed in Proposition 4, the stationary bias  $B(\hat{\boldsymbol{\theta}}_{\mathbf{P}_\alpha})$  and the stationary variance  $V(\hat{\boldsymbol{\theta}}_{\mathbf{P}_\alpha})$  can be simplified to

$$B(\hat{\boldsymbol{\theta}}_{\mathbf{P}_\alpha}) = \frac{m'_\alpha(0)}{m_\alpha^2(0)} \mathbb{E} \frac{v_x}{(1 + v_x f(v_x; \alpha) m_\alpha(0))^2} \quad \text{and} \quad V(\hat{\boldsymbol{\theta}}_{\mathbf{P}_\alpha}) = \sigma^2 \cdot \left( \frac{m'_\alpha(0)}{m_\alpha^2(0)} - 1 \right),$$

where  $m_\alpha(z)$  and  $m'_\alpha(z)$  satisfy

$$1 = -z m_\alpha(z) + \gamma \mathbb{E} \frac{v_x f(v_x; \alpha) m_\alpha(z)}{1 + v_x f(v_x; \alpha) m_\alpha(z)} \quad (\text{C.7})$$

$$\frac{m'_\alpha(z)}{m_\alpha^2(z)} = \frac{1}{1 - \gamma \mathbb{E} \left( \frac{f(v_x; \alpha) m_\alpha(z)}{1 + f(v_x; \alpha) m_\alpha(z)} \right)^2}. \quad (\text{C.8})$$

For notation convenience, let  $f_\alpha := v_x f(v_x; \alpha)$ . From (C.8), we have the following equivalent expressions.

$$B(\hat{\boldsymbol{\theta}}_{\mathbf{P}_\alpha}) = \frac{\mathbb{E} \frac{v_x}{(1 + f_\alpha m_\alpha(0))^2}}{1 - \gamma \mathbb{E} \left( \frac{f_\alpha m_\alpha(0)}{1 + f_\alpha m_\alpha(0)} \right)^2}, \quad (\text{C.9})$$

$$V(\hat{\boldsymbol{\theta}}_{\mathbf{P}_\alpha}) = \sigma^2 \left( \frac{1}{1 - \gamma \mathbb{E} \left( \frac{f_\alpha m_\alpha(0)}{1 + f_\alpha m_\alpha(0)} \right)^2} - 1 \right). \quad (\text{C.10})$$

We first show that (b) holds. Note that from (C.10), we have

$$\frac{\partial V(\hat{\boldsymbol{\theta}}_{\mathbf{P}_\alpha})}{\partial \alpha} = \gamma \sigma^2 \left( \frac{1}{1 - \gamma \mathbb{E} \left( \frac{f_\alpha m_\alpha(0)}{1 + f_\alpha m_\alpha(0)} \right)^2} \right)^2 \mathbb{E} \left[ \frac{2 f_\alpha m_\alpha(0)}{(1 + f_\alpha m_\alpha(0))^3} \left( f_\alpha \frac{\partial m_\alpha(z)}{\partial \alpha} \Big|_{z=0} + \frac{\partial f_\alpha}{\partial \alpha} m_\alpha(0) \right) \right]. \quad (\text{C.11})$$

To calculate  $\frac{\partial m_\alpha(z)}{\partial \alpha} \Big|_{z=0}$ , we take derivatives with respect to  $\alpha$  on both sides of (C.7),

$$0 = \gamma \mathbb{E} \left[ \frac{1}{(1 + f_\alpha m_\alpha(0))^2} \cdot \left( f_\alpha \frac{\partial m_\alpha(z)}{\partial \alpha} \Big|_{z=0} + \frac{\partial f_\alpha}{\partial \alpha} m_\alpha(0) \right) \right]. \quad (\text{C.12})$$

Therefore, plugging (C.12) into (C.11) yields

$$\begin{aligned} \frac{\partial V(\hat{\boldsymbol{\theta}}_{\mathbf{P}_\alpha})}{\partial \alpha} &= 2\gamma \sigma^2 \left( \frac{m_\alpha(0)}{1 - \gamma \mathbb{E} \left( \frac{f_\alpha m_\alpha(0)}{1 + f_\alpha m_\alpha(0)} \right)^2} \right)^2 \left( \mathbb{E} \frac{f_\alpha}{(1 + f_\alpha m_\alpha(0))^2} \right)^{-1} \\ &\quad \times \left( \mathbb{E} \frac{f_\alpha \frac{\partial f_\alpha}{\partial \alpha}}{(1 + f_\alpha m_\alpha(0))^3} \mathbb{E} \frac{f_\alpha}{(1 + f_\alpha m_\alpha(0))^2} - \mathbb{E} \frac{f_\alpha^2}{(1 + f_\alpha m_\alpha(0))^3} \mathbb{E} \frac{\frac{\partial f_\alpha}{\partial \alpha}}{(1 + f_\alpha m_\alpha(0))^2} \right) \end{aligned}$$

Hence, showing  $V(\hat{\theta}_{\mathbf{P}_\alpha})$  is a decreasing function of  $\alpha$  is equivalent to showing that

$$\mathbb{E} \frac{f_\alpha^2}{(1+f_\alpha m_\alpha(0))^3} \mathbb{E} \frac{\frac{\partial f_\alpha}{\partial \alpha}}{(1+f_\alpha m_\alpha(0))^2} \geq \mathbb{E} \frac{f_\alpha \frac{\partial f_\alpha}{\partial \alpha}}{(1+f_\alpha m_\alpha(0))^3} \mathbb{E} \frac{f_\alpha}{(1+f_\alpha m_\alpha(0))^2}. \quad (\text{C.13})$$

Let  $\mu_x$  be the probability measure of  $v_x$ . We define a new measure  $\tilde{\mu}_x = \frac{f_\alpha \mu_x}{(1+f_\alpha m_\alpha(0))^2}$ , and let  $\tilde{v}_x$  follow the new measure. Since  $\frac{\partial f(x;\alpha)}{\partial \alpha} / f(x;\alpha)$  is a decreasing function of  $x$  and  $xf(x;\alpha)$  is a monotonic function of  $x$ ,

$$\mathbb{E} \frac{\tilde{v}_x f(\tilde{v}_x; \alpha)}{1 + \tilde{v}_x f(\tilde{v}_x; \alpha) m_\alpha(0)} \mathbb{E} \frac{\frac{\partial \tilde{v}_x f(\tilde{v}_x; \alpha)}{\partial \alpha}}{\tilde{v}_x f(\tilde{v}_x; \alpha)} \geq \mathbb{E} \frac{\frac{\partial \tilde{v}_x f(\tilde{v}_x; \alpha)}{\partial \alpha}}{1 + \tilde{v}_x f(\tilde{v}_x; \alpha) m_\alpha(0)}.$$

Changing  $\tilde{v}_x$  back to  $v_x$ , we arrive at (C.13) and thus (b).

For the bias term  $B(\hat{\theta}_{\mathbf{P}_\alpha})$ , note that from (C.7) and (C.9), we have

$$\begin{aligned} \frac{\partial B(\hat{\theta}_{\mathbf{P}_\alpha})}{\partial \alpha} &= \frac{1}{\gamma} \left( \frac{1}{\gamma} - \mathbb{E} \left( \frac{f_\alpha m_\alpha(0)}{1+f_\alpha m_\alpha(0)} \right)^2 \right)^{-2} \\ &\quad \times \left( -\mathbb{E} \left[ 2 \frac{v_x}{(1+f_\alpha m_\alpha(0))^3} \cdot \left( f_\alpha \frac{\partial m_\alpha(z)}{\partial \alpha} \Big|_{z=0} + \frac{\partial f_\alpha}{\partial \alpha} m_\alpha(0) \right) \right] \mathbb{E} \frac{f_\alpha m_\alpha(0)}{(1+f_\alpha m_\alpha(0))^2} \right. \\ &\quad \left. + \mathbb{E} \frac{v_x}{(1+f_\alpha m_\alpha(0))^2} \mathbb{E} \left[ 2 \frac{f_\alpha m_\alpha(0)}{(1+f_\alpha m_\alpha(0))^3} \cdot \left( f_\alpha \frac{\partial m_\alpha(z)}{\partial \alpha} \Big|_{z=0} + \frac{\partial f_\alpha}{\partial \alpha} m_\alpha(0) \right) \right] \right). \quad (\text{C.14}) \end{aligned}$$

Similarly, we plug (C.12) in (C.14) and simplify the expression. To verify  $B(\hat{\theta}_{\mathbf{P}_\alpha})$  is an increasing function of  $\alpha$ , we need to show

$$\begin{aligned} 0 \leq & \left( \mathbb{E} \frac{v_x f_\alpha m_\alpha(0)}{(1+f_\alpha m_\alpha(0))^3} \mathbb{E} \frac{\frac{\partial f_\alpha}{\partial \alpha}}{(1+f_\alpha m_\alpha(0))^2} - \mathbb{E} \frac{v_x \frac{\partial f_\alpha}{\partial \alpha}}{(1+f_\alpha m_\alpha(0))^3} \mathbb{E} \frac{f_\alpha m_\alpha(0)}{(1+f_\alpha m_\alpha(0))^2} \right) \mathbb{E} \frac{f_\alpha m_\alpha(0)}{(1+f_\alpha m_\alpha(0))^2} \\ & - \mathbb{E} \frac{v_x}{(1+f_\alpha m_\alpha(0))^2} \left( \mathbb{E} \frac{(f_\alpha m_\alpha(0))^2}{(1+f_\alpha m_\alpha(0))^3} \mathbb{E} \frac{\frac{\partial f_\alpha}{\partial \alpha}}{(1+f_\alpha m_\alpha(0))^2} - \mathbb{E} \frac{f_\alpha m_\alpha(0) \frac{\partial f_\alpha}{\partial \alpha}}{(1+f_\alpha m_\alpha(0))^3} \mathbb{E} \frac{f_\alpha m_\alpha(0)}{(1+f_\alpha m_\alpha(0))^2} \right), \quad (\text{C.15}) \end{aligned}$$

Let  $h_\alpha \triangleq f_\alpha m_\alpha(0) = v_x f(v_x; \alpha) m_\alpha(0)$  and  $g_\alpha \triangleq \frac{\partial f_\alpha}{\partial \alpha} = v_x \frac{\partial f(v_x; \alpha)}{\partial \alpha}$ . Then (C.15) can be further simplified to the following equation

$$\begin{aligned} 0 \leq & \underbrace{\mathbb{E} \frac{v_x h_\alpha}{(1+h_\alpha)^3} \mathbb{E} \frac{g_\alpha}{(1+h_\alpha)^3} \mathbb{E} \frac{h_\alpha}{(1+h_\alpha)^3} - \mathbb{E} \frac{v_x}{(1+h_\alpha)^3} \mathbb{E} \frac{g_\alpha}{(1+h_\alpha)^3} \mathbb{E} \frac{h_\alpha^2}{(1+h_\alpha)^3}}_{\text{part 1}} \\ & + \underbrace{\mathbb{E} \frac{v_x}{(1+h_\alpha)^3} \mathbb{E} \frac{g_\alpha h_\alpha}{(1+h_\alpha)^3} \mathbb{E} \frac{h_\alpha}{(1+h_\alpha)^3} - \mathbb{E} \frac{v_x g_\alpha}{(1+h_\alpha)^3} \mathbb{E} \frac{h_\alpha}{(1+h_\alpha)^3} \mathbb{E} \frac{h_\alpha}{(1+h_\alpha)^3}}_{\text{part 2}} \\ & + \underbrace{2 \mathbb{E} \frac{v_x h_\alpha}{(1+h_\alpha)^3} \mathbb{E} \frac{g_\alpha h_\alpha}{(1+h_\alpha)^3} \mathbb{E} \frac{h_\alpha}{(1+h_\alpha)^3} - 2 \mathbb{E} \frac{v_x g_\alpha}{(1+h_\alpha)^3} \mathbb{E} \frac{h_\alpha^2}{(1+h_\alpha)^3} \mathbb{E} \frac{h_\alpha}{(1+h_\alpha)^3}}_{\text{part 3}} \\ & + \underbrace{\mathbb{E} \frac{v_x h_\alpha}{(1+h_\alpha)^3} \mathbb{E} \frac{g_\alpha h_\alpha}{(1+h_\alpha)^3} \mathbb{E} \frac{h_\alpha^2}{(1+h_\alpha)^3} - \mathbb{E} \frac{v_x g_\alpha}{(1+h_\alpha)^3} \mathbb{E} \frac{h_\alpha^2}{(1+h_\alpha)^3} \mathbb{E} \frac{h_\alpha^2}{(1+h_\alpha)^3}}_{\text{part 4}}. \quad (\text{C.16}) \end{aligned}$$

Note that under condition of (a), we know that both  $h_\alpha$  and  $v_x/h_\alpha$  are increasing functions of  $v_x$ ; and both  $g_\alpha/h_\alpha$  and  $g_\alpha$  are decreasing functions of  $v_x$ . Hence, with calculation similar to (C.13), we know part 1,2,3,4 in (C.16) are all non-negative, and therefore (C.16) holds.  $\square$

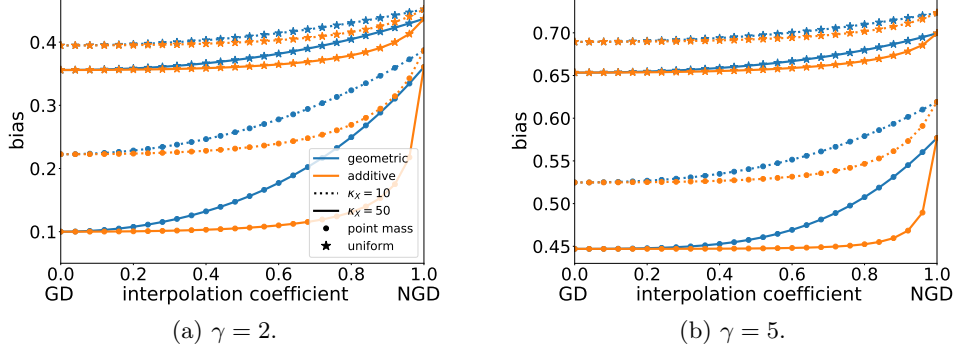


Figure 21: Illustration of the monotonicity of the bias term under  $\Sigma_{\theta} = \mathbf{I}_d$ . We consider two distributions of eigenvalues for  $\Sigma_{\mathbf{X}}$ : two equally weighted point masses (circle) and a uniform distribution (star), and vary the condition number  $\kappa_{\mathbf{X}}$  and overparameterization level  $\gamma$ . In all cases the bias is monotone in  $\alpha \in [0, 1]$ .

**Remark.** The above characterization provides sufficient but not necessary conditions for the monotonicity of the bias term. In general, the expression of the bias is rather opaque, and determining the sign of its derivative can be tedious, except for certain special cases (e.g.  $\gamma = 2$  and the eigenvalues of  $\Sigma_{\mathbf{X}}$  are two equally weighted point masses, for which  $m_{\alpha}$  has a simple form and one may analytically check the monotonicity). We conjecture that the bias is monotone for  $\alpha \in [0, 1]$  for a much wider class of  $\Sigma_{\mathbf{X}}$ , as shown in Figure 21.

## C.6 Proof of Proposition 5

**Proof.** Taking the derivative of  $V(\boldsymbol{\theta}_{\mathbf{P}}(t))$  w.r.t. time yields (omitting the scalar  $\sigma^2$ ),

$$\begin{aligned} \frac{dV(\boldsymbol{\theta}_{\mathbf{P}}(t))}{dt} &= \frac{d}{dt} \left\| \Sigma_{\mathbf{X}}^{1/2} \mathbf{P} \mathbf{X}^{\top} \left( \mathbf{I}_n - \exp\left(-\frac{t}{n} \mathbf{X} \mathbf{P} \mathbf{X}^{\top}\right) \right) \left( \mathbf{X} \mathbf{P} \mathbf{X}^{\top} \right)^{-1} \right\|_F^2 \\ &\stackrel{(i)}{=} \frac{1}{n} \text{tr} \left( \underbrace{\Sigma_{\mathbf{X} \mathbf{P}} \bar{\mathbf{X}}^{\top} \mathbf{S}_{\mathbf{P}} \exp\left(-\frac{t}{n} \mathbf{S}_{\mathbf{P}}\right) \mathbf{S}_{\mathbf{P}}^{-2} \left( \mathbf{I}_n - \exp\left(-\frac{t}{n} \mathbf{S}_{\mathbf{P}}\right) \right) \bar{\mathbf{X}}}_{p.s.d.} \right) \stackrel{(ii)}{>} 0, \end{aligned}$$

where we defined  $\bar{\mathbf{X}} = \mathbf{X} \mathbf{P}^{1/2}$  and  $\mathbf{S}_{\mathbf{P}} = \mathbf{X} \mathbf{P} \mathbf{X}^{\top}$  in (i), and (ii) is due to (A2-3) the inequality  $\text{tr}(\mathbf{A} \mathbf{B}) \geq \lambda_{\min}(\mathbf{A}) \text{tr}(\mathbf{B})$  for positive semi-definite  $\mathbf{A}$  and  $\mathbf{B}$ .  $\square$

## C.7 Proof of Proposition 6

**Proof.** Recall the definition of the bias (well-specified) of  $\hat{\boldsymbol{\theta}}_{\mathbf{P}}(t)$ ,

$$\begin{aligned} B(\boldsymbol{\theta}_{\mathbf{P}}(t)) &\stackrel{(i)}{=} \frac{1}{d} \text{tr} \left( \Sigma_{\theta} \left( \mathbf{I}_d - \mathbf{P} \mathbf{X}^{\top} \mathbf{W}_{\mathbf{P}}(t) \mathbf{S}_{\mathbf{P}}^{-1} \mathbf{X} \right)^{\top} \Sigma_{\mathbf{X}} \left( \mathbf{I}_d - \mathbf{P} \mathbf{X}^{\top} \mathbf{W}_{\mathbf{P}}(t) \mathbf{S}_{\mathbf{P}}^{-1} \mathbf{X} \right) \right) \\ &\stackrel{(ii)}{=} \frac{1}{d} \text{tr} \left( \Sigma_{\theta/\mathbf{P}} \left( \mathbf{I}_d - \bar{\mathbf{X}}^{\top} \mathbf{W}_{\mathbf{P}}(t) \mathbf{S}_{\mathbf{P}}^{-1} \bar{\mathbf{X}} \right)^{\top} \Sigma_{\mathbf{X} \mathbf{P}} \left( \mathbf{I}_d - \bar{\mathbf{X}}^{\top} \mathbf{W}_{\mathbf{P}}(t) \mathbf{S}_{\mathbf{P}}^{-1} \bar{\mathbf{X}} \right) \right) \\ &\stackrel{(iii)}{\geq} \frac{1}{d} \text{tr} \left( \left( \Sigma_{\mathbf{X} \mathbf{P}}^{1/2} \left( \mathbf{I}_d - \bar{\mathbf{X}}^{\top} \mathbf{W}_{\mathbf{P}}(t) \mathbf{S}_{\mathbf{P}}^{-1} \bar{\mathbf{X}} \right) \Sigma_{\theta/\mathbf{P}}^{1/2} \right)^2 \right), \end{aligned} \tag{C.17}$$

where we defined  $\mathbf{S}_{\mathbf{P}} = \mathbf{X} \mathbf{P} \mathbf{X}^{\top}$ ,  $\mathbf{W}_{\mathbf{P}}(t) = \mathbf{I}_n - \exp\left(-\frac{t}{n} \mathbf{S}_{\mathbf{P}}\right)$  in (i),  $\bar{\mathbf{X}} = \mathbf{X} \mathbf{P}^{1/2}$  in (ii), and (iii) is due to the inequality  $\text{tr}(\mathbf{A}^{\top} \mathbf{A}) \geq \text{tr}(\mathbf{A}^2)$ .

When  $\Sigma_{\mathbf{X}} = \Sigma_{\boldsymbol{\theta}}^{-1}$ , i.e. NGD achieves lowest stationary bias, (C.17) simplifies to

$$B(\boldsymbol{\theta}_{\mathbf{P}}(t)) \geq \frac{1}{d} \text{tr} \left( \left( \mathbf{I}_d - \bar{\mathbf{X}}^\top \mathbf{W}_{\mathbf{P}}(t) \mathbf{S}_{\mathbf{P}}^{-1} \bar{\mathbf{X}} \right)^2 \right) = \left( 1 - \frac{1}{\gamma} \right) + \frac{1}{d} \sum_{i=1}^n \exp \left( -\frac{t}{n} \bar{\lambda}_i \right)^2, \quad (\text{C.18})$$

where  $\bar{\lambda}$  is the eigenvalue of  $\mathbf{S}_{\mathbf{P}}$ . On the other hand, since  $\mathbf{F} = \Sigma_{\mathbf{X}}$ , for the NGD iterate  $\hat{\boldsymbol{\theta}}_{\mathbf{F}^{-1}}(t)$  we have

$$B(\boldsymbol{\theta}_{\mathbf{F}^{-1}}(t)) = \frac{1}{d} \text{tr} \left( \left( \mathbf{I}_d - \hat{\mathbf{X}}^\top \mathbf{W}_{\mathbf{F}^{-1}}(t) \mathbf{S}_{\mathbf{F}^{-1}}^{-1} \hat{\mathbf{X}} \right)^2 \right) = \left( 1 - \frac{1}{\gamma} \right) + \frac{1}{d} \sum_{i=1}^n \exp \left( -\frac{t}{n} \hat{\lambda}_i \right)^2, \quad (\text{C.19})$$

where  $\hat{\mathbf{X}} = \mathbf{X} \Sigma_{\mathbf{X}}^{-1/2}$  and  $\bar{\lambda}$  is the eigenvalue of  $\mathbf{S}_{\mathbf{F}^{-1}} = \hat{\mathbf{X}} \hat{\mathbf{X}}^\top$ . Comparing (C.18)(C.19), we see that given  $\hat{\boldsymbol{\theta}}_{\mathbf{P}}(t)$  at a fixed  $t$ , if we run NGD for time  $T > \frac{\bar{\lambda}_{\max}}{\bar{\lambda}_{\min}} t$  (note that  $T/t = O(1)$  by (A2-3)), then we have  $B(\boldsymbol{\theta}_{\mathbf{P}}(t)) \geq B(\boldsymbol{\theta}_{\mathbf{F}^{-1}}(T))$  for any  $\mathbf{P}$  satisfying (A3). This thus implies that  $B^{\text{opt}}(\boldsymbol{\theta}_{\mathbf{P}}) \geq B^{\text{opt}}(\boldsymbol{\theta}_{\mathbf{F}^{-1}})$ .

On the other hand, when  $\Sigma_{\boldsymbol{\theta}} = \mathbf{I}_d$ , we can show that the bias term of GD is monotonically decreasing through time by taking its derivative,

$$\begin{aligned} \frac{d}{dt} B(\boldsymbol{\theta}_{\mathbf{I}}(t)) &= \frac{1}{d} \frac{d}{dt} \text{tr} \left( \left( \mathbf{I}_d - \mathbf{X}^\top \mathbf{W}_{\mathbf{I}}(t) \mathbf{S}_{\mathbf{I}}^{-1} \mathbf{X} \right)^\top \Sigma_{\mathbf{X}} \left( \mathbf{I}_d - \mathbf{X}^\top \mathbf{W}_{\mathbf{I}}(t) \mathbf{S}_{\mathbf{I}}^{-1} \mathbf{X} \right) \right) \\ &= -\frac{1}{nd} \text{tr} \left( \underbrace{\Sigma_{\mathbf{X}} \mathbf{X}^\top \mathbf{S} \exp \left( -\frac{t}{n} \mathbf{S} \right) \mathbf{S}^{-1} \mathbf{X} \left( \mathbf{I}_d - \mathbf{X}^\top \mathbf{W}_{\mathbf{I}}(t) \mathbf{S}_{\mathbf{I}}^{-1} \mathbf{X} \right)}_{p.s.d.} \right) < 0. \end{aligned} \quad (\text{C.20})$$

Similarly, one can verify that the expected bias of NGD is monotonically decreasing for all choices of  $\Sigma_{\mathbf{X}}$  and  $\Sigma_{\boldsymbol{\theta}}$  satisfying (A2-4),

$$\begin{aligned} &\frac{d}{dt} \text{tr} \left( \Sigma_{\boldsymbol{\theta}} \left( \mathbf{I}_d - \mathbf{F}^{-1} \mathbf{X}^\top \mathbf{W}_{\mathbf{F}^{-1}}(t) \mathbf{S}_{\mathbf{F}^{-1}}^{-1} \mathbf{X} \right)^\top \Sigma_{\mathbf{X}} \left( \mathbf{I}_d - \mathbf{F}^{-1} \mathbf{X}^\top \mathbf{W}_{\mathbf{F}^{-1}}(t) \mathbf{S}_{\mathbf{F}^{-1}}^{-1} \mathbf{X} \right) \right) \\ &= \frac{d}{dt} \text{tr} \left( \Sigma_{\mathbf{X} \boldsymbol{\theta}} \left( \mathbf{I}_d - \hat{\mathbf{X}}^\top \mathbf{W}_{\mathbf{F}^{-1}}(t) \mathbf{S}_{\mathbf{F}^{-1}}^{-1} \hat{\mathbf{X}} \right)^\top \left( \mathbf{I}_d - \hat{\mathbf{X}}^\top \mathbf{W}_{\mathbf{F}^{-1}}(t) \mathbf{S}_{\mathbf{F}^{-1}}^{-1} \hat{\mathbf{X}} \right) \right) \stackrel{(i)}{<} 0, \end{aligned}$$

where (i) follows from calculation similar to (C.20). Since the expected bias is decreasing through time for both GD and NGD when  $\Sigma_{\boldsymbol{\theta}} = \mathbf{I}_d$ , and from Theorem 2 we know that  $B(\boldsymbol{\theta}_{\mathbf{I}}) \leq B(\hat{\boldsymbol{\theta}}_{\mathbf{F}^{-1}})$ , we conclude that  $B^{\text{opt}}(\boldsymbol{\theta}_{\mathbf{I}}) \leq B^{\text{opt}}(\boldsymbol{\theta}_{\mathbf{F}^{-1}})$ .  $\square$

## C.8 Proof of Theorem 7

### C.8.1 Setup and Result

We first state the setting and assumptions (which has been slightly updated compare to that of the main text).  $\mathcal{H}$  is an RKHS included in  $L_2(P_X)$  equipped with a bounded kernel function  $k$ .  $K_{\mathbf{x}} \in \mathcal{H}$  is the Riesz representation of the kernel function  $k(\mathbf{x}, \cdot)$ , that is,  $k(\mathbf{x}, \mathbf{y}) = \langle K_{\mathbf{x}}, K_{\mathbf{y}} \rangle_{\mathcal{H}}$ .  $S$  is the canonical embedding operator from  $\mathcal{H}$  to  $L_2(P_X)$ . We write  $\Sigma = S^* S : \mathcal{H} \rightarrow \mathcal{H}$  and  $L = S S^*$ . Note that the boundedness of the kernel gives  $\|Sf\|_{L_2(P_X)} \leq \sup_{\mathbf{x}} |f(\mathbf{x})| = \sup_{\mathbf{x}} |\langle K_{\mathbf{x}}, f \rangle| \leq \|K_{\mathbf{x}}\|_{\mathcal{H}} \|f\|_{\mathcal{H}} \leq \|f\|_{\mathcal{H}}$ . Hence we know  $\|\Sigma\| \leq 1$  and  $\|L\| \leq 1$ . We make the following assumptions.

- there exist  $r \in (0, \infty)$  and  $M > 0$  such that  $f^* = L^r h^*$  for some  $h^* \in L_2(P_X)$  and  $\|f^*\|_{\infty} \leq M$ .
- there exists  $s > 1$  s.t.  $\text{tr}(\Sigma^{1/s}) < \infty$  and  $2r + s^{-1} > 1$ .
- There exist  $\mu \in [s^{-1}, 1]$  and  $C_{\mu} > 0$  such that  $\sup_{\mathbf{x} \in \text{supp}(P_X)} \|\Sigma^{1/2-1/\mu} K_{\mathbf{x}}\|_{\mathcal{H}} \leq C_{\mu}$ .
- $\sup_{\mathbf{x} \in \text{supp}(P_X)} k(\mathbf{x}, \mathbf{x}) \leq 1$ .

The training data is generated as  $y_i = f^*(\mathbf{x}_i) + \varepsilon_i$ , where  $\varepsilon_i$  is an i.i.d. noise satisfying  $|\varepsilon_i| \leq \sigma$  almost surely. Let  $\mathbf{y} \in \mathbb{R}^n$  be the label vector. We identify  $\mathbb{R}^n$  with  $L_2(P_n)$  and define

$$\hat{\Sigma} = \frac{1}{n} \sum_{i=1}^n K_{\mathbf{x}_i} \otimes K_{\mathbf{x}_i} : \mathcal{H} \rightarrow \mathcal{H}, \quad \hat{S}^* Y = \frac{1}{n} \sum_{i=1}^n Y_i K_{\mathbf{x}_i}, \quad (Y \in L_2(P_n)).$$

We consider the following preconditioned update on  $f_t \in \mathcal{H}$ :

$$f_t = f_{t-1} - \eta(\Sigma + \lambda I)^{-1}(\hat{\Sigma} f_{t-1} - \hat{S}^* Y), \quad f_0 = 0.$$

We aim to show the following theorem:

**Theorem 8.** *Given the assumptions above, if the sample size  $n$  is sufficiently large so that  $1/(n\lambda) \ll 1$ , then for  $\eta < \|\Sigma\|$  with  $\eta t \geq 1$  and  $0 < \delta < 1$  and  $0 < \lambda < 1$ , it holds that*

$$\|Sf_t - f^*\|_{L_2(P_X)}^2 \leq C(B(t) + V(t)),$$

with probability  $1 - 3\delta$ , where  $C$  is a constant and

$$B(t) := \exp(-\eta t) \vee \left(\frac{\lambda}{\eta t}\right)^{2r},$$

$$V(t) := V_1(t) + (1 + \eta t) \left( \frac{\lambda^{-1} B(t) + \sigma^2 \text{tr}(\Sigma^{1/s}) \lambda^{-1/s}}{n} + \frac{\lambda^{-1}(\sigma + M + (1 + t\eta)\lambda^{-(\frac{1}{2}-r)_+})^2}{n^2} \right) \log(1/\delta)^2,$$

in which

$$V_1(t) := \left[ \exp(-\eta t) \vee \left(\frac{\lambda}{\eta t}\right)^{2r} + (t\eta)^2 \left( \frac{\beta'(1 \vee \lambda^{2r-\mu}) \text{tr}(\Sigma^{1/s}) \lambda^{-1/s}}{n} + \frac{\beta'^2(1 + \lambda^{-\mu}(1 \vee \lambda^{2r-\mu}))}{n^2} \right) \right] (1 + t\eta)^2,$$

for  $\beta' = \log\left(\frac{28C_\mu^2(2^{2r-\mu} \vee \lambda^{-\mu+2r}) \text{tr}(\Sigma^{1/s}) \lambda^{-1/s}}{\delta}\right)$ . When  $r \geq 1/2$ , if we set  $\lambda = n^{-\frac{s}{2rs+1}} =: \lambda^*$  and  $t = \Theta(\log(n))$ , then the overall convergence rate becomes

$$\|Sg_t - f^*\|_{L_2(P_X)}^2 = \tilde{O}_p\left(n^{-\frac{2rs}{2rs+1}}\right),$$

which is the minimax optimal rate ( $\tilde{O}_p(\cdot)$  hides a poly-log( $n$ ) factor). On the other hand, when  $r < 1/2$ , the bound is also  $\tilde{O}_p\left(n^{-\frac{2rs}{2rs+1}}\right)$  except the term  $V_1(t)$ . In this case, if  $2r \geq \mu$  holds additionally, we have  $V_t(t) = \tilde{O}_p\left(n^{-\frac{2rs}{2rs+1}}\right)$ , which again recovers the optimal rate.

Note that if the naive GD (with iterates  $\tilde{f}_t$ ) is employed, from previous works [LR17], we know that the bias term  $\left(\frac{\lambda}{\eta t}\right)^{2r}$  is replaced by  $\left(\frac{1}{\eta t}\right)^{2r}$ , and therefore the upper bound translates to

$$\|S\tilde{f}_t - f^*\|_{L_2(P_X)}^2 \leq C \left\{ (\eta t)^{-2r} + \frac{1}{n} \left( \text{tr}(\Sigma^{1/s}) (\eta t)^{1/s} + \frac{\eta t}{n} \right) \left( \sigma^2 + \left(\frac{1}{\eta t}\right)^{2r} + \frac{M^2 + (\eta t)^{-(2r-1)}}{n} \right) \right\},$$

with high probability. In other words, by the condition  $\eta = O(1)$ , we need  $t = \Theta(n^{\frac{2rs}{2rs+1}})$  steps to sufficiently diminish the bias term. In contrast, the preconditioned update that interpolates between GD and NGD (4.1) only require  $t = O(\log(n))$  steps to make the bias term negligible. This is because the NGD amplifies the high frequency component and rapidly captures the detailed ‘‘shape’’ of the target function  $f^*$ .

### C.8.2 Proof of Main Result

**Proof.** We follow the proof strategy of [LR17]. First we define a reference optimization problem with iterates  $\bar{f}_t$  that directly minimize the population risk:

$$\bar{f}_t = \bar{f}_{t-1} - \eta(\Sigma + \lambda I)^{-1}(\Sigma \bar{f}_{t-1} - S^* f^*), \quad \bar{f}_0 = 0.$$

Note that  $\mathbb{E}[f_t] = \bar{f}_t$ . In addition, we define the degrees of freedom and its related quantity as

$$\mathcal{N}_\infty(\lambda) := \mathbb{E}_{\mathbf{x}}[\langle K_{\mathbf{x}}, \Sigma_\lambda^{-1} K_{\mathbf{x}} \rangle_{\mathcal{H}}] = \text{tr}(\Sigma \Sigma_\lambda^{-1}), \quad \mathcal{F}_\infty(\lambda) := \sup_{\mathbf{x} \in \text{supp}(P_X)} \|\Sigma_\lambda^{-1/2} K_{\mathbf{x}}\|_{\mathcal{H}}^2.$$

We can see that the risk admits the following bias-variance decomposition

$$\|Sf_t - f^*\|_{L_2(P_X)}^2 \leq 2 \underbrace{\|Sf_t - S\bar{f}_t\|_{L_2(P_X)}^2}_{V(t), \text{ variance}} + \underbrace{\|\bar{f}_t - f^*\|_{L_2(P_X)}^2}_{B(t), \text{ bias}}.$$

We upper bound the bias and variance separately.

**Bounding the bias term  $B(t)$ :** Note that by the update rule (4.1), it holds that

$$\begin{aligned} S\bar{f}_t - f^* &= S\bar{f}_{t-1} - f^* - \eta S(\Sigma + \lambda I)^{-1}(\Sigma \bar{f}_{t-1} - S^* f^*) \\ \Leftrightarrow S\bar{f}_t - f^* &= (I - \eta S(\Sigma + \lambda I)^{-1} S^*)(S\bar{f}_{t-1} - f^*). \end{aligned}$$

Therefore, unrolling the recursion gives  $S\bar{f}_t - f^* = (I - \eta S(\Sigma + \lambda I)^{-1} S^*)^t (S\bar{f}_0 - f^*) = (I - \eta S(\Sigma + \lambda I)^{-1} S^*)^t (-f^*) = -(I - \eta S(\Sigma + \lambda I)^{-1} S^*)^t L^r h^*$ . Write the spectral decomposition of  $L$  as  $L = \sum_{j=1}^{\infty} \sigma_j \phi_j \phi_j^*$  for  $\phi_j \in L_2(P_X)$  for  $\sigma_j \geq 0$ . We have  $\|(I - \eta S(\Sigma + \lambda I)^{-1} S^*)^t L^r h^*\|_{L_2(P_X)} = \sum_{j=1}^{\infty} (1 - \eta \frac{\sigma_j}{\sigma_j + \lambda})^{2t} \sigma_j^{2r} h_j^2$ , where  $h = \sum_{j=1}^{\infty} h_j \phi_j$ . We then apply Lemma 9 to obtain

$$B(t) \leq \exp(-\eta t) \sum_{j: \sigma_j \geq \lambda} h_j^2 + \left(\frac{2r}{e} \frac{\lambda}{\eta t}\right)^{2r} \sum_{j: \sigma_j < \lambda} h_j^2 \leq C \left[ \exp(-\eta t) \vee \left(\frac{\lambda}{\eta t}\right)^{2r} \right] \|h^*\|_{L_2(P_X)}^2,$$

where  $C$  is a constant depending only on  $r$ .

**Bounding the variance term  $V(t)$ :** We now handle the variance term  $V(t)$ . For notational convenience, we write  $A_\lambda := A + \lambda I$  for a linear operator  $A$  from a Hilbert space  $H$  to  $H$ . By the definition of  $f_t$ , we know

$$\begin{aligned} f_t &= (I - \eta(\Sigma + \lambda I)^{-1} \hat{\Sigma}) f_{t-1} + \eta(\Sigma + \lambda I)^{-1} \hat{S}^* Y \\ &= \sum_{j=0}^{t-1} (I - \eta(\Sigma + \lambda I)^{-1} \hat{\Sigma})^j \eta(\Sigma + \lambda I)^{-1} \hat{S}^* Y \\ &= \Sigma_\lambda^{-1/2} \eta \left[ \sum_{j=0}^{t-1} (I - \eta \Sigma_\lambda^{-1/2} \hat{\Sigma} \Sigma_\lambda^{-1/2})^j \right] \Sigma_\lambda^{-1/2} \hat{S}^* Y =: \Sigma_\lambda^{-1/2} G_t \Sigma_\lambda^{-1/2} \hat{S}^* Y, \end{aligned}$$

where we defined  $G_t := \eta \left[ \sum_{j=0}^{t-1} (I - \eta \Sigma_\lambda^{-1/2} \hat{\Sigma} \Sigma_\lambda^{-1/2})^j \right]$ . Accordingly, we decompose  $V(t)$  as

$$\begin{aligned} \|Sf_t - S\bar{f}_t\|_{L_2(P_X)}^2 &\leq 2 \underbrace{\|S(f_t - \Sigma_\lambda^{-1/2} G_t \Sigma_\lambda^{-1/2} \hat{\Sigma} \bar{f}_t)\|_{L_2(P_X)}^2}_{(a)} \\ &\quad + \underbrace{\|S(\Sigma_\lambda^{-1/2} G_t \Sigma_\lambda^{-1/2} \hat{\Sigma} \bar{f}_t - \bar{f}_t)\|_{L_2(P_X)}^2}_{(b)}. \end{aligned}$$

We bound (a) and (b) separately.

**Step 1. Bounding (a).** Decompose (a) as

$$\begin{aligned} & \|S(f_t - \Sigma_\lambda^{-1/2} G_t \Sigma_\lambda^{-1/2} \hat{\Sigma} \bar{f}_t)\|_{L_2(P_X)}^2 = \|S \Sigma_\lambda^{-1/2} G_t \Sigma_\lambda^{-1/2} (\hat{S}^* Y - \hat{\Sigma} \bar{f}_t)\|_{L_2(P_X)}^2 \\ & \leq \|S \Sigma_\lambda^{-1/2}\|^2 \|G_t \Sigma_\lambda^{-1/2} \hat{\Sigma} \Sigma_\lambda^{-1/2}\|^2 \|\Sigma_\lambda^{1/2} \hat{\Sigma}^{-1} \Sigma_\lambda^{1/2}\|^2 \|\Sigma_\lambda^{-1/2} (\hat{S}^* Y - \hat{\Sigma} \bar{f}_t)\|_{\mathcal{H}}^2. \end{aligned}$$

We bound the terms in the RHS individually.

(i)  $\|S \Sigma_\lambda^{-1/2}\|^2 = \|\Sigma_\lambda^{-1/2} \Sigma \Sigma_\lambda^{-1/2}\| \leq 1.$

(ii) Note that  $\Sigma_\lambda^{-1/2} \hat{\Sigma} \Sigma_\lambda^{-1/2} = I - \Sigma_\lambda^{-1/2} (\Sigma - \hat{\Sigma}) \Sigma_\lambda^{-1/2} \succeq (1 - \|\Sigma_\lambda^{-1/2} (\Sigma - \hat{\Sigma}) \Sigma_\lambda^{-1/2}\|) I.$

Proposition 6 of [RR17] and its proof implies that for  $\lambda \leq \|\Sigma\|$  and  $0 < \delta < 1$ , it holds that

$$\|\Sigma_\lambda^{-1/2} (\Sigma - \hat{\Sigma}) \Sigma_\lambda^{-1/2}\| \leq \sqrt{\frac{2\beta \mathcal{F}_\infty(\lambda)}{n}} + \frac{2\beta(1 + \mathcal{F}_\infty(\lambda))}{3n} =: \Xi_n, \quad (\text{C.21})$$

with probability  $1 - \delta$ , where  $\beta = \log\left(\frac{4\text{tr}(\Sigma \Sigma_\lambda^{-1})}{\delta}\right) = \log\left(\frac{4\mathcal{N}_\infty(\lambda)}{\delta}\right)$ . By Lemma 12,  $\beta \leq \log\left(\frac{4\text{tr}(\Sigma^{1/s}) \lambda^{-1/s}}{\delta}\right)$  and  $\mathcal{F}_\infty(\lambda) \leq \lambda^{-1}$ . Therefore, if  $\lambda = o(n^{-1} \log(n))$  and  $\lambda = \Omega(n^{-1/s})$ , the right hand side can be smaller than  $1/2$  for sufficiently large  $n$ , i.e.  $\Xi_n = O(\sqrt{\log(n)/(n\lambda)}) \leq 1/2$ . In this case we have,

$$\Sigma_\lambda^{-1/2} \hat{\Sigma} \Sigma_\lambda^{-1/2} \succeq \frac{1}{2} I.$$

We denote this event as  $\mathcal{E}_1$ .

(iii) Note that

$$\begin{aligned} G_t \Sigma_\lambda^{-1/2} \hat{\Sigma} \Sigma_\lambda^{-1/2} &= \eta \left[ \sum_{j=0}^{t-1} (I - \eta \Sigma_\lambda^{-1/2} \hat{\Sigma} \Sigma_\lambda^{-1/2})^j \right] \Sigma_\lambda^{-1/2} \hat{\Sigma} \Sigma_\lambda^{-1/2} \\ &= \eta \left[ \sum_{j=0}^{t-1} (I - \eta \Sigma_\lambda^{-1/2} \hat{\Sigma} \Sigma_\lambda^{-1/2})^j \right] (\Sigma_\lambda^{-1/2} \hat{\Sigma} \Sigma_\lambda^{-1/2} + \lambda \Sigma_\lambda^{-1}). \end{aligned}$$

Thus, by Lemma 10 we have

$$\begin{aligned} & \|G_t \Sigma_\lambda^{-1/2} \hat{\Sigma} \Sigma_\lambda^{-1/2}\| \\ & \leq \underbrace{\left\| \eta \left[ \sum_{j=0}^{t-1} (I - \eta \Sigma_\lambda^{-1/2} \hat{\Sigma} \Sigma_\lambda^{-1/2})^j \right] \Sigma_\lambda^{-1/2} \hat{\Sigma} \Sigma_\lambda^{-1/2} \right\|}_{\leq 1 \text{ (due to Lemma 10)}} + \left\| \eta \left[ \sum_{j=0}^{t-1} (I - \eta \Sigma_\lambda^{-1/2} \hat{\Sigma} \Sigma_\lambda^{-1/2})^j \right] \lambda \Sigma_\lambda^{-1} \right\| \\ & \leq 1 + \eta \sum_{j=0}^{t-1} \|(I - \eta \Sigma_\lambda^{-1/2} \hat{\Sigma} \Sigma_\lambda^{-1/2})^j\| \|\lambda \Sigma_\lambda^{-1}\| \leq 1 + \eta t. \end{aligned}$$

(iv) Note that

$$\|\Sigma_\lambda^{-1/2} (\hat{S}^* Y - \hat{\Sigma} \bar{f}_t)\|_{\mathcal{H}}^2 \leq 2(\|\Sigma_\lambda^{-1/2} [(\hat{S}^* Y - \hat{\Sigma} \bar{f}_t) - (S^* f^* - \Sigma \bar{f}_t)]\|_{\mathcal{H}}^2 + \|\Sigma_\lambda^{-1/2} (S^* f^* - \Sigma \bar{f}_t)\|_{\mathcal{H}}^2).$$

First we bound the first term of the right hand side. Let  $\xi_i = \Sigma_\lambda^{-1/2} [K_{\mathbf{x}_i} y_i - K_{\mathbf{x}_i} \bar{f}_t(\mathbf{x}_i) - (S^* f^* - \Sigma \bar{f}_t)]$ . Then,  $\{\xi_i\}_{i=1}^n$  is an i.i.d. sequence of zero-centered random variables taking value in  $\mathcal{H}$  and thus we have

$$\|\Sigma_\lambda^{-1/2} [(\hat{S}^* Y - \hat{\Sigma} \bar{f}_t) - (S^* f^* - \Sigma \bar{f}_t)]\|_{\mathcal{H}}^2 = \left\| \frac{1}{n} \sum_{i=1}^n \xi_i \right\|_{\mathcal{H}}^2.$$

The right hand side can be bounded by using Bernstein's inequality in Hilbert space [CDV07]. To apply the inequality, we need to bound the variance and sup-norm of the random variable. The variance can be bounded as

$$\begin{aligned}
\mathbb{E}[\|\xi_i\|_{\mathcal{H}}^2] &\leq \mathbb{E}_{(\mathbf{x},y)} \left[ \|\Sigma_\lambda^{-1/2}(K_{\mathbf{x}}(f^*(\mathbf{x}) - \bar{f}_t(\mathbf{x})) + K_\xi \epsilon)\|_{\mathcal{H}}^2 \right] \\
&\leq 2 \left\{ \mathbb{E}_{(\mathbf{x},y)} \left[ \|\Sigma_\lambda^{-1/2}(K_{\mathbf{x}}(f^*(\mathbf{x}) - \bar{f}_t(x))\|_{\mathcal{H}}^2 + \|\Sigma_\lambda^{-1/2}(K_{\mathbf{x}}\epsilon)\|_{\mathcal{H}}^2 \right] \right\} \\
&\leq 2 \left\{ \sup_{\mathbf{x} \in \text{supp}(P_X)} \|\Sigma_\lambda^{-1/2} K_{\mathbf{x}}\|^2 \|f^* - S\bar{f}_t\|_{L_2(P_X)}^2 + \sigma^2 \text{tr}(\Sigma_\lambda^{-1} \Sigma) \right\} \\
&\leq 2 \{ \mathcal{F}_\infty(\lambda) B(t) + \sigma^2 \text{tr}(\Sigma_\lambda^{-1} \Sigma) \} \\
&\leq 2 \{ \lambda^{-1} B(t) + \sigma^2 \text{tr}(\Sigma_\lambda^{-1} \Sigma) \},
\end{aligned}$$

The sup-norm can be bounded as follows. Observe that  $\|\bar{f}_t\|_\infty \leq \|\bar{f}_t\|_{\mathcal{H}}$ , and thus by Lemma 11,

$$\begin{aligned}
\|\xi_i\|_{\mathcal{H}} &\leq 2 \sup_{\mathbf{x} \in \text{supp}(P_X)} \|\Sigma_\lambda^{-1/2} K_{\mathbf{x}}\|_{\mathcal{H}} (\sigma + \|f^*\|_\infty + \|\bar{f}_t\|_\infty) \\
&\lesssim \mathcal{F}_\infty^{1/2}(\lambda) (\sigma + M + (1 + t\eta) \lambda^{-(1/2-r)_+}) \\
&\lesssim \lambda^{-1/2} (\sigma + M + (1 + t\eta) \lambda^{-(1/2-r)_+}).
\end{aligned}$$

Therefore, for  $0 < \delta < 1$ , Bernstein's inequality (see Proposition 2 of [CDV07]) yields that

$$\left\| \frac{1}{n} \sum_{i=1}^n \xi_i \right\|_{\mathcal{H}}^2 \leq C \left( \sqrt{\frac{\lambda^{-1} B(t) + \sigma^2 \text{tr}(\Sigma_\lambda^{-1} \Sigma)}{n}} + \frac{\lambda^{-1/2} (\sigma + M + (1 + t\eta) \lambda^{-(1/2-r)_+})}{n} \right)^2 \log(1/\delta)^2$$

with probability  $1 - \delta$  where  $C$  is a universal constant. We define this event as  $\mathcal{E}_2$ .

For the second term  $\|\Sigma_\lambda^{-1/2}(S^* f^* - \Sigma \bar{f}_t)\|_{\mathcal{H}}^2$  we have

$$\|\Sigma_\lambda^{-1/2}(S^* f^* - \Sigma \bar{f}_t)\|_{\mathcal{H}}^2 \leq \|\Sigma_\lambda^{-1/2}(f^* - S\bar{f}_t)\|_{\mathcal{H}}^2 = \|f^* - S\bar{f}_t\|_{L_2(P_X)}^2 \leq B(t).$$

Combining these evaluations, on the event  $\mathcal{E}_2$  where  $P(\mathcal{E}_2) \geq 1 - \delta$  for  $0 < \delta < 1$  we have

$$\begin{aligned}
&\|\Sigma_\lambda^{-1/2}(\hat{S}^* Y - \hat{\Sigma} \bar{f}_t)\|_{\mathcal{H}}^2 \\
&\stackrel{(i)}{\leq} C \left( \sqrt{\frac{\lambda^{-1} B(t) + \sigma^2 \text{tr}(\Sigma_\lambda^{-1} \Sigma)}{n}} + \frac{\lambda^{-1/2} (\sigma + M + (1 + t\eta) \lambda^{-(1/2-r)_+})}{n} \right)^2 \log(1/\delta)^2 + B(t).
\end{aligned}$$

where we used Lemma 12 in (i).

**Step 2. Bounding (b).** On the event  $\mathcal{E}_1$ , the term (b) can be evaluated as

$$\begin{aligned}
&\|S(\Sigma_\lambda^{-1/2} G_t \Sigma_\lambda^{-1/2} \hat{\Sigma} \bar{f}_t - \bar{f}_t)\|_{L_2(P_X)}^2 \\
&\leq \|\Sigma^{1/2}(\Sigma_\lambda^{-1/2} G_t \Sigma_\lambda^{-1/2} \hat{\Sigma} \bar{f}_t - \bar{f}_t)\|_{\mathcal{H}}^2 \\
&\leq \|\Sigma^{1/2} \Sigma_\lambda^{-1/2} (G_t \Sigma_\lambda^{-1/2} \hat{\Sigma} \Sigma_\lambda^{-1/2} - I) \Sigma_\lambda^{1/2} \bar{f}_t\|_{\mathcal{H}}^2 \\
&\leq \|\Sigma^{1/2} \Sigma_\lambda^{-1/2} \| (G_t \Sigma_\lambda^{-1/2} \hat{\Sigma} \Sigma_\lambda^{-1/2} - I) \Sigma_\lambda^{1/2} \bar{f}_t\|_{\mathcal{H}}^2 \\
&\leq \|(G_t \Sigma_\lambda^{-1/2} \hat{\Sigma} \Sigma_\lambda^{-1/2} - I) \Sigma_\lambda^{1/2} \bar{f}_t\|_{\mathcal{H}}^2.
\end{aligned} \tag{C.22}$$

where we used Lemma 11 in the last inequality,  $C$  is a positive universal constant. The term  $\|(G_t \Sigma_\lambda^{-1/2} \hat{\Sigma} \Sigma_\lambda^{-1/2} - I) \Sigma_\lambda^{1/2} \bar{f}_t\|_{\mathcal{H}}$  can be bounded as follows. First, note that

$$(G_t \Sigma_\lambda^{-1/2} \hat{\Sigma} \Sigma_\lambda^{-1/2} - I) \Sigma_\lambda^{1/2} = \left\{ \eta \left[ \sum_{j=0}^{t-1} (I - \eta \Sigma_\lambda^{-1/2} \hat{\Sigma} \Sigma_\lambda^{-1/2})^j \right] \Sigma_\lambda^{-1/2} \hat{\Sigma} \Sigma_\lambda^{-1/2} - I \right\} \Sigma_\lambda^{1/2}$$

$$= (I - \eta \Sigma_\lambda^{-1/2} \hat{\Sigma} \Sigma_\lambda^{-1/2})^t \Sigma_\lambda^{1/2}.$$

Therefore, the right hand side of (C.22) can be further bounded by

$$\begin{aligned}
& \|(I - \eta \Sigma_\lambda^{-1/2} \hat{\Sigma} \Sigma_\lambda^{-1/2})^t \Sigma_\lambda^{1/2} \bar{f}_t\|_{\mathcal{H}} \\
&= \|(I - \eta \Sigma_\lambda^{-1/2} \Sigma \Sigma_\lambda^{-1/2} + \eta \Sigma_\lambda^{-1/2} (\Sigma - \hat{\Sigma}) \Sigma_\lambda^{-1/2})^t \Sigma_\lambda^{1/2} \bar{f}_t\|_{\mathcal{H}} \\
&= \left\| \sum_{k=0}^{t-1} (I - \eta \Sigma_\lambda^{-1/2} \hat{\Sigma} \Sigma_\lambda^{-1/2})^k (\eta \Sigma_\lambda^{-1/2} (\Sigma - \hat{\Sigma}) \Sigma_\lambda^{-1/2}) (I - \eta \Sigma_\lambda^{-1} \Sigma)^{t-k-1} \Sigma_\lambda^{1/2} \bar{f}_t - (I - \eta \Sigma_\lambda^{-1} \Sigma)^t \Sigma_\lambda^{1/2} \bar{f}_t \right\|_{\mathcal{H}} \\
&\stackrel{(i)}{\leq} \|(I - \eta \Sigma_\lambda^{-1} \Sigma)^t \Sigma_\lambda^{1/2} \bar{f}_t\|_{\mathcal{H}} \\
&\quad + \eta \sum_{k=0}^{t-1} \|(I - \eta \Sigma_\lambda^{-1/2} \hat{\Sigma} \Sigma_\lambda^{-1/2})^k \Sigma_\lambda^{-1/2} (\Sigma - \hat{\Sigma}) \Sigma_\lambda^{-1/2+r} (I - \eta \Sigma_\lambda^{-1} \Sigma)^{t-k-1} \Sigma_\lambda^{1/2-r} \bar{f}_t\|_{\mathcal{H}} \\
&\leq \|(I - \eta \Sigma_\lambda^{-1} \Sigma)^t \Sigma_\lambda^{1/2} \bar{f}_t\|_{\mathcal{H}} + t\eta \|\Sigma_\lambda^{-1/2} (\Sigma - \hat{\Sigma}) \Sigma_\lambda^{-1/2+r}\| \|\Sigma_\lambda^{1/2-r} \bar{f}_t\|_{\mathcal{H}} \\
&= \|(I - \eta \Sigma_\lambda^{-1} \Sigma)^t \Sigma_\lambda^r\| \|\Sigma_\lambda^{1/2-r} \bar{f}_t\|_{\mathcal{H}} + t\eta \|\Sigma_\lambda^{-1/2} (\Sigma - \hat{\Sigma}) \Sigma_\lambda^{-1/2+r}\| \|\Sigma_\lambda^{1/2-r} \bar{f}_t\|_{\mathcal{H}} \\
&\lesssim \|(I - \eta \Sigma_\lambda^{-1} \Sigma)^t \Sigma_\lambda^r\| + t\eta \|\Sigma_\lambda^{-1/2} (\Sigma - \hat{\Sigma}) \Sigma_\lambda^{-1/2+r}\| (1 + t\eta) \|h^*\|_{L_2(P_X)}, \tag{C.23}
\end{aligned}$$

where (i) is due to exchangeability of  $\Sigma_\lambda$  and  $\Sigma$ . By Lemma 9, for the right hand side we have

$$\|(I - \eta \Sigma_\lambda^{-1} \Sigma)^t \Sigma_\lambda^r\| \leq \exp(-\eta t/2) \vee \left(\frac{1}{e} \frac{\lambda}{\eta t}\right)^r.$$

Next, as in the (C.21), by applying the Bernstein inequality for asymmetric operators (Corollary 3.1 of [Min17] with the argument in its Section 3.2), it holds that

$$\begin{aligned}
& \|\Sigma_\lambda^{-1/2} (\Sigma - \hat{\Sigma}) \Sigma_\lambda^{-1/2+r}\| \\
&\leq C' \left( \sqrt{\frac{\beta' C_\mu^2 (2^{2r-\mu} \vee \lambda^{2r-\mu}) \mathcal{N}_\infty(\lambda)}{n}} + \frac{\beta' ((1+\lambda)^r + C_\mu^2 \lambda^{-\mu/2} (2^{2r-\mu} \vee \lambda^{r-\mu/2}))}{n} \right) =: \Xi'_n,
\end{aligned}$$

with probability  $1 - \delta$ , where  $C'$  is a universal constant and  $\beta' \leq \log\left(\frac{28C_\mu^2 (2^{2r-\mu} \vee \lambda^{-\mu+2r}) \text{tr}(\Sigma^{1/s}) \lambda^{-1/s}}{\delta}\right)$ . We also used the following bounds on the sup-norm and the second order moments:

$$\begin{aligned}
(\text{sup-norm}) \quad & \|\Sigma_\lambda^{-1/2} (K_{\mathbf{x}} K_{\mathbf{x}}^* - \Sigma) \Sigma_\lambda^{-1/2+r}\| \\
& \leq \|\Sigma_\lambda^{-1/2} K_{\mathbf{x}} K_{\mathbf{x}}^* \Sigma_\lambda^{-1/2+r}\| + \|\Sigma_\lambda^r\| \\
& \leq \|\Sigma_\lambda^{-\mu/2} \Sigma_\lambda^{\mu/2-1/2} K_{\mathbf{x}} K_{\mathbf{x}}^* \Sigma_\lambda^{-1/2+\mu/2} \Sigma_\lambda^{r-\mu/2}\| + \|\Sigma_\lambda^r\| \\
& \leq C_\mu^2 \lambda^{-\mu/2} (2^{r-\mu/2} \vee \lambda^{r-\mu/2}) + (1+\lambda)^r \quad (\text{a.s.}), \\
(2\text{nd order moment 1}) \quad & \|\mathbb{E}_{\mathbf{x}} [\Sigma_\lambda^{-1/2} (K_{\mathbf{x}} K_{\mathbf{x}}^* - \Sigma) \Sigma_\lambda^{-1+2r} (K_{\mathbf{x}} K_{\mathbf{x}}^* - \Sigma) \Sigma_\lambda^{-1/2}]\| \\
& \leq \|\Sigma_\lambda^{-1/2} \Sigma \Sigma_\lambda^{-1/2}\| \sup_{\mathbf{x} \in \text{supp}(P_X)} [K_{\mathbf{x}}^* \Sigma_\lambda^{-1/2+\mu/2} \Sigma_\lambda^{-\mu+2r} \Sigma_\lambda^{-1/2+\mu/2} K_{\mathbf{x}}] \\
& \leq C_\mu^2 (2^{2r-\mu} \vee \lambda^{2r-\mu}), \\
(2\text{nd order moment 2}) \quad & \|\mathbb{E}_{\mathbf{x}} [\Sigma_\lambda^{-1/2+r} (K_{\mathbf{x}} K_{\mathbf{x}}^* - \Sigma) \Sigma_\lambda^{-1/2} \Sigma_\lambda^{-1/2} (K_{\mathbf{x}} K_{\mathbf{x}}^* - \Sigma) \Sigma_\lambda^{-1/2+r}]\| \\
& \leq \|\mathbb{E}_{\mathbf{x}} [\Sigma_\lambda^{-1/2+r} K_{\mathbf{x}} K_{\mathbf{x}}^* \Sigma_\lambda^{-1} K_{\mathbf{x}} K_{\mathbf{x}}^* \Sigma_\lambda^{-1/2+r}]\| \\
& \leq C_\mu^2 (2^{2r-\mu} \vee \lambda^{2r-\mu}) \mathbb{E}_{\mathbf{x}} [K_{\mathbf{x}}^* \Sigma_\lambda^{-1} K_{\mathbf{x}}] \\
& = C_\mu^2 (2^{2r-\mu} \vee \lambda^{2r-\mu}) \text{tr}(\Sigma \Sigma_\lambda^{-1}) \\
& = C_\mu^2 (2^{2r-\mu} \vee \lambda^{2r-\mu}) \mathcal{N}_\infty(\lambda).
\end{aligned}$$

We define this event as  $\mathcal{E}_3$ . Therefore, the right hand side of (C.23) can be further bounded by

$$\begin{aligned} & \|[(I - \eta \Sigma_\lambda^{-1} \Sigma)^t \Sigma_\lambda^r] + Ct\eta \|\Sigma_\lambda^{-1/2} (\Sigma - \hat{\Sigma}) \Sigma_\lambda^{-1/2+r}\| \|h^*\|_{L_2(P_X)} \\ & \leq \left[ \exp(-\eta t/2) \vee \left( \frac{1}{e} \frac{\lambda}{\eta t} \right)^r + t\eta \Xi'_n \right] (1 + t\eta) \|h^*\|_{L_2(P_X)}. \end{aligned}$$

Finally, note that when  $\lambda = \lambda^*$  and  $2r \geq \mu$ ,

$$\Xi_n^{r/2} = \tilde{O} \left( \frac{\lambda^{*2r-\mu-1/s}}{n} + \frac{\lambda^{*2(r-\mu)}}{n^2} \right) \leq \tilde{O} \left( n^{-\frac{s(4r-\mu)}{2rs+1}} + n^{-\frac{s(4r-2\mu)+2}{2rs+1}} \right) \leq \tilde{O} \left( n^{-\frac{2rs}{2rs+1}} \right).$$

**Step 3.** Combining the calculations in Step 1 and 2 leads to the desired result.  $\square$

### C.8.3 Auxiliary lemmas

**Lemma 9.** For  $t \in \mathbb{N}$ ,  $0 < \eta < 1$ ,  $0 < \sigma \leq 1$  and  $0 \leq \lambda$ , it holds that

$$\left( 1 - \eta \frac{\sigma}{\sigma + \lambda} \right)^t \sigma^r \leq \begin{cases} \exp(-\eta t/2) & (\sigma \geq \lambda) \\ \left( \frac{2r}{e} \frac{\lambda}{\eta t} \right)^r & (\sigma < \lambda) \end{cases}.$$

**Proof.** When  $\sigma \geq \lambda$ , we have

$$\left( 1 - \eta \frac{\sigma}{\sigma + \lambda} \right)^t \sigma^r \leq \left( 1 - \eta \frac{\sigma}{2\sigma} \right)^t \sigma^r = (1 - \eta/2)^t \sigma^r \leq \exp(-\eta t/2) \sigma^r \leq \exp(-\eta t/2)$$

due to  $\sigma \leq 1$ . On the other hand, note that

$$\begin{aligned} \left( 1 - \eta \frac{\sigma}{\sigma + \lambda} \right)^t \sigma^r & \leq \exp\left(-\eta t \frac{\sigma}{\sigma + \lambda}\right) \times \left( \frac{\sigma \eta t}{\sigma + \lambda} \right)^r \left( \frac{\sigma + \lambda}{\eta t} \right)^r \\ & \leq \sup_{x>0} \exp(-x) x^r \left( \frac{\sigma + \lambda}{\eta t} \right)^r \leq \left( \frac{\sigma + \lambda}{\eta t e} \right)^r, \end{aligned}$$

where we used  $\sup_{x>0} \exp(-x) x^r = (r/e)^r$ .  $\square$

**Lemma 10.** For  $t \in \mathbb{N}$ ,  $0 < \eta$  and  $0 \leq \sigma$  such that  $\eta\sigma < 1$ , it holds that  $\eta \sum_{j=0}^{t-1} (1 - \eta\sigma)^j \sigma \leq 1$ .

**Proof.** If  $\sigma = 0$ , then the statement is obvious. Assume that  $\sigma > 0$ , then

$$\sum_{j=0}^{t-1} (1 - \eta\sigma)^j \sigma = \frac{1 - (1 - \eta\sigma)^t}{1 - (1 - \eta\sigma)} \sigma = \frac{1}{\eta} [1 - (1 - \eta\sigma)^t] \leq \eta^{-1}.$$

This yields the desired claim.  $\square$

**Lemma 11.** Under (A5-7), for any  $0 < \lambda < 1$  and  $q \leq r$ , it holds that

$$\|\Sigma_\lambda^{-s} \bar{f}_t\|_{\mathcal{H}} \lesssim (1 + \lambda^{-(1/2+(q-r))_+} + \lambda t \eta \lambda^{-(3/2+(q-r))_+}) \|h^*\|_{L_2(P_X)}.$$

**Proof.** Recall that

$$\bar{f}_t = (I - \eta(\Sigma + \lambda I)^{-1} \Sigma) \bar{f}_{t-1} + \eta(\Sigma + \lambda I)^{-1} S^* f^* = \sum_{j=0}^{t-1} (I - \eta(\Sigma + \lambda I)^{-1} \Sigma)^j \eta(\Sigma + \lambda I)^{-1} S^* f^*.$$

Therefore, we obtain the following

$$\begin{aligned}
\|\Sigma_\lambda^{-q} \bar{f}_t\|_{\mathcal{H}} &= \eta \left\| \sum_{j=0}^{t-1} (I - \eta \Sigma_\lambda^{-1} \Sigma)^j \Sigma_\lambda^{-1-q} S^* L^r h^* \right\|_{\mathcal{H}} \\
&= \eta \left\| \sum_{j=0}^{t-1} (I - \eta \Sigma_\lambda^{-1} \Sigma)^j \Sigma_\lambda^{-1} (\Sigma + \lambda I) \Sigma_\lambda^{-q-1} S^* L^r h^* \right\|_{\mathcal{H}} \\
&\leq \eta \left\| \sum_{j=0}^{t-1} (I - \eta \Sigma_\lambda^{-1} \Sigma)^j \Sigma_\lambda^{-1} \Sigma \Sigma_\lambda^{-q-1} S^* L^r h^* \right\|_{\mathcal{H}} + \lambda \eta \left\| \sum_{j=0}^{t-1} (I - \eta \Sigma_\lambda^{-1} \Sigma)^j \Sigma_\lambda^{-1} \Sigma_\lambda^{-q-1} S^* L^r h^* \right\|_{\mathcal{H}} \\
&\leq \eta \left\| \sum_{j=0}^{t-1} (I - \eta \Sigma_\lambda^{-1} \Sigma)^j \Sigma_\lambda^{-1} \Sigma \right\| \left\| \Sigma_\lambda^{-q-1} S^* L^r h^* \right\|_{\mathcal{H}} + \lambda \eta \left\| \sum_{j=0}^{t-1} (I - \eta \Sigma_\lambda^{-1} \Sigma)^j \Sigma_\lambda^{-1} \Sigma_\lambda^{-q-1} S^* L^r h^* \right\|_{\mathcal{H}} \\
&\leq \left\| \Sigma_\lambda^{-q-1} S^* L^r h^* \right\|_{\mathcal{H}} + \lambda t \eta \left\| \Sigma_\lambda^{-1} \Sigma_\lambda^{-q-1} S^* L^r h^* \right\|_{\mathcal{H}} \\
&\leq \left\| S^* L_\lambda^{-q-1+r} h^* \right\|_{\mathcal{H}} + \lambda t \eta \left\| S^* L_\lambda^{-q-2+r} h^* \right\|_{\mathcal{H}} \\
&\leq \sqrt{\langle h^*, L_\lambda^{-q-1+r} S S^* L_\lambda^{-q-1+r} h^* \rangle_{L_2(P_X)}} + \lambda t \eta \sqrt{\langle h^*, L_\lambda^{-q-2+r} S S^* L_\lambda^{-q-2+r} h^* \rangle_{L_2(P_X)}} \\
&= \sqrt{\langle h^*, L_\lambda^{-q-1+r} L L_\lambda^{-q-1+r} h^* \rangle_{L_2(P_X)}} + \lambda t \eta \sqrt{\langle h^*, L_\lambda^{-q-2+r} L L_\lambda^{-q-2+r} h^* \rangle_{L_2(P_X)}} \\
&\leq (\lambda^{-1/2-(q-r)} + \lambda t \eta \lambda^{-3/2-(q-r)}) \|h^*\|_{L_2(P_X)} \leq (1 + t \eta) \lambda^{-1/2-(q-r)} \|h^*\|_{L_2(P_X)}.
\end{aligned}$$

□

**Lemma 12.** Under (A5-7) and for  $\lambda \in (0, 1)$ , it holds that  $\mathcal{N}_\infty(\lambda) \leq \text{tr}(\Sigma^{1/s}) \lambda^{-1/s}$ , and  $\mathcal{F}_\infty(\lambda) \leq 1/\lambda$ .

**Proof.** For the first inequality, we have

$$\begin{aligned}
\mathcal{N}_\infty(\lambda) &= \text{tr}(\Sigma \Sigma_\lambda^{-1}) = \text{tr}(\Sigma^{1/s} \Sigma^{1-1/s} \Sigma_\lambda^{-(1-1/s)} \Sigma_\lambda^{-1/s}) \\
&\leq \text{tr}(\Sigma^{1/s} \Sigma^{1-1/s} \Sigma_\lambda^{-(1-1/s)}) \lambda^{-1/s} \leq \text{tr}(\Sigma^{1/s}) \lambda^{-1/s}.
\end{aligned}$$

As for the second inequality, note that

$$\mathcal{F}_\infty(\lambda) = \sup_{\mathbf{x}} \langle K_{\mathbf{x}}, \Sigma_\lambda^{-1} K_{\mathbf{x}} \rangle_{\mathcal{H}} \leq \sup_{\mathbf{x}} \lambda^{-1} \langle K_{\mathbf{x}}, K_{\mathbf{x}} \rangle_{\mathcal{H}} \leq \lambda^{-1} \sup_{\mathbf{x}} k(\mathbf{x}, \mathbf{x}) \leq \lambda^{-1}.$$

□

## D Experiment Setup

### D.1 Processing the Datasets

To obtain extra unlabeled data to estimate the Fisher, we zero pad pixels on the borders of each image before randomly cropping; a random horizontal flip is also applied for CIFAR10 images. We preprocess all images by dividing pixel values by 255 before centering them to be located within  $[-0.5, 0.5]$  with the subtraction by  $1/2$ . For experiments on CIFAR10, we downsample the original images using a max pooling layer with kernel size 2 and stride 2.

## D.2 Setup and Implementation for Optimizers

In all settings, GD uses a learning rate of 0.01 that is exponentially decayed every 1k updates with the parameter value 0.999. For NGD, we use a fixed learning rate of 0.03. Since inverting a parameter-by-parameter-sized Fisher estimate per iteration would be costly, we adopt the Hessian free approach [Mar10] which computes approximate matrix-inverse-vector products using the conjugate gradient (CG) method [NW06, BBV04]. For each approximate inversion, we run CG for 200 iterations starting from the solution returned by the previous CG run. The precise number of CG iterations and the initialization heuristic roughly follow [MS12]. For the first run of CG, we initialize the vector from a standard Gaussian, and run CG for 5k iterations. To ensure invertibility, we apply a very small amount of damping (0.00001) in most scenarios.

## D.3 Other Details

For experiments in the label noise and misspecification sections, we pretrain the teacher using the Adam optimizer [KB14] with its default hyperparameters and a learning rate of 0.001.

For experiments in the misalignment section, we downsample all images twice using max pooling with kernel size 2 and stride 2. Moreover, only for experiments in this section, we implement natural gradient descent by exactly computing the Fisher on a large batch of unlabeled data and inverting the matrix by calling PyTorch’s `torch.inverse` before right multiplying the gradient.